U.S. DEPARTMENT OF THE INTERIOR
U.S. GEOLOGICAL SURVEY

A Direct-Current Resistivity Survey near Mineral Hot Springs, San Luis Valley, Colorado.

By

Adel A.R. Zohdy [1]
Robert J. Bisdorf [1]

Open-File Report 93-282

1993

1. Box 25046, M.S. 964, Denver Federal Center, Denver, Colorado 80225

A DIRECT-CURRENT RESISTIVITY SURVEY NEAR MINERAL HOT SPRINGS, SAN LUIS VALLEY, COLORADO.

By

Adel A.R. Zohdy and Robert J. Bisdorf

INTRODUCTION

In August 1991, the U.S. Geological Survey made a direct-current resistivity survey to study the subsurface geoelectrical structure in the area near Mineral Hot Springs, in the northern part of the San Luis Valley, Colorado. The resistivity survey consisted of 30 deep Schlumberger soundings (Kunetz, 1966; Zohdy and others, 1974) and was completed in ten days.

The study area is bound on the east by the Sangre de Cristo Mountains, with outcrops of Paleozoic limestones and gneissic Precambrian rocks, and on the west by outcrops of Precambrian gneissic quartz monzonite rocks (Knepper, 1974) and Precambrian granodiorite (Scott and others, 1978) which are thrusted over Paleozoic carbonate rocks. At the foot of the Sangre de Cristo Mountains, there is another hot springs area: Valley View Hot Springs with warm waters of 32 to 34 degrees Celsius (Barrett and Pearl, 1978). The resistivity survey did not include the Valley View Hot Springs area.

The Mineral Hot Springs consist of three groups of springs scattered over an area of about 80 acres (0.324 square kilometers). These springs are located within a few hundred meters east of state-highway Colorado 17 and approximately nine kilometers south of Villa Grove. The temperature of the springs is 60 degrees Celsius, the total dissolved solids concentration is about 650 mg/l, and the waters are of the sodium-bicarbonate type (Barrett and Pearl, 1978). In the past, warm waters from the springs were piped to mineral baths and to a swimming pool.

In this report we present: a) the field data of the 30 Schlumberger soundings, b) interpretation of all the sounding curves, c) two recontoured bipole-dipole total-field apparent-resistivity maps based on data obtained by Jordan (1974), d) three interpreted-resistivity cross sections, and e) an interpreted-resistivity three-dimensional block diagram, which helps visualize the 3-D subsurface geoelectric structure.

SCHLUMBERGER ELECTRODE CONFIGURATION AND SOUNDING PROCEDURE

Figure 1 shows a schematic of the symmetric Schlumberger electrode configuration with two current electrodes (A and B) and two potential electrodes (M and N). The figure also shows a current power supply, an ammeter for measuring the intensity of the electric current, and a potentiometric chart recorder for measuring the electric potential difference between the electrodes M and N. The direction of expanding the distance between the current electrodes is indicated by the arrows. Note that the current-electrode spacing (AB/2) is defined as half the distance between the current electrodes A and B, and that the potential-electrode spacing (MN/2) is defined as half the distance between the potential electrodes M and N.

To make a sounding, the current-electrode spacings are increased at a logarithmically nearly equal increment (usually at the rate of 7 points per decade) while the potential electrode spacings are held fixed. After several measurements are made at successive AB/2 spacings, the expansion of AB/2 is stopped, the spacing between the electrodes M and N is increased, the measurement is repeated, and then the expansion of AB/2 is resumed. The condition that the ratio AB/MN must be greater than or equal to 5 is maintained (Zohdy and others, 1974). Listings of current-electrode spacings (AB/2) are given beneath each field-sounding curve in the appendix.

From a knowledge of the current- and potential-electrode spacings, the intensity of the electric current injected into the ground via the electrodes A and B, and the potential difference measured between the electrodes M and N, an apparent resistivity can be calculated. The apparent resistivity is plotted against the current-electrode spacing (AB/2) on a log-log scale (Zohdy and others, 1974) and the resulting curve is called a Schlumberger sounding curve.

SCHLUMBERGER SOUNDING STATIONS

Figure 2 shows the location of all the Schlumberger-sounding stations and the direction of current-electrode expansions, which were generally parallel to the available roads. The soundings were expanded to maximum current-electrode spacings, AB/2, that ranged from 914 m (3000 ft) to 7,315 m (24,000 ft) with the majority of the soundings being expanded to 3048 m (10,000 ft).

FIELD CONDITIONS AND MEASUREMENT PROCEDURES

At the time of the survey (August, 1991), the field conditions in the study area were favorable for making direct current resistivity soundings. The weather was generally good (except for a severe thunderstorm that approached from the north on the afternoon of the last day of the survey). Only a few fences with metal posts were present (except along U.S. Route 285, where a long metal fence exists). The effects of man-made structures on a few of the sounding curves are discussed in the section on distorted sounding curves.

Electrode-Spacing Measurements:

All current- and potential-electrode spacings were measured in feet and later converted to meters during interpretation. In this section, to simplify the discussion, we will refer to the electrode-spacing distances in feet (as they were measured in the field). The current-electrode spacings (AB/2) from 10 to 100 ft were measured using a cloth tape. At 140 ft and at 200 ft, they were measured using markings on the laid-out potential-electrode cable, and for greater than 200 ft they were measured using truck-mounted precision foot-odometers.

In this survey, several of the field-sounding curves are composed of four segments. A segment on a sounding curve is defined as a sequence of measurements made with increasing current-electrode spacings (AB/2) at fixed potential-electrode spacings (MN/2). The segments on the field-sounding curves correspond to fixed MN/2 spacings of: 2, 20, 200, and 600 ft, respectively. The MN/2 spacing of 600 ft was only needed to make measurements at large current-electrode spacings (AB/2) that reached 24,000 ft.

For each sounding curve, the first segment was obtained by successively expanding the current-electrode spacing (AB/2) from 10 ft to 100 ft with the potential-electrode spacing (MN/2) held fixed at 2 ft. At AB/2 = 100 ft, the MN/2 spacing was expanded from 2 ft to 20 ft and the second segment on the sounding curve was obtained by successively expanding AB/2 from 100 to 1000 ft. At AB/2 = 1000 ft, the MN/2 spacing was expanded from 20 ft to 200 ft and the third segment of the sounding curve was obtained by successively expanding AB/2 from 1000 ft to 3000 or up to 10,000 ft.

Some sounding stations were reoccupied and the sounding was expanded from AB/2 = 8000 ft to AB/2 = 24,000 ft and the potential-electrode spacing (MN/2) was increased from 200 ft to 600 ft at AB/2 = 8000 ft (see for example sounding 1).

Other soundings were pre-planned for expansion to 24,000 ft, and therefore the potential electrodes were expanded from 200 to 600 ft at the current-electrode spacing of 3000 or 4000 ft.

A few soundings were expanded to current-electrode spacings that were longer than the available straight-line road by following the turn in the road (see for example soundings 24, 25, and 26). These soundings were corrected for non-linear geometry using a method that we developed for making soundings along winding roads in the Medicine Lake area, California (Zohdy and Bisdorf, 1990).

Trucks and Other Equipment:

Three trucks were used for making the resistivity survey: an instrument truck (a carryall) that remained stationary at the center of the sounding, and two pickup trucks that were used to lay out and pick up the current cable. Communication between operator and crew was maintained using 90-watt FM radios. A 5-KVA generator was used for current-power supply and a potentiometric-chart recorder was used for measuring the potential difference between the potential electrodes.

Data Acquisition Procedure:

The sounding curves were plotted in the field as the measurements were made. We always use this procedure in order to identify (and to correct or minimize) spurious readings caused by operator or crew errors, by man-made structures (fences, buried cables, etc), by current leakage from damaged cable insulation, or by equipment malfunction. At the end of each sounding, a test for current leakage (Zohdy, 1968) was made. No current-leakage effects were observed for any of the tests.

SCHLUMBERGER SOUNDING DATA

The field sounding curves and their interpretations are given in the appendix. The soundings are numbered consecutively from Mineral Hot Springs 1 to Mineral Hot Springs 30. All the sounding curves were processed and interpreted using an automatic interpretation computer program (Zohdy, 1989; Zohdy and Bisdorf, 1989). The result is a step-function curve that shows the interpreted variation of resistivity with depth for a horizontally-layered earth model. We refer to the resistivities in such a model as interpreted resistivities.

Automatic-Data Processing and Interpretation:

The automatic data processing of the sounding curves consists of:

a) Converting the current-electrode spacings (AB/2) from feet to meters.

b) Shifting the observed-curve segments, obtained with fixed potential-electrode spacings (MN/2), upward or downward to obtain a continuous unsegmented curve. Generally, the segment measured with the largest potential-electrode spacing is kept fixed and the other segments are shifted up or down.

c) Sampling the continuous curve at the rate of 6 points per logarithmic cycle to obtain a digitized-sounding curve. The sampling of apparent resistivities is done from right to left, starting at the largest current-electrode spacing.

The digitized sounding curve resulting from the above processing is fed into the automatic-interpretation portion of the program to obtain depths and resistivities of a horizontally-stratified earth model. The obtained model is assumed to exist directly beneath the sounding station.

DISTORTED SOUNDING CURVES

Distorted sounding curves often are defined as curves which do not resemble those measured over horizontally stratified media. Here, we use the term "distorted" to describe sounding curves that are affected by man-made structures or by measurement errors. Two sounding curves (soundings 23 and 24) were distorted by a fence and by a pipe line, respectively. A third sounding (sounding 27) also may have been subtly distorted by a long fence along the highway. The effect of a metal fence on the measured signal varies as a function of: (a) the distance of the current and potential electrodes from the nearest metal post, (b) the grounding of the various metal posts, (c) the direction of the sounding expansion with respect to the orientation of the fence, and (d) the continuity of the metal fence. The largest effects are observed when the sounding expansion parallels the orientation of the fence.

Sounding 23 was expanded in a north-south direction, perpendicular to a metal fence located at a distance of about 1500 ft north of the center of the sounding. At that distance, the fence turns at a 90 degree angle and parallels the direction of expansion of the sounding line for an additional distance of about 4000 ft. The effect of the fence

was not significant or noticeable until the current-electrode spacing reached 4000 ft. At that distance the measured apparent resistivity suddenly increased as the metal posts of the fence acted as several small current-sources located at distances extending between 1500 ft and 4000 ft from the center of the sounding.

We conducted a small experiment to study the effect of this metal fence on the apparent resistivity measurement made at the current-electrode spacing AB/2 = 4000 ft. We made several measurements in which the distance from the current-electrode to the fence varied from 0 (zero) to a about 50 feet away from the fence. The apparent resistivity readings decreased from 86 ohm-m when the current line was at zero distance to about half as much (48 ohm-m) when the current electrode was placed at merely 4 feet away from the fence. As the current electrode was moved in steps to about 50 ft away from the fence the readings dropped asymptotically from 48 to 40 ohm-m, which is a more reasonable value for an undistorted sounding curve. It is interesting to note the quick drop from 86 to 48 ohm-m, even when the current electrode was only 4 feet from the fence. This suggests that similar experiments may be used to correct or at least to reduce the effect of a fence under similar field conditions. Hooking the current electrode to the fence, however, is not recommended for safety reasons and is unnecessary. The readings made at 2000, and 3000 ft may be slightly higher (about 3 to 5 percent) than they could have been if the fence was not present. The fence ended at a distance of 5300 feet from the center of the sounding.

Sounding 24, was made near a buried metal-pipe-line that formed an acute angle with the direction of the sounding line. No distortion from the pipe line was observed until the potential-electrode spacing was increased from 200 ft to 600 ft. The sounding-curve segment obtained with MN/2 = 600 feet dropped below the segment obtained with MN/2 = 200 ft. Because of the relatively large displacement, we made a complete overlap of the two segments (see the field curve of sounding 24C in the appendix). The buried pipeline intersected the sounding line at a distance of about 600 ft and therefore it was located directly under the potential electrode west of the center of the sounding. By scouting the area we could see a segment of the pipeline lying above the ground at a distance of about 150 feet north of the road where the sounding center was located. Interestingly, a downward-pointing cusp was not formed at the current-electrode spacing of 600 ft where the current electrode crosse the buried pipeline.

Sounding 27 was made parallel to US 285 and its center was located approximately 100 feet from a long fence with

metal posts. Surprisingly, no significant distortions were observed at any electrode spacings (see sounding 27 in appendix), but significant negative IP (induced polarization) effects were observed at current-electrode spacings greater than 2000 ft. The seeming absence of strong distortions is attributable to the continuity of the fence along the highway (discontinuous fences often cause more readily observable distortions on sounding curves). The IP effects attest to the detection of a polarizable material nearby which is the metal fence. The reduction in resistivity at electrode spacings greater than AB/2 = 1400 ft may be caused by the fence and to a lesser extent by the conductive materials of the valley fill to the east of the sounding 27.

EFFECT OF LATERAL-GEOLOGIC INHOMOGENEITIES ON SOUNDING CURVES

On some sounding curves (see for example soundings 1 and 2 in the appendix) we measured cusps caused by large lateral-geologic inhomogeneities. Cusps are formed on a sounding curve as the current electrodes are moved across lateral inhomogeneities during the sounding expansion. There are two types of cusps: downward-pointing cusps and upward-pointing cusps. A downward-pointing cusp is formed when a current electrode crosses over a conductive lateral inhomogeneity, whereas an upward-pointing cusp is formed when a current electrode crosses over a resistive inhomogeneity. A knowledge of the behaviour of theoretical Schlumberger sounding curves obtained near lateral inhomogeneities is essential in interpreting the cusps on field curves. Sets of theoretical Schlumberger sounding curves were published for the following configurations: a) electrode array expanded at various azimuths near a single vertical contact (Zohdy, 1974), b) soundings expanded perpendicular to the strike of three vertical layers (Zohdy, 1980), c) soundings made near dipping contacts and over combined vertical and horizontal contacts (Alpin and others, 1966; Kunetz, 1966).

Cusps (of either type) which are measured at short electrode spacings are usually caused by small lateral inhomogeneities such as boulders and buried stream channels; whereas, cusps measured at large current-electrode spacings are usually caused by much larger geologic units (assuming that the cusps are not caused by inaccurate measurements). Small lateral inhomogeneities of natural origin (not man-made pipes and fences, etc), crossed by the current electrodes at large spacings, do not affect the measurements to any measurable degree.

On sounding 1 (see appendix) two downward-pointing cusps are observed, one at the current-electrode spacing of 6000 ft

and the other at the current-electrode spacing of 16,000 ft. Each cusp represents the crossing of at least one of the current electrodes over one or more near-vertical contacts. Both cusps indicate near-vertical contacts separating resistive material (beneath the center of the sounding) from conductive material (on the other side of the contact). Because of the symmetry of the Schlumberger electrode array, it is not possible to know, from conventional measurements, on which side of the sounding center do the lateral inhomogeneities at 6000 and 16,000 ft exist. However, data from other soundings and from the total field data helped resolve this problem. For example, the data from sounding 2, which is located 3300 ft (one kilometer) south of sounding 1 and expanded in the same north-south direction as sounding 1, shows a well pronounced downward-pointing cusp at the electrode spacing of 3000 ft. The formation of this cusp at the current-electrode spacing of 3000 ft correlates very well with the cusp observed on sounding 1 at the electrode spacing of 6000 ft, and indicates that a near-vertical lateral inhomogeneity must be present at about 3000 ft south of sounding 2 and about 6000 ft south of sounding 1. **This interpretation places a near vertical contact (geologic fault?) at a distance of about 1000 ft north of Mineral Hot Springs, separating a low resistivity region south of the contact from a high resistivity region north of the contact.** Visual examination of the area in the vicinity of this low resistivity region did not reveal man-made structures (at the time of the survey) that could have caused these cusps. Supporting evidence on the presence of a low-resistivity inhomogeneity in that area is provided from the qualitative and quantitative interpretation of other soundings (soundings 3, 5, 6, and 7) south of sounding 1 and from the recontoured total-field apparent resistivity map derived from Jordan's data (Jordan, 1974).

The downward-pointing cusp on the curve of sounding 1 at the current-electrode spacing of 16,000 ft is probably caused by both current electrodes (north and south of the sounding center) symmetrically crossing near-vertical contacts to the north and to the south of the sounding center. The presence of low-resistivity bodies at nearly equal distance to the south and to the north of the sounding station causes the cusp to be more pronounced even for relatively small resistivity contrasts (Zohdy, 1980). The presence of a possible fault to the south of sounding 1 (at a distance of about 16000 ft) is supported by the interpretation of soundings to the south of it (see interpretation of soundings 6 and 7 in the section on resistivity cross sections), whereas the presence of a near vertical contact separating the resistive material beneath sounding 1 from conductive material to the north (at a distance of about 16000 ft) is supported by the total-field resistivity map shown in Figure 4-a, and by a geologically

inferred fault (Knepper, 1974). Soundings 8, 9, and 10 which were made north of sounding 1 and south of the contact, show little or no evidence on the presence of this contact. This is interpreted to indicate that the near-vertical electrical contact at that northern location is deep.

The location of most other observed cusps on the sounding curves were found to correspond to geologic lateral inhomogeneities that were revealed by the quantitative interpretation of ensembles of sounding data collected along profiles, from the study of Jordan's total-field bipole-dipole apparent resistivity data (Jordan, 1974), and from geologic maps (Knepper, 1974, Scott and others, 1978).

JORDAN'S DIRECT-CURRENT RESISTIVITY DATA

John M. Jordan (1974) made several geoelectrical surveys in the Mineral Hot Springs area in 1971, including six Schlumberger soundings, several time-domain electromagnetic soundings, and two direct-current bipole-dipole total-field apparent resistivity maps. His work also included a brief analysis of gravity, aeromagnetic, and remote sensing data, and was published in a thesis submitted to the Colorado School of Mines for a Master of Science Degree. Jordan's total-field apparent resistivity data were of the simple-total field type (Zohdy, 1978) which means that only the magnitude of the electric-field vector was used to compute the apparent resistivity.

The maximum current-electrode spacings in Jordan's Schlumberger soundings ranged from about 800 m (about 2600 ft) to 1548 m (about 5000 ft) and therefore, only few of his soundings detected the presence of a resistive basement.

Our sounding 8 (made in 1991) was accidentally located very near to Jordan's sounding 1 (made in 1971). The near coincidence of the two sets of sounding data which were obtained 20 years apart is remarkable (see Figure 3). Our sounding 13 was made near Jordan's sounding 3. Here the two sounding curves coincide at current-electrode spacings ranging from 3000 ft to 10,000 ft, where Jordan's sounding was terminated. At shorter electrode spacings, Jordan's sounding-3 curve shows higher apparent resistivities than our sounding-13 curve. A plot comparing Jordan's sounding 3 to our sounding 13 is not shown here.

BIPOLE-DIPOLE TOTAL FIELD MAPS

Jordan's direct current, bipole-dipole total field data are based on two different current-bipole locations and orientations: one east-west bipole and one north-south bipole. Figure 4, shows two apparent resistivity maps that we compiled and recontoured using Jordan's bipole-dipole data. The location of the current bipoles and of the measuring-dipole stations, and associated apparent resistivity values were taken from Jordan's Figures 7 and 10, respectively.

Fortunately, Jordan included the measuring-dipole station location and the associated apparent resistivity values in his Figures 7 and 10, because the tabulated data (in appendix II of his thesis) could not be used for regenerating the total-field apparent resistivity maps. Jordan tabulated the distances R1 and R2 from the measuring dipole station to each of the current-bipole electrodes and the value of the angle between R1 and R2. This information is sufficient to calculate the value of the geometric factor to compute an apparent resistivity; but without specifying the quadrant in which a station is located, it is impossible to determine uniquely the location of a station on the map. Thus although there is data in Jordan's tabulation for a few additional stations (which he did not plot on his maps) it was impossible for us to include these data on the maps we generated.

Jordan used the contour values of 25, 50, 70, and 200 ohm-m for contouring his maps. These values are neither linearly nor logarithmically equally spaced. In so doing, interesting and potentially important apparent resistivity anomalies were missed in Jordan's Figure 7 (with the east-west current-bipole orientation).

Figure 4 (a and b) shows the results of recontouring the apparent resistivity data given in Jordan's Figures 7 and 10, respectively. The maps in Figure 4 (a and b) were generated using the program Kolor-Map & Section (Zohdy, 1993) and are contoured at the logarithmically nearly-equal interval of six contours per decade. The contour values we used in the computer program are: 4.5, 7, 10, 15, 20, 30, 45, 70, 100, 150, 200, 300, and 450 ohm-m.

Bipole-dipole total-field apparent resistivity maps have different forms which depend on the subsurface geoelectric structures and also on the orientation of the current bipole; this is valid even for horizontally layered media (Zohdy, 1978). When examining such maps one should remember that: a) the closer a station is to one of the current electrodes, the lesser the depth of exploration and conversely, b) stations located along the polar axis of the current bipole are influenced by the effect of layers at shallower depths than

stations located at comparable distances along the equatorial axis of the current bipole, and c) lateral variations in resistivity affect measurements made along the polar axis of the bipole much more, and in a different manner, than those measured along the equatorial axis. Therefore, it is not surprising that the two maps shown in Figure 4-a and 4-b are different.

We found that the map in Figure 4-a is more useful, than the map in Figure 4-b, in depicting some of the features that are of interest in this survey. The map in Figure 4-b, as compared to the map in Figure 4-a, is based on fewer stations, covers a smaller area, and seems to be mostly affected by the proximity of resistive materials on the eastern part of the survey area (the Sangre de Cristo Mountains).

Figure 4-a shows that the area nearest Mineral Hot Springs is characterized by two stations of moderately lower apparent resistivities. The small embayment in the apparent-resistivity contours is outlined in Figure 4-a by a circle. The contours in that encircled area are 70 and 100 ohm-m which are moderately lower than the apparent resistivity contours nearby.

In geothermal exploration one usually looks for targets of low resistivity that seem to be governed by the presence of faults and other structures. In general, however, low resistivity alone is not necessarily indicative of a heat source and a low resistivity body associated with the presence of a fault is not necessarily indicative of the presence of an active heat source; because clays and high concentrations of dissolved solids, by themselves, cause low resistivities. However, *in a geothermal area*, heat can alter rock materials into clays and other conductive minerals and generally increases the amount of dissolved solids in the hot or warm waters, thus low resistivity bodies occurring near faults are still a good indication for the location of a potential heat source in a given geothermal area.

The Mud Volcano area in Yellowstone National Park is a vapor-dominated geothermal system which is electrically characterized by a cap rock of low interpreted resistivity (2 to 7 ohm-m) underlain by a body of moderate interpreted resistivity (75 to 135 ohm-m) which represents the vapor dominated geothermal reservoir (Zohdy and others, 1973). In the Mineral Hot Springs area, we do not observe a low resistivity cap rock but we do detect the presence of a moderately-low resistivity structure (45 to 70 ohm-m) associated with the presence of inferred faults at large depths beneath Mineral Hot Springs. The waters at the Mud Volcano are rich in sulfates and low in chlorides, and the waters at Mineral Hot Springs are rich in bicarbonates and low

in chlorides. The presence of a deep vapor-dominated geothermal system in the Mineral Hot Springs area is not very likely.

Figure 4-a shows a second low resistivity embayment on the total-field apparent resistivity map at a distance of about 4 to 5 kilometers north of the A current electrode of the bipole A-B, and at less than one kilometer south of Villa Grove. The apparent-resistivity low is defined by three total-field stations. As mentioned earlier, the location of this apparent-resistivity low is in very good agreement with the location of the low-resistivity body detected by a cusp at the 16,000 ft (4.8 km) current-electrode spacing on sounding 1. The total-field apparent-resistivity data indicates that two east-west faults probably exist in that area. The two faults are separated by a distance of about 1.5 to 2 km and they enclose a relatively low-resistivity material between them (a graben structure ?). In addition, a geologically-inferred fault is located in this area (Knepper, 1974). Unfortunately, we did not make a sounding at that location. The lack of well developed cusps on soundings 8, 9 and 10, north of sounding 1 indicates that this is a relatively deep structure, covered by a relatively thick overburden, and can be detected laterally, by the formation of a cusp, only on sounding curves whose centers are located at large distances from the structure.

Figure 4-a shows two apparent resistivity gradients striking approximately north-south. One gradient is located between the electrodes A and B of the current bipole, and the other is located near the eastern edge of the map. Most likely, these two gradients represent the presence of north-south trending faults. An inferred north-south trending fault that passes near Mineral Hot Springs is shown on some geologic maps (Barrett and Pearl, 1978; Scott and others, 1978), and several northwest-southeast faults forming scarps in the alluvium near the foot of the Sangre de Cristo mountains are shown on other geologic maps (Knepper, 1974; Scott and others, 1978).

INTERPRETED-RESISTIVITY CROSS SECTIONS

Three interpreted-resistivity cross sections were prepared based on the automatic interpretation of the sounding curves. Two are north-south cross sections and one is an east-west cross section. The cross sections were generated using the Kolor-Map & Section program (Zohdy, 1993) and were edited and annotated using the commercial program Deluxe Paint III (Silva, 1989). The step-function layering model, of each sounding, resulting from the automatic interpretation program (Zohdy and Bisdorf, 1989) is sampled in the Kolor-Map &

Section program at the logarithmic center of each horizontal and vertical line. These sampled interpreted-resistivity values are used to generate the cross section and are shown as black points beneath each sounding station (triangles). The plotting of these points (which may be hard to see on the printed copy of the cross section) is a good reminder of the depth of exploration of each sounding when the cross section is displayed on the computer monitor. White areas (with question marks) beneath some soundings on the cross sections indicate the limited depth of exploration beneath these soundings. However, not all areas beneath shallow soundings are whitened when it is reasonable to interpolate the data between two adjacent deep soundings.

The three interpreted-resistivity cross sections are shown in figures 5, 6, and 7. Each figure is composed of two parts: the upper part shows the top portion of the cross section, vertically exaggerated five times (to show the near surface formations in more detail), whereas the lower part of the figure shows the complete cross section without vertical exaggeration.

On all three cross sections, the depth to the 100 ohm-m contour represents the minimum-interpreted depth to basement whereas the depth to the 450 ohm-m contour represents the maximum-interpreted depth to basement. We consider the depth to the 200 ohm-m contour to be the most reasonable depth estimate to the geoelectric basement. It is possible to interpret the zone of high resistivity contours (100 to 450 ohm-m) as a zone of gradual change from highly weathered basement rocks at the 100 ohm-m contour levels to a much-less weathered basement at the 450 ohm-m contour levels. The exact depth to basement (without additional knowledge from deep wells) is beyond the resolution of electrical methods and is disguised by the various possibilities of equivalent geoelectric models (Zohdy and others, 1974, Zohdy, 1989). The geoelectric basement probably represents either Paleozoic carbonate rocks or Precambrian granitic rocks.

Cross-Section 10-7:

Figure 5 shows the interpreted resistivity cross-section extending from sounding 10 in the north to sounding 7 in the south (see figure 2 for location). The length of this cross section is approximately 9 km. The cross section shows a considerable degree of complexity and clearly indicates the possible presence of several near-vertical faults in the deep subsurface.

The geoelectric layering in the northern part of the cross section (from sounding 10 to sounding 2) is basically

different from the geoelectric layering in the southern part of the cross section (from sounding 2 to sounding 7). The northern part of the cross section appears more like a typical basin whereas the southern part is more complicated with a thick resistive layer dominating the cross section from a depth of about 100 to 600 m. This division in the cross section is supported by the mapped geology and by the total-field maps of Jordan, which all indicate predominantly north-northwest south-southeast trending faults on the west side of the valley, and a few geologically inferred faults that trend nearly east west (Knepper, 1974). We believe that this geoelectric section, in the vicinity of sounding 3 - near Mineral Hot Springs, intersects some of these north-northwest south-southeast inferred faults (Barrett and Pearl, 1978; Scott and others, 1978) at an acute angle, and also intersects the inferred east-west faults (Knepper, 1974) at nearly right angles.

In the northern part of the cross section, there is a top layer of moderately high resistivity (70 to 150 ohm-m), probably composed of coarse sand and gravel, with a thickness of about 100 to 150 meters (about 300 to 450 ft). It is underlain by a low to medium resistivity layer (20 to 70 ohm-m), probably representing sedimentary rocks with greater clay or shale content, and having a thickness of 600 to 700 m (about 1800 to 2200 ft), except beneath sounding 9 where its thickness is even greater and may reach 1200 m (about 3600 ft). The two faults shown in Figure 5 at large depth beneath sounding 9 are questionable.

The southern part of the cross section (from sounding 2 to sounding 7) is characterized by a moderately resistive layer of 100 to 200 ohm-m extending from a depth of about 150 m to about 700 m. It is unlikely that this layer, with a thickness of 500 to 600 m (1500 to 1800 ft), is composed of sand and gravel. Its thickness and resistivity are more indicative of a fractured limestone or of a highly weathered granitic layer. It may also be a layer of fine sediments but with a cemented matrix which was deposited by geothermal fluids. Without deep drill-hole information we can only speculate as to the nature and type of rocks based on their interpreted resistivity and geometry.

The most significant features in this southern part of the cross section are the presence of several prominent inferred faults and the presence of materials with moderately-low interpreted-resistivity (less than 45 ohm-m to 70 ohm-m) in the depth range from about 1000 m to 2200 m beneath sounding 3 near the Mineral Hot Springs area. Thus there are three pieces of information that indicate that the Mineral Hot Springs area is underlain at great depths by a low resistivity body: a) the interpretation of sounding 3, b) the formation

of cusps at the proper current-electrode spacings on soundings 1, 2, 5, 6, and 7, and c) the formation of an embayment of low resistivity in the total-field apparent resistivity map shown in Figure 4-a. All these indications are manifested on the measured data in an almost subtle manner, but collectively they distinctly support one another. It is interesting to note that the near surface materials beneath sounding 3 are not particularly conductive and that shallow electrical exploration in the study area would not have yielded the information presented here.

A significant inferred fault is shown south of sounding 5. The deepening of the basement in this area is also supported by the formation of a cusp at the electrode spacing of 16,000 ft on sounding 1. The presence of a second inferred fault south of sounding 6 is less certain.

Cross-Section 28-26:

Figure 6 shows the interpreted resistivity cross-section extending from sounding 28 in the west to sounding 26 in the east (see figure 2 for location). The length of this cross section is approximately 11.5 km.

In the western part of the cross section, the interpretation of soundings 28, 29, 27 and 30 indicates that at most locations, a resistive material with interpreted resistivities in the range of 150 to 300 ohm-m exists at shallow depth and extends to depths of at least 500 m. These resistivities can be indicative of fractured limestone or weathered granitic rocks. The geologic maps (Knepper, 1974, Scott and others, 1978) show Precambrian granitic rocks in the area to the west and south of sounding 28. These granitic rocks are thrusted over Paleozoic carbonates which outcrop to the northwest of sounding 28. In the area of soundings 28, 27, and 29, the alluvium conceals the underlying rocks.

Sounding 30 on the cross section was expanded east-west. To the east of sounding 30, there is strong evidence for the presence of a fault as indicated by the abrupt change in interpreted resistivity beneath sounding 30 and sounding 1. In fact, the fault is probably at a distance of about 70 m east of sounding 30 as evidenced by the formation of a downward-pointing cusp at that current-electrode spacing (see appendix). Furthermore, the location of this electrically inferred fault is in very good agreement with the location of a geologically inferred north-northwest south-southeast fault (Barrett and Pearl, 1978, Scott and others, 1978).

The interpretation of sounding 1 on cross section 28-26, shows a much greater depth to the geoelectric basement, not

only with respect to soundings 30, 27, 29 and 28 to the west, but also with respect to soundings 11, 12, and 13 to the east. There are at least three possible explanations for this: a) sounding 1 is located in a graben-like structure with another fault to the east of it (as shown on the cross section), b) inasmuch as sounding 1 was expanded in a north-south direction, whereas all the soundings to the east of it were expanded in an east-west direction, it is possible that sounding 1 was affected, at large current electrode spacings, by the presence of conductive materials to the east of it; the same conductive materials will not affect soundings expanded in the east-west direction to the same degree (Alpin and others, 1966; Zohdy, 1970), and c) as discussed earlier, sounding 1 is definitely influenced by strong lateral inhomogeneities at near right angles to the direction of expansion resulting in the formation of two cusps, and a different smoothing of the sounding curve could result into a smaller interpreted-depth to basement.

The part of the cross section between soundings 11 and 14 shows a typical basin with low resistivity materials in the middle of the basin. These low resistivity materials probably represent an increase in silts and clays. It is unlikely that these low resistivities indicate a conductive body of geothermal potential. Had the geologic setting been in a basin filled with volcanic materials, then these low resistivity materials would have been of much more geothermal significance. There are two inferred faults in this part of the section. The inferred fault between sounding 11 and 12 is uncertain, but the inferred fault between soundings 13 and 14 is very likely. Here all soundings are expanded in an east-west direction.

To the east of sounding 15 the interpreted resistivity at depths ranging from 500 to 1500 m increases steadily and it is very likely that there is at least one fault between soundings 15 and 24. There is a bend in the section at sounding 24, and soundings 25 and 26 were made on a road that trends northeast. The high resistivity of the alluvial fans is clearly shown on the vertically exaggerated part of the cross section beneath soundings 15, 24, 25, and 26. It is difficult to ascertain whether the high resistivity materials (at a depth of about 500 m) beneath soundings 24 and 25 represent basement rocks or not. If they do then they probably represent the geologically mapped Paleozoic carbonates which outcrop to the east (Knepper, 1974; Scott and others, 1978).

Cross Section 23-20:

Figure 7 shows the interpreted resistivity cross-section extending from sounding 23 in the north to sounding 20 in the south (see figure 2 for location). The length of this cross section is approximately 9.8 km. The cross section is relatively simple except for the rise of the basement surface beneath sounding 13 and the possible existance of a wide graben between soundings 13 and sounding 19 where a depression in the basement surface is detected beneath soundings 16, 17, and 18. In this cross section all the soundings were expanded north south except for sounding 13 which was expanded east west. It is possible to force the automatic interpretation of sounding 13 (using some of the program options) to deepen the basement surface to the same depth as beneath soundings 23, 22, and 21 which are located north of sounding 13. The results of this exercise in sounding interpretation are not presented here, and suffice it to say that even if the interpretation of sounding 13 is altered to agree more with soundings 23, 22, and 21, the possibility of a fault to the south of sounding 13 would still exist.

It is quite probable that had we made a sounding near sounding 13 and expanded it in the north-south direction that we would have obtained a sounding curve that would have been in better agreement with the other soundings on the cross section. Such a sounding also may have shown the effect of lateral pseudo anisotropy often manifested on crossed soundings.

BLOCK DIAGRAM

Figure 8 shows a three dimensional block diagram constructed from segments of the three interpreted-resistivity cross sections discussed above. The purpose of presenting this block diagram is to help visualize the three dimensional view of the subsurface geoelectrical structure. The location of the viewer is in the south of the survey area and the view is to the north. The block diagram is self explanatory, because all the interpreted-resistivity features already have been described above.

MAP OF INFERRED FAULTS

Figure 9 shows a map of the location and direction of throw of all the geoelectrically and some of the geologically inferred faults. This compilation is primarily based on the quantitative interpretation of the sounding curves (including the detection of cusps on the curves), the construction of interpreted resistivity cross sections, and on the qualitative

analysis of the total-field apparent resistivity map shown in Figure 4-a. Almost all the faults are concealed by a large thickness of alluvium and overburden rocks. The faults are dashed where their continuity is uncertain. The north-south fault west of sounding 1 agrees very well with a geologically inferred fault (Scott and others, 1978), whereas the east-west faults agree in principle with other geologically postulated faults (Knepper, 1974). The map in Figure 9 shows that the Mineral Hot Springs are located above a graben-like structure formed by two deep inferred faults.

CONCLUSIONS

The geoelectrical survey proved capable of delineating the geoelectric structure in the area of Mineral Hot Springs and vicinity at depths reaching 2 to 3 kilometers with a reasonable amount of detail. The careful study of the formation of cusps, which often are ignored and smoothed out in conventional interpretation of sounding curves, proved to be very useful in delineating the location of inferred faults. This information when coupled with the layering interpretation of the sounding curves and with the examination of the bipole-dipole total-field apparent resistivity data, proved to be useful in constructing an electrically consistent concept of the subsurface structure. The Mineral Hot Springs were found to occur above a deeply seated, relatively low resistivity, zone bound by two deep faults.

COMPUTERS AND PERIPHERALS

The sounding interpretations were made on a 386 IBM-compatible computer. The resistivity maps and cross sections were generated in color on an Amiga 3000 computer using the Kolor-Map & Section (Zohdy, 1993). The commercial program Deluxe Paint III (Silva, 1989) was used exclusively on the Amiga for editing and annotating the interpreted-resistivity maps and cross sections, and in constructing the three dimensional block diagram. The maps and cross sections were printed on a Xerox 4020 ink-jet color printer.

The tabulations and log-log plots of the sounding curves shown in the appendix were made as follows. The data files from the automatic interpretation program were used to generate graphics and text files compatible with WordPerfect 5.1, using a program written by the second author in Microsoft QuickBASIC 4.5. The output was printed on an HP LaserJet III printer.

ACKNOWLEDGEMENTS

This work was made with support from the U.S. Department of Energy to the U.S. Geological Survey - National Geothermal Research Program under contract number LAno. DE-AIo101-91CE31020.

REFERENCES

Alpin, L.M., Berdichevskii, M.N., Vedrintsev, G.A., and Zagarmistr, 1966, Dipole methods for measuring earth conductivity [translated by George V. Keller]: Consultant Bureau, New York, 300 p.

Barrett, James K. and Pearl, Richard Howard, 1978, An appraisal of Colorado's Geothermal Resources: Colorado Geol. Survey, Dept. of Natural Resources, Bull. 39, 224 p.

Jordan, J. M., 1974, Geothermal investigations in the San Luis Valley, south-central Colorado: Master of Science thesis, Colorado School of Mines, 89 p.

Knepper, Daniel H., 1974, Tectonic analysis of the Rio Grande rift zone central Colorado: Ph.D. thesis, Colorado School of Mines, 237 p.

Kunetz, Geza, 1966, Principles of direct current resistivity prospecting: Gebruder-Borntraeger, 103 p.

Silva, Daniel, 1989, Deluxe Paint III, Amiga version: Electronic Arts, 1820 Gateway Drive, San Mateo, CA 94403

Scott, Glenn R., Taylor, Richard B., Epis, Rudy C., and Wobus, Reinhard A., 1978, Geologic map of the Pueblo 1^{o} x 2^{o} quadrangle, south-central Colorado.: U.S. Geol. Survey Miscellaneous Investigations Series, Map I-1022.

Zohdy, A.A.R., 1968, The effect of current leakage and electrode spacing errors on resistivity measurements: U.S. Geological Survey Prof. Paper 600D, p. D258-D264.

_____, 1970, Variable azimuth Schlumberger resistivity sounding and profiling near a vertical contact: U.S. Geol. Survey Bulletin 1313-A, 22 p.

_____, 1978, Total field resistivity mapping and sounding over horizontally layered media: Geophysics, v. 3, p 748-766.

_____, 1980, Master curves of Schlumberger soundings over three vertical layers, array expanded at right angles to strike: U.S. Geol. Survey Open-File Report 80-249, 166 p.

_____, 1989, A new method for the automatic interpretation of Schlumberger and Wenner sounding curves: Geophysics, v. 54, p. 245-253.

_____, 1993, Program Kolor-Map & Section - Amiga version 1.0: U.S. Geol. Survey Open-File Report 93-13, 86 p. + Disk.

Zohdy, A.A.R., L.A. Anderson, and L.J.P. Muffler, 1973, Resistivity, self-potential, and induced polarization surveys of a vapor-dominated geothermal system: Geophysics, v. 38, no. 6, p 1130-1144.

Zohdy, A.A.R. and Bisdorf, R.J., 1989, Programs for the automatic processing and interpretation of Schlumberger sounding curves in QuickBASIC 4.0: U.S. Geological Survey Open-File Report 89-137 A&B, 64 p. + 1 Disk.

Zohdy, A.A.R. and Bisdorf, R.J., 1990, Schlumberger soundings near Medicine Lake, California: Geophysics, v. 55, p. 956-964.

Zohdy, A.A.R., Eaton, G.P., and Mabey, D.R., 1974, Application of Surface Geophysics to Ground-Water Investigations: Techniques of Water-Resources investigations of the United States Geological Survey, Book 2, Chapter D1, 116 p.

APPENDIX

On the following pages, the data for each sounding curve includes:

1) A sounding title which is designated by the name of the survey area followed by the sounding number. On the title of the observed and interpreted curves, the suffix C means that the sounding curve was corrected for a non-linear electrode array. On the title of interpreted curves, the suffix S indicates that the sounding curve was smoothed, trimmed, or truncated, prior to interpretation, and the suffix X indicates the sounding curve was extrapolated to smaller or larger electrode spacings.

2) A tabulation of the current-electrode spacings (AB/2) in meters (and in feet) and corresponding apparent resistivities in ohm-meters.

3) A log-log plot of the field-sounding data. Data points made with the same potential-electrode spacing (MN/2) are connected with a solid line to form a continuous segment on the curve. Measurements were made with the potential-electrode spacings fixed at 2, 20, 200, and 600 ft.

4) A tabulation of the automatically interpreted layering; with depths in meters (and in feet) and corresponding interpreted resistivities in ohm-meters.

5) A log-log plot of the output of the automatic interpretation program. Circles represent the shifted-digitized sounding curve. The continuous curve represents the calculated sounding curve. The step-function curve represents the interpreted layering model. Note that the abscissa is used to represent the current-electrode spacing for both the digitized and calculated sounding curves as well as the interpreted depth to the various layers. Similarly, the ordinate is used to represent the digitized and calculated apparent resistivities as well as the interpreted resistivity of the various layers in the step-function model.

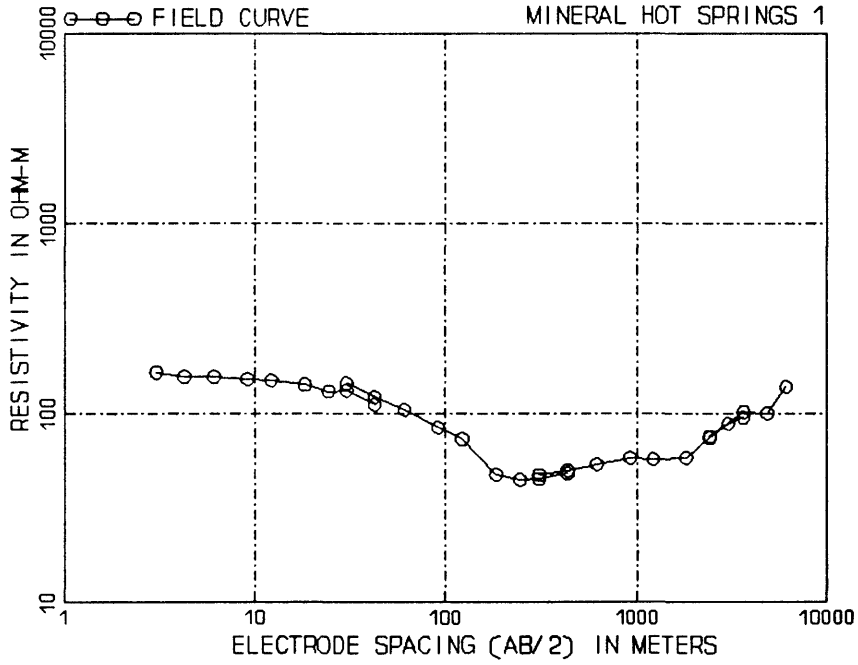

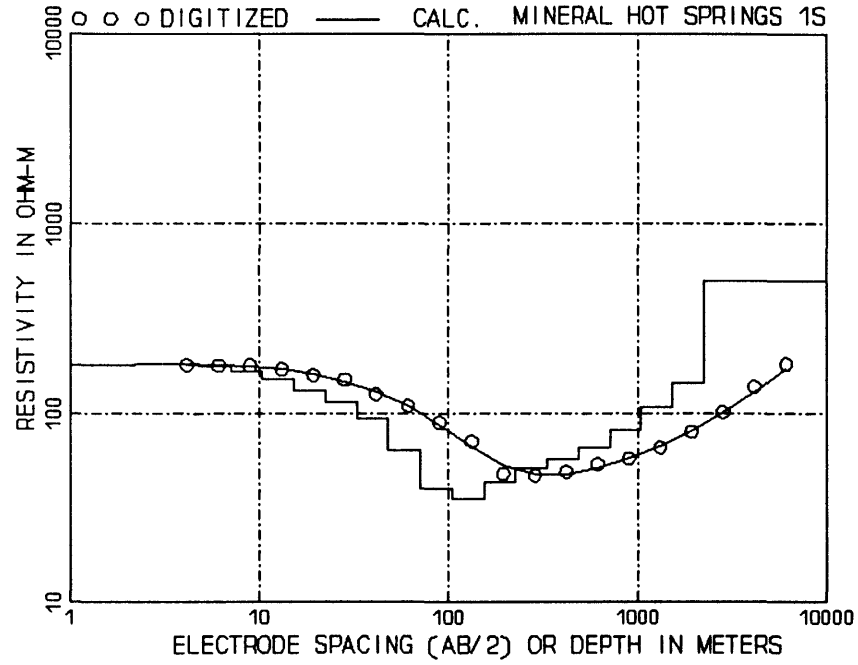

AB/2, m (ft)	App. Res.	AB/2, m (ft)	App. Res.
3.05 (10.00)	165.00	243.84 (800.00)	44.50
4.27 (14.00)	156.00	304.80 (1000.00)	45.00
6.10 (20.00)	156.00	426.72 (1400.00)	48.00
9.14 (30.00)	152.00	304.80 (1000.00)	47.20
12.19 (40.00)	150.00	426.72 (1400.00)	50.00
18.29 (60.00)	142.00	609.60 (2000.00)	54.00
24.38 (80.00)	131.00	914.40 (3000.00)	58.00
30.48 (100.00)	132.00	1219.20 (4000.00)	57.10
42.67 (140.00)	111.00	1828.80 (6000.00)	58.00
30.48 (100.00)	144.00	2438.40 (8000.00)	74.00
42.67 (140.00)	122.00	3048.00 (10000.00)	88.00
60.96 (200.00)	105.00	3657.60 (12000.00)	95.00
91.44 (300.00)	84.00	2438.40 (8000.00)	75.00
121.92 (400.00)	73.00	3657.60 (12000.00)	102.00
182.88 (600.00)	47.50	4876.80 (16000.00)	100.50
		6096.00 (20000.00)	138.00

DEPTH, m (ft)	RESIS.	DEPTH, m (ft)	RESIS.
2.24 (7.36)	180.52	104.10 (341.53)	40.03
3.29 (10.80)	182.49	152.79 (501.29)	35.60
4.83 (15.85)	182.66	224.27 (735.80)	42.91
7.09 (23.27)	177.36	329.18 (1080.00)	51.02
10.41 (34.15)	166.58	483.18 (1585.22)	57.07
15.28 (50.13)	150.63	709.21 (2326.79)	65.30
22.43 (73.58)	131.50	1040.97 (3415.26)	81.13
32.92 (108.00)	114.04	1527.94 (5012.92)	108.03
48.32 (158.52)	93.62	2242.71 (7357.96)	145.87
70.92 (232.68)	63.67	99999.00 (99999.00)	500.00

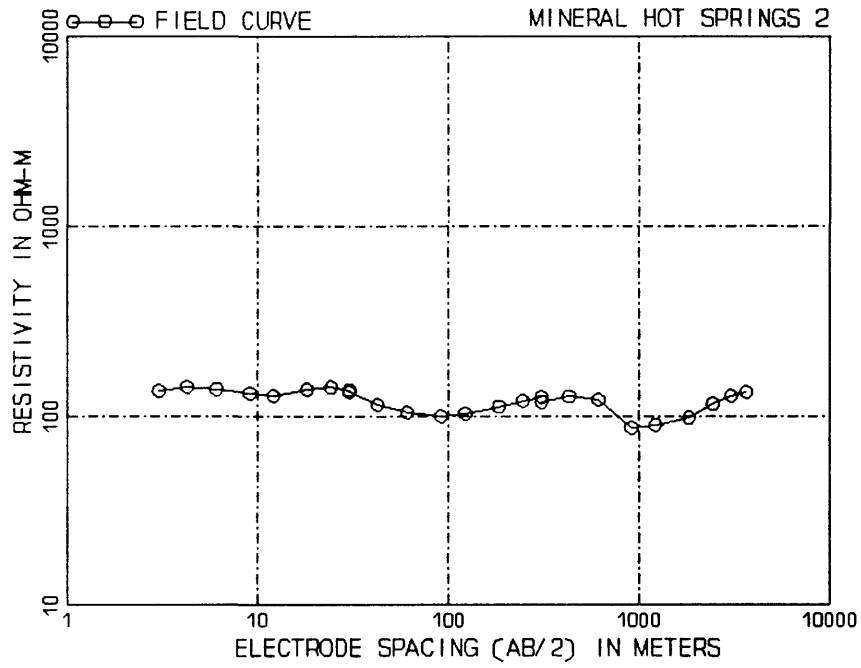

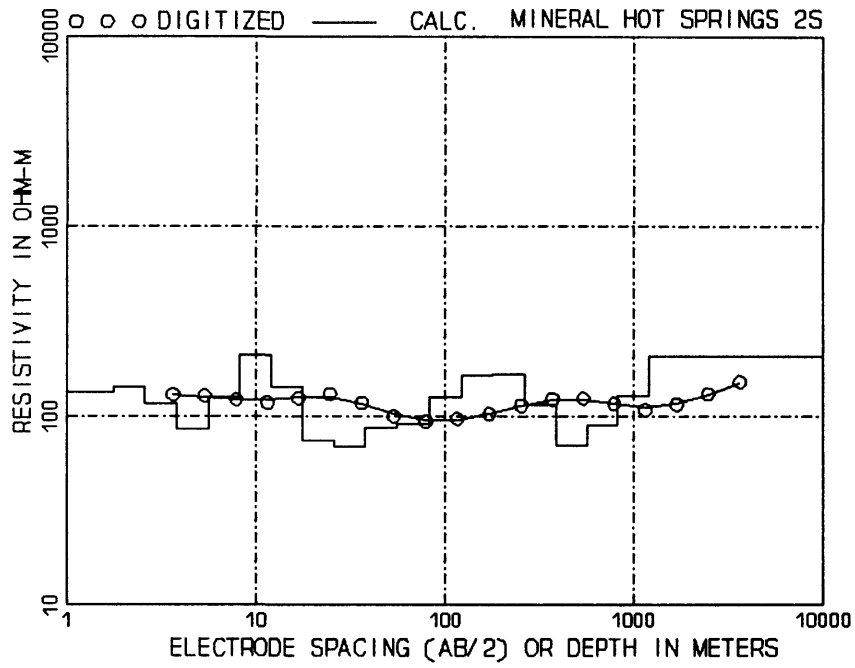

AB/2, m (ft)	App. Res.	AB/2, m (ft)	App. Res.
3.05 (10.00)	136.00	121.92 (400.00)	103.00
4.27 (14.00)	143.00	182.88 (600.00)	112.00
6.10 (20.00)	139.00	243.84 (800.00)	120.00
9.14 (30.00)	132.00	304.80 (1000.00)	126.00
12.19 (40.00)	128.00	304.80 (1000.00)	119.00
18.29 (60.00)	138.00	426.72 (1400.00)	127.00
24.38 (80.00)	142.00	609.60 (2000.00)	122.00
30.48 (100.00)	137.00	914.40 (3000.00)	87.00
30.48 (100.00)	134.00	1219.20 (4000.00)	90.00
42.67 (140.00)	115.00	1828.80 (6000.00)	98.00
60.96 (200.00)	105.00	2438.40 (8000.00)	116.00
91.44 (300.00)	100.00	3048.00 (10000.00)	128.00
		3657.60 (12000.00)	134.00

DEPTH, m (ft)	RESIS.	DEPTH, m (ft)	RESIS.
1.78 (5.83)	133.60	56.21 (184.42)	86.79
2.61 (8.56)	141.54	82.51 (270.70)	90.35
3.83 (12.56)	116.29	121.11 (397.33)	126.31
5.62 (18.44)	84.89	177.76 (583.20)	165.12
8.25 (27.07)	126.73	260.92 (856.02)	167.49
12.11 (39.73)	210.77	382.97 (1256.47)	115.03
17.78 (58.32)	142.17	562.12 (1844.24)	69.40
26.09 (85.60)	74.65	825.09 (2706.98)	89.17
38.30 (125.65)	68.27	1211.06 (3973.30)	126.89
		99999.00 (99999.00)	207.44

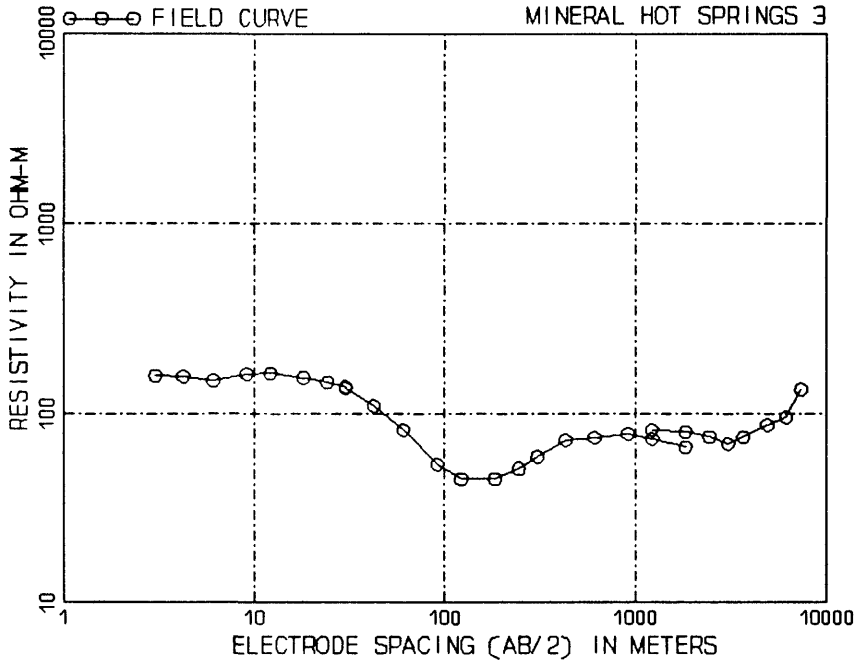

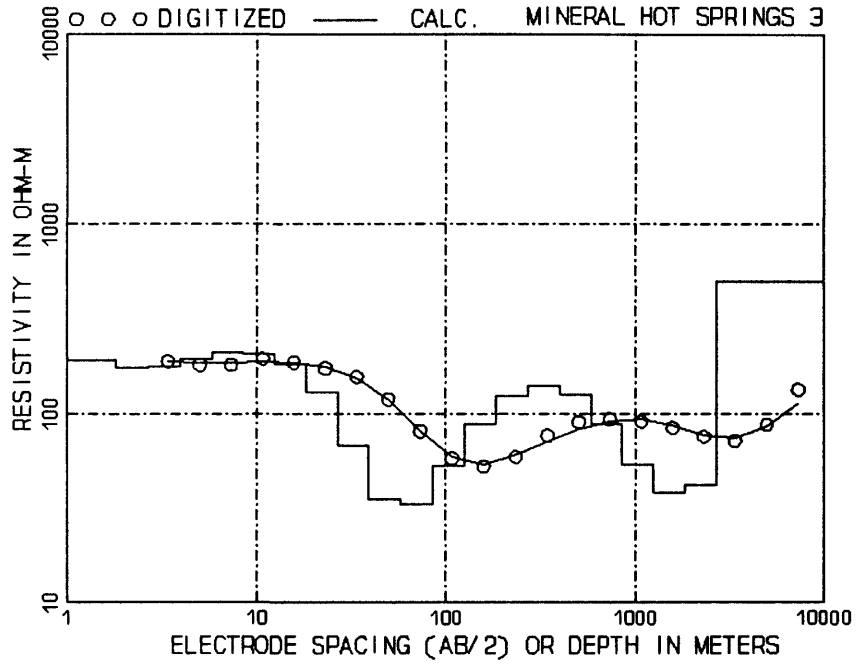

AB/2, m (ft)	App. Res.	AB/2, m (ft)	App. Res.
3.05 (10.00)	158.00	304.80 (1000.00)	59.00
4.27 (14.00)	157.00	304.80 (1000.00)	59.00
6.10 (20.00)	149.00	426.72 (1400.00)	72.00
9.14 (30.00)	162.00	609.60 (2000.00)	74.50
12.19 (40.00)	163.00	914.40 (3000.00)	78.00
18.29 (60.00)	155.00	1219.20 (4000.00)	73.30
24.38 (80.00)	146.00	1828.80 (6000.00)	66.25
30.48 (100.00)	138.00	1219.20 (4000.00)	82.00
30.48 (100.00)	136.00	1828.80 (6000.00)	80.00
42.67 (140.00)	110.00	2438.40 (8000.00)	75.00
60.96 (200.00)	82.00	3048.00 (10000.00)	69.00
91.44 (300.00)	54.00	3657.60 (12000.00)	75.00
121.92 (400.00)	45.00	4876.80 (16000.00)	87.00
182.88 (600.00)	45.00	6096.00 (20000.00)	95.60
243.84 (800.00)	51.00	7315.20 (24000.00)	134.00

DEPTH, m (ft)	RESIS.	DEPTH, m (ft)	RESIS.
1.83 (6.02)	191.27	85.10 (279.21)	33.35
2.69 (8.83)	173.15	124.92 (409.83)	52.76
3.95 (12.96)	176.76	183.35 (601.55)	88.15
5.80 (19.02)	195.88	269.12 (882.95)	124.47
8.51 (27.92)	209.25	395.02 (1296.00)	140.44
12.49 (40.98)	207.09	579.81 (1902.27)	124.96
18.34 (60.15)	183.18	851.05 (2792.15)	88.02
26.91 (88.30)	128.96	1249.17 (4098.31)	53.57
39.50 (129.60)	67.84	1833.52 (6015.50)	38.17
57.98 (190.23)	35.57	2691.25 (8829.55)	41.64
		99999.00 (99999.00)	500.00

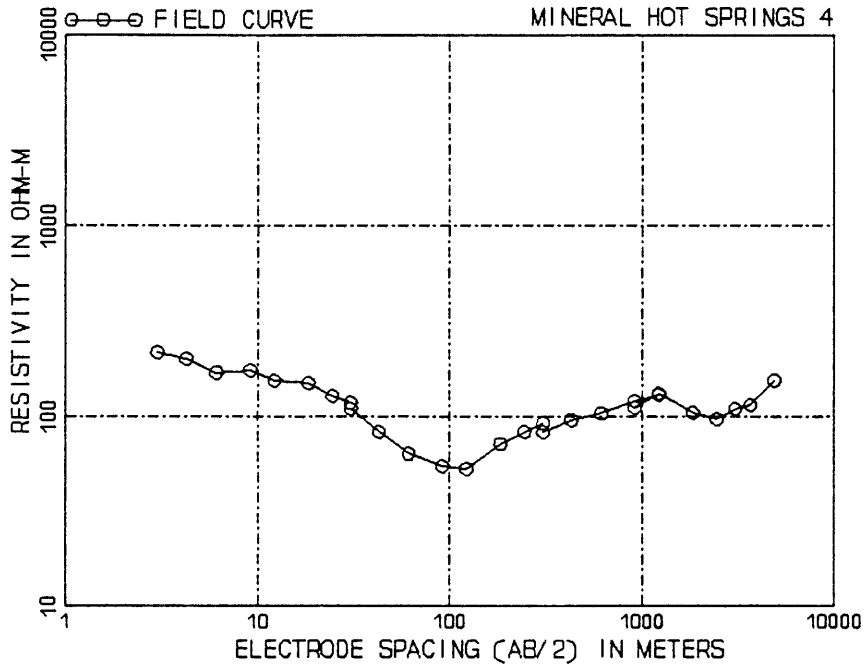

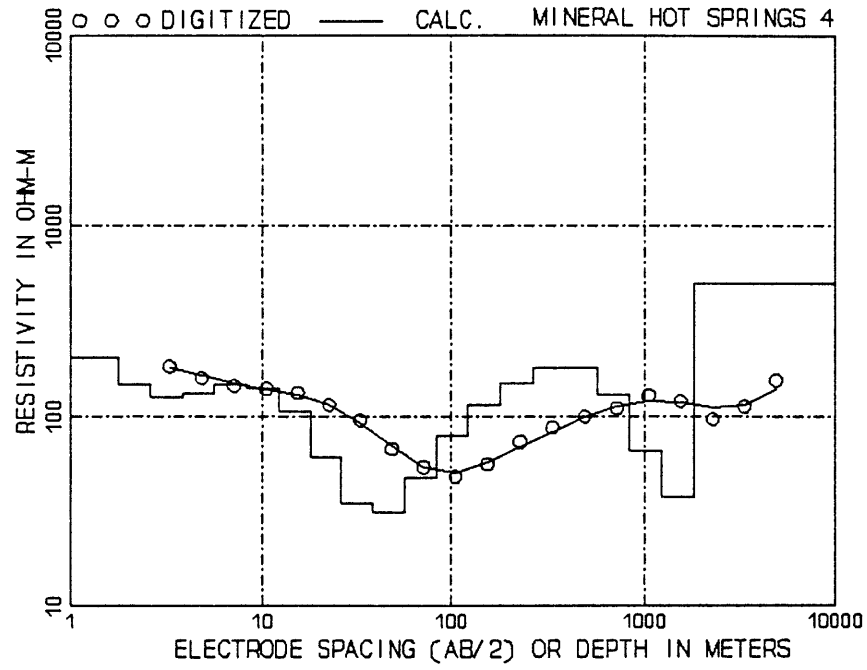

AB/2, m (ft)	App. Res.	AB/2, m (ft)	App. Res.
3.05 (10.00)	217.00	243.84 (800.00)	83.00
4.27 (14.00)	200.00	304.80 (1000.00)	92.00
6.10 (20.00)	170.00	304.80 (1000.00)	83.00
9.14 (30.00)	175.00	426.72 (1400.00)	96.00
12.19 (40.00)	154.00	609.60 (2000.00)	104.00
18.29 (60.00)	150.00	914.40 (3000.00)	120.00
24.38 (80.00)	128.00	1219.20 (4000.00)	130.00
30.48 (100.00)	118.00	914.40 (3000.00)	111.50
30.48 (100.00)	110.00	1219.20 (4000.00)	132.00
42.67 (140.00)	83.00	1828.80 (6000.00)	105.00
60.96 (200.00)	63.50	2438.40 (8000.00)	97.00
91.44 (300.00)	54.50	3048.00 (10000.00)	110.00
121.92 (400.00)	53.00	3657.60 (12000.00)	115.00
182.88 (600.00)	71.50	4876.80 (16000.00)	155.00

DEPTH, m (ft)	RESIS.	DEPTH, m (ft)	RESIS.
1.79 (5.89)	203.15	83.28 (273.22)	47.55
2.63 (8.64)	147.99	122.23 (401.03)	78.84
3.87 (12.68)	125.04	179.42 (588.64)	115.31
5.67 (18.61)	131.97	263.35 (864.00)	150.40
8.33 (27.32)	146.04	386.54 (1268.18)	179.33
12.22 (40.10)	140.39	567.36 (1861.43)	180.33
17.94 (58.86)	105.76	832.78 (2732.21)	129.14
26.33 (86.40)	61.25	1222.35 (4010.33)	65.32
38.65 (126.82)	34.78	1794.16 (5886.36)	37.51
56.74 (186.14)	31.41	99999.00 (99999.00)	500.00

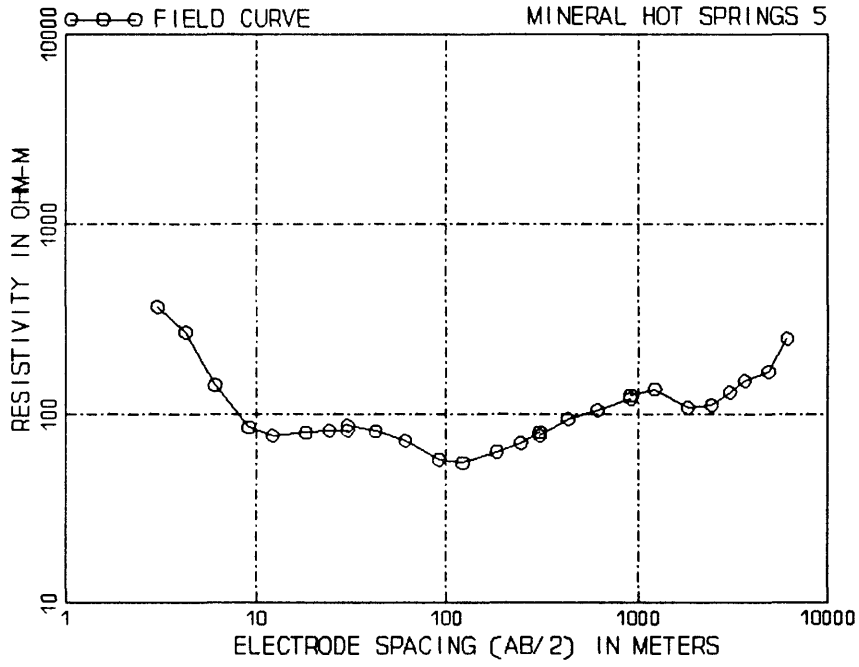

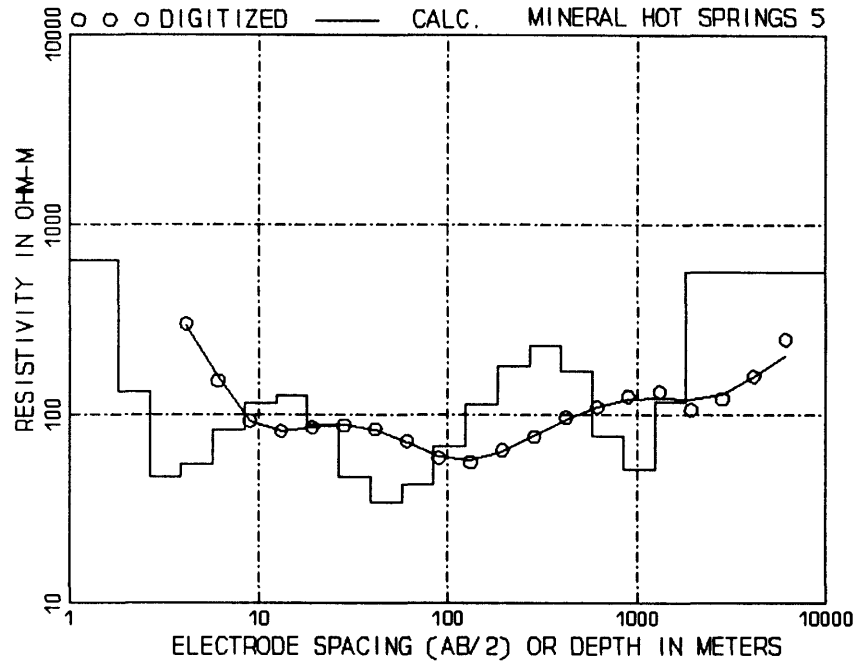

AB/2, m (ft)	App. Res.	AB/2, m (ft)	App. Res.
3.05 (10.00)	367.00	243.84 (800.00)	70.00
4.27 (14.00)	270.00	304.80 (1000.00)	80.00
6.10 (20.00)	142.00	304.80 (1000.00)	77.00
9.14 (30.00)	85.00	426.72 (1400.00)	94.00
12.19 (40.00)	77.00	609.60 (2000.00)	105.00
18.29 (60.00)	80.00	914.40 (3000.00)	120.00
24.38 (80.00)	82.00	914.40 (3000.00)	125.00
30.48 (100.00)	82.00	1219.20 (4000.00)	135.00
30.48 (100.00)	87.00	1828.80 (6000.00)	108.00
42.67 (140.00)	81.00	2438.40 (8000.00)	111.00
60.96 (200.00)	72.00	3048.00 (10000.00)	130.00
91.44 (300.00)	57.50	3657.60 (12000.00)	150.00
121.92 (400.00)	55.00	4876.80 (16000.00)	167.00
182.88 (600.00)	63.00	6096.00 (20000.00)	250.00

DEPTH, m (ft)	RESIS.	DEPTH, m (ft)	RESIS.
1.82 (5.96)	651.82	84.32 (276.64)	42.74
2.67 (8.75)	131.48	123.76 (406.05)	67.44
3.91 (12.84)	47.04	181.66 (595.99)	112.40
5.74 (18.85)	54.68	266.64 (874.80)	181.14
8.43 (27.66)	82.59	391.37 (1284.03)	228.89
12.38 (40.60)	115.54	574.46 (1884.70)	169.32
18.17 (59.60)	125.08	843.19 (2766.36)	76.55
26.66 (87.48)	88.00	1237.63 (4060.46)	51.35
39.14 (128.40)	46.78	1816.59 (5959.94)	116.40
57.45 (188.47)	34.21	99999.00 (99999.00)	562.64

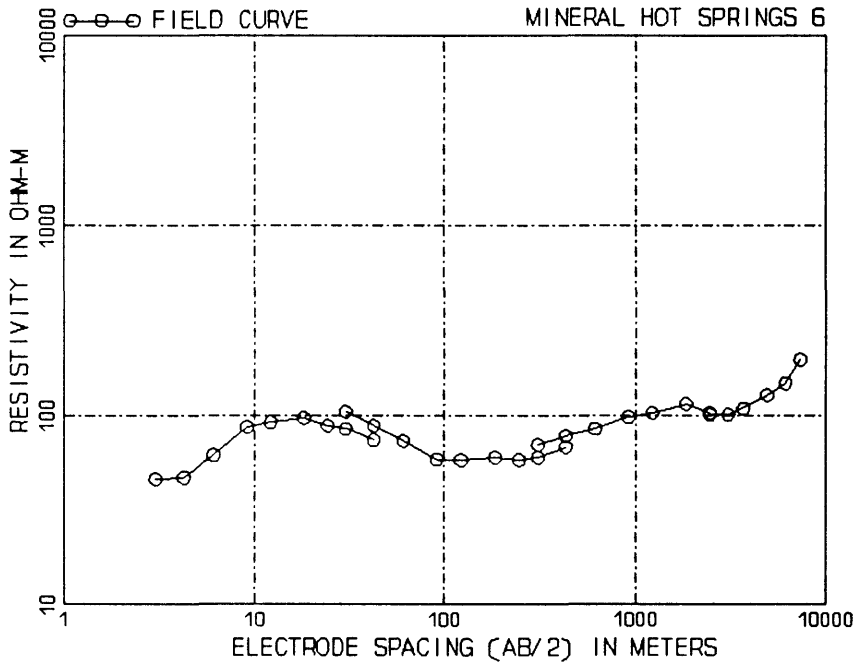

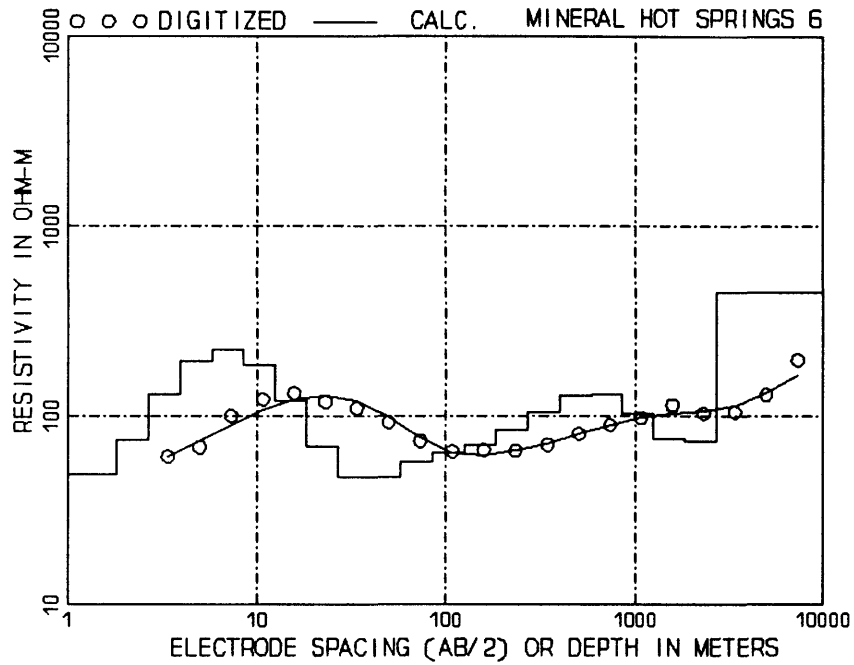

AB/2, m	(ft)	App. Res.	AB/2, m	(ft)	App. Res.
3.05	(10.00)	46.00	243.84	(800.00)	58.00
4.27	(14.00)	47.00	304.80	(1000.00)	60.00
6.10	(20.00)	61.50	426.72	(1400.00)	68.00
9.14	(30.00)	87.00	304.80	(1000.00)	70.00
12.19	(40.00)	92.00	426.72	(1400.00)	78.00
18.29	(60.00)	97.00	609.60	(2000.00)	85.00
24.38	(80.00)	88.00	914.40	(3000.00)	98.00
30.48	(100.00)	85.00	1219.20	(4000.00)	103.00
42.67	(140.00)	74.00	1828.80	(6000.00)	115.00
30.48	(100.00)	105.00	2438.40	(8000.00)	103.00
42.67	(140.00)	88.00	2438.40	(8000.00)	101.00
60.96	(200.00)	73.50	3048.00	(10000.00)	101.00
91.44	(300.00)	58.50	3657.60	(12000.00)	109.00
121.92	(400.00)	58.00	4876.80	(16000.00)	128.00
182.88	(600.00)	60.00	6096.00	(20000.00)	148.00
			7315.20	(24000.00)	197.00

DEPTH, m	(ft)	RESIS.	DEPTH, m	(ft)	RESIS.
1.83	(6.02)	48.65	85.10	(279.21)	57.39
2.69	(8.83)	74.05	124.92	(409.83)	63.45
3.95	(12.96)	128.98	183.35	(601.55)	70.23
5.80	(19.02)	196.07	269.12	(882.95)	84.13
8.51	(27.92)	223.79	395.02	(1296.00)	105.31
12.49	(40.98)	186.67	579.81	(1902.27)	127.84
18.34	(60.15)	120.02	851.05	(2792.15)	130.48
26.91	(88.30)	69.16	1249.17	(4098.31)	102.18
39.50	(129.60)	47.18	1833.52	(6015.50)	75.26
57.98	(190.23)	47.67	2691.25	(8829.55)	73.60
			99999.00	(99999.00)	450.00

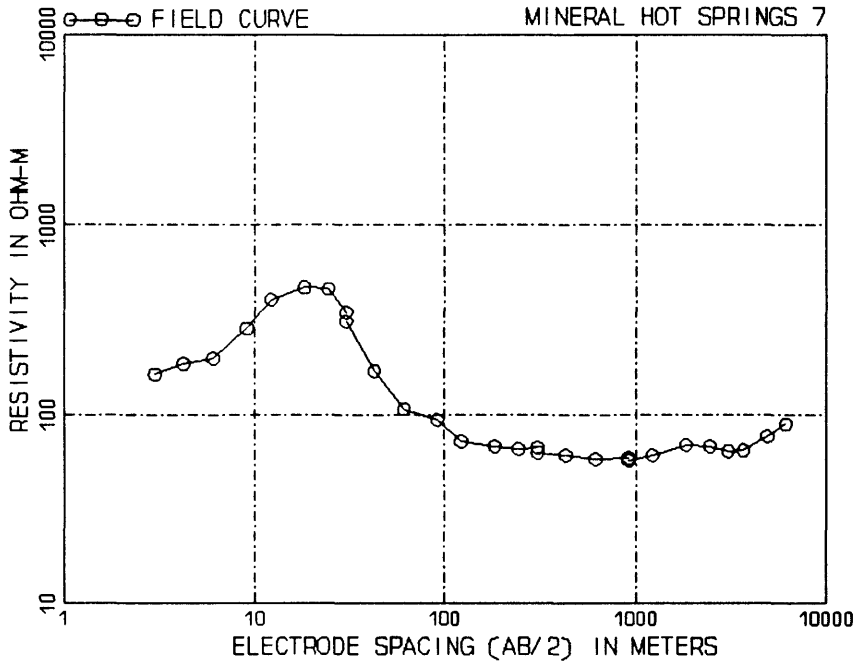

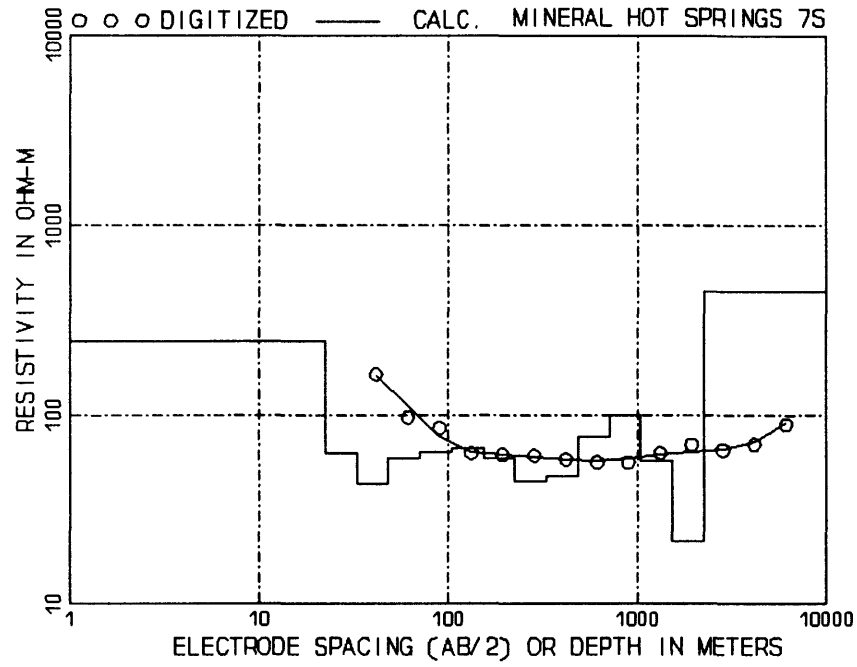

AB/2, m (ft)	App. Res.	AB/2, m (ft)	App. Res.
3.05 (10.00)	163.00	243.84 (800.00)	66.00
4.27 (14.00)	185.00	304.80 (1000.00)	67.00
6.10 (20.00)	197.00	304.80 (1000.00)	63.00
9.14 (30.00)	285.00	426.72 (1400.00)	61.00
12.19 (40.00)	402.00	609.60 (2000.00)	58.00
18.29 (60.00)	468.00	914.40 (3000.00)	59.00
24.38 (80.00)	460.00	914.40 (3000.00)	57.00
30.48 (100.00)	345.00	1219.20 (4000.00)	61.00
30.48 (100.00)	310.00	1828.80 (6000.00)	69.00
42.67 (140.00)	170.00	2438.40 (8000.00)	68.00
60.96 (200.00)	107.00	3048.00 (10000.00)	64.00
91.44 (300.00)	94.00	3657.60 (12000.00)	64.50
121.92 (400.00)	72.00	4876.80 (16000.00)	77.00
182.88 (600.00)	68.00	6096.00 (20000.00)	89.00

DEPTH, m (ft)	RESIS.	DEPTH, m (ft)	RESIS.
22.43 (73.58)	246.17	329.18 (1080.00)	44.57
32.92 (108.00)	62.78	483.18 (1585.22)	47.19
48.32 (158.52)	43.04	709.21 (2326.79)	76.99
70.92 (232.68)	59.37	1040.97 (3415.26)	99.21
104.10 (341.53)	63.84	1527.94 (5012.92)	57.45
152.79 (501.29)	66.91	2242.71 (7357.96)	21.64
224.27 (735.80)	58.71	99999.00 (99999.00)	450.00

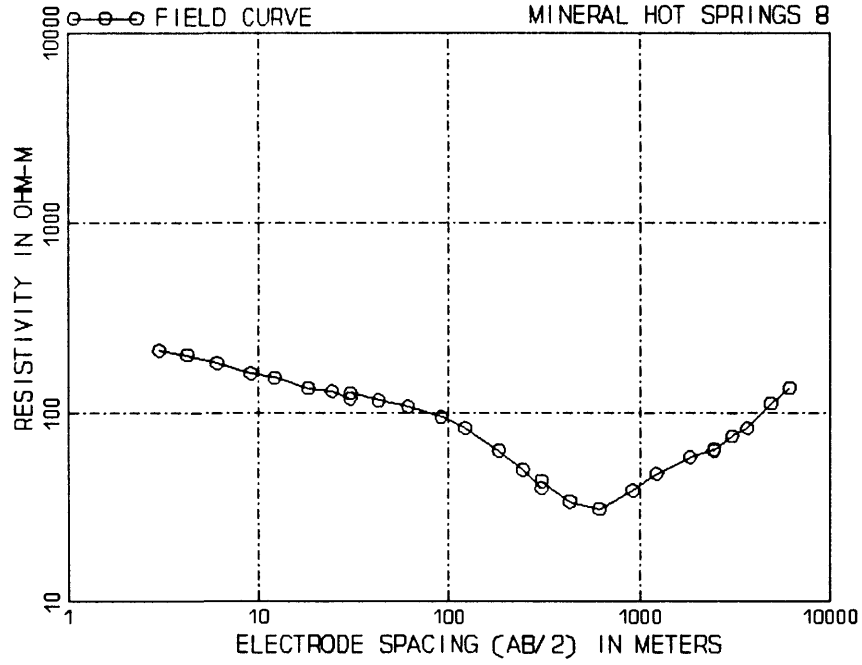

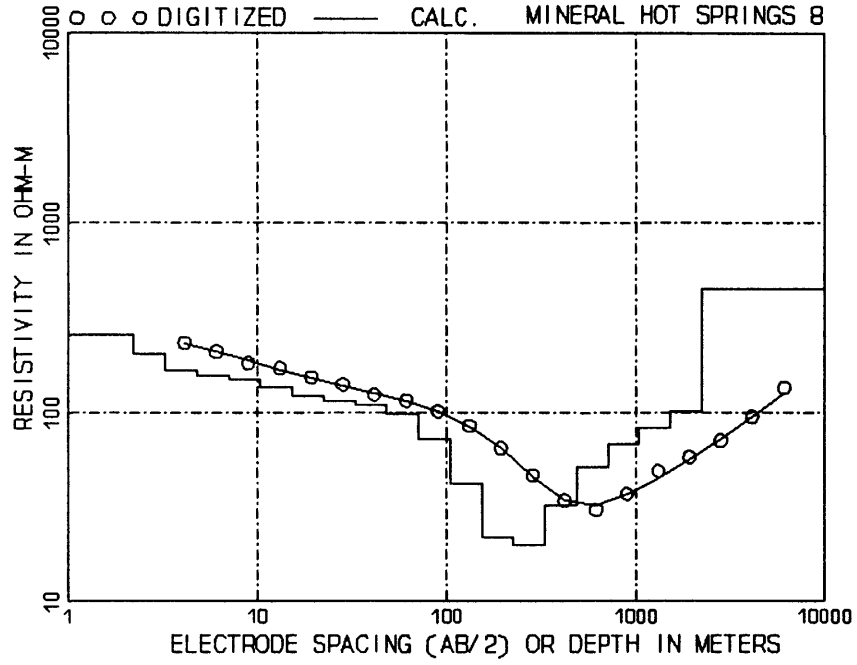

AB/2, m (ft)	App. Res.	AB/2, m (ft)	App. Res.
3.05 (10.00)	213.00	243.84 (800.00)	50.00
4.27 (14.00)	202.00	304.80 (1000.00)	40.00
6.10 (20.00)	183.00	304.80 (1000.00)	43.50
9.14 (30.00)	161.00	426.72 (1400.00)	34.00
12.19 (40.00)	153.00	609.60 (2000.00)	31.00
18.29 (60.00)	135.00	914.40 (3000.00)	38.80
24.38 (80.00)	130.00	1219.20 (4000.00)	47.50
30.48 (100.00)	119.00	1828.80 (6000.00)	58.00
30.48 (100.00)	127.00	2438.40 (8000.00)	64.00
42.67 (140.00)	116.00	2438.40 (8000.00)	63.00
60.96 (200.00)	108.00	3048.00 (10000.00)	75.00
91.44 (300.00)	95.00	3657.60 (12000.00)	83.00
121.92 (400.00)	83.00	4876.80 (16000.00)	112.00
182.88 (600.00)	63.00	6096.00 (20000.00)	135.00

DEPTH, m (ft)	RESIS.	DEPTH, m (ft)	RESIS.
2.24 (7.36)	258.46	104.10 (341.53)	72.58
3.29 (10.80)	203.66	152.79 (501.29)	41.70
4.83 (15.85)	167.73	224.27 (735.80)	21.91
7.09 (23.27)	156.25	329.18 (1080.00)	19.90
10.41 (34.15)	150.30	483.18 (1585.22)	32.10
15.28 (50.13)	136.38	709.21 (2326.79)	51.26
22.43 (73.58)	122.03	1040.97 (3415.26)	68.01
32.92 (108.00)	115.22	1527.94 (5012.92)	82.25
48.32 (158.52)	110.39	2242.71 (7357.96)	101.16
70.92 (232.68)	97.72	99999.00 (99999.00)	450.00

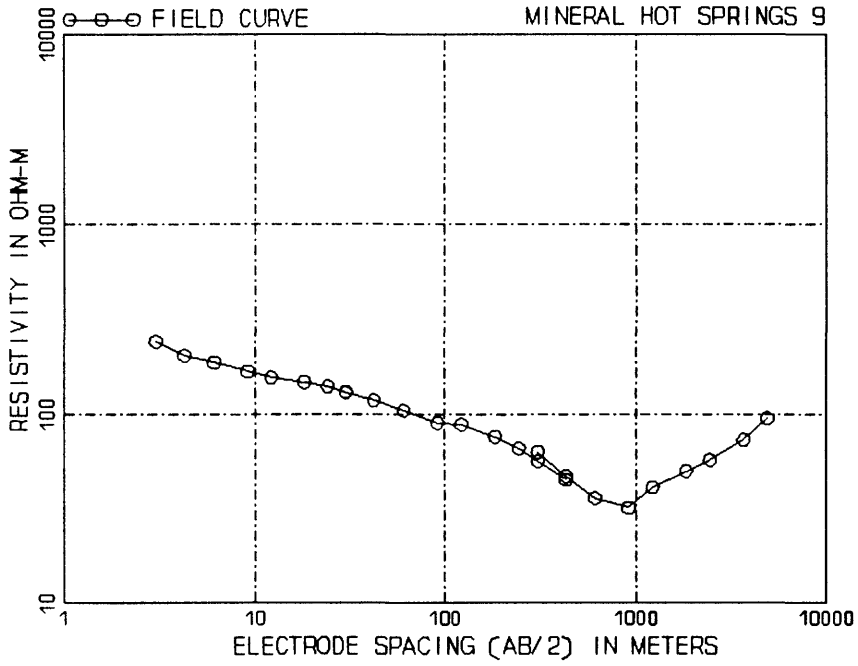

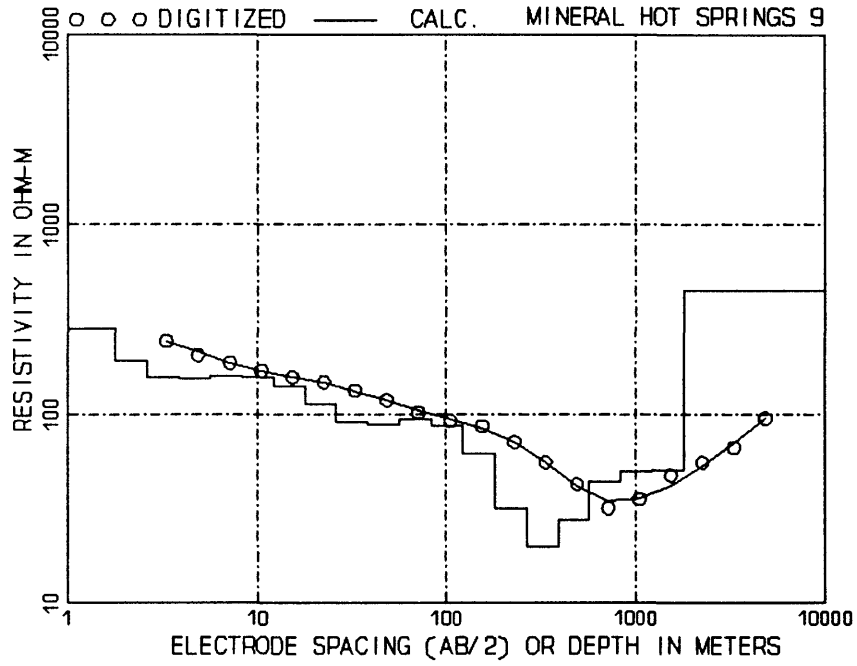

AB/2, m (ft)	App. Res.	AB/2, m (ft)	App. Res.
3.05 (10.00)	242.00	182.88 (600.00)	76.00
4.27 (14.00)	204.00	243.84 (800.00)	66.00
6.10 (20.00)	187.00	304.80 (1000.00)	56.50
9.14 (30.00)	168.00	426.72 (1400.00)	45.00
12.19 (40.00)	156.00	304.80 (1000.00)	63.00
18.29 (60.00)	148.00	426.72 (1400.00)	47.00
24.38 (80.00)	140.00	609.60 (2000.00)	36.00
30.48 (100.00)	130.00	914.40 (3000.00)	32.00
30.48 (100.00)	131.00	1219.20 (4000.00)	41.00
42.67 (140.00)	118.00	1219.20 (4000.00)	41.00
60.96 (200.00)	105.00	1828.80 (6000.00)	50.00
91.44 (300.00)	90.00	2438.40 (8000.00)	57.00
121.92 (400.00)	88.00	3657.60 (12000.00)	73.00
		4876.80 (16000.00)	95.00

DEPTH, m (ft)	RESIS.	DEPTH, m (ft)	RESIS.
1.79 (5.89)	280.08	83.28 (273.22)	93.93
2.63 (8.64)	191.70	122.23 (401.03)	87.51
3.87 (12.68)	155.24	179.42 (588.64)	61.57
5.67 (18.61)	152.83	263.35 (864.00)	31.81
8.33 (27.32)	158.65	386.54 (1268.18)	19.85
12.22 (40.10)	157.35	567.36 (1861.43)	27.52
17.94 (58.86)	140.86	832.78 (2732.21)	43.90
26.33 (86.40)	112.88	1222.35 (4010.33)	49.76
38.65 (126.82)	91.08	1794.16 (5886.36)	50.81
56.74 (186.14)	87.82	99999.00 (99999.00)	450.00

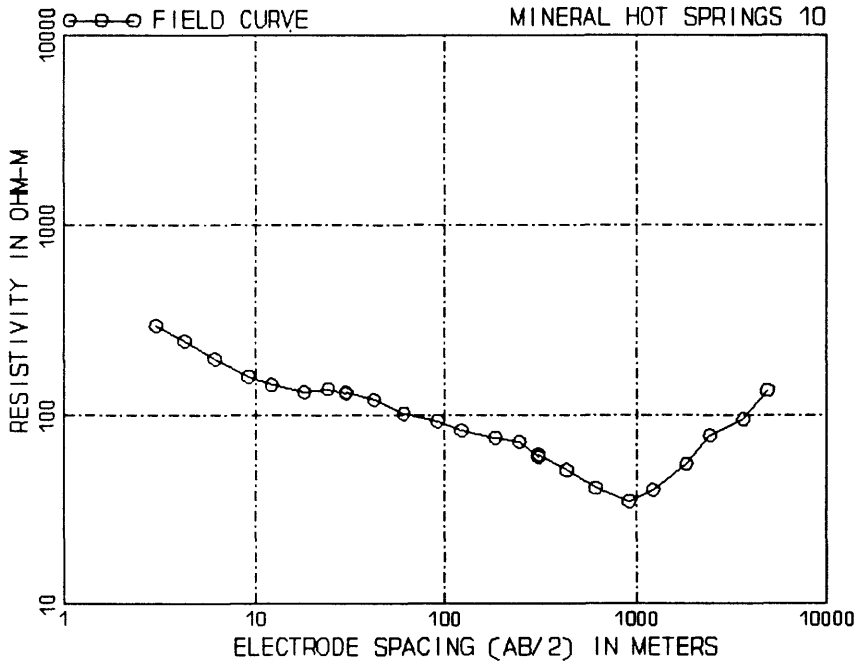

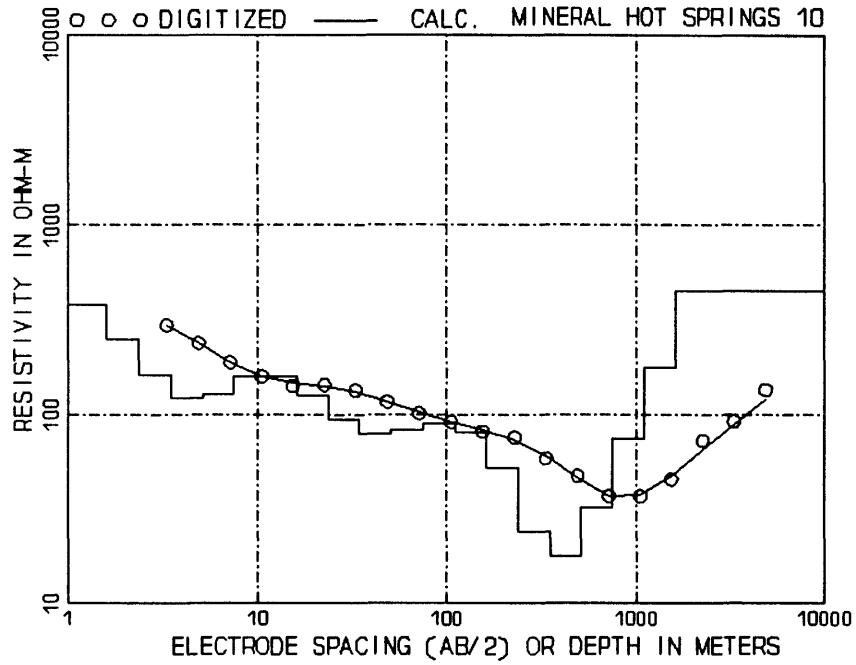

AB/2, m	(ft)	App. Res.	AB/2, m	(ft)	App. Res.
3.05	(10.00)	295.00	182.88	(600.00)	76.00
4.27	(14.00)	245.00	243.84	(800.00)	72.00
6.10	(20.00)	198.00	304.80	(1000.00)	60.00
9.14	(30.00)	160.00	304.80	(1000.00)	62.00
12.19	(40.00)	144.00	426.72	(1400.00)	51.00
18.29	(60.00)	132.00	609.60	(2000.00)	41.00
24.38	(80.00)	137.00	914.40	(3000.00)	35.00
30.48	(100.00)	130.00	914.40	(3000.00)	35.00
30.48	(100.00)	132.00	1219.20	(4000.00)	40.00
42.67	(140.00)	120.00	1828.80	(6000.00)	55.00
60.96	(200.00)	102.00	2438.40	(8000.00)	78.00
91.44	(300.00)	93.00	3657.60	(12000.00)	95.00
121.92	(400.00)	83.00	4876.80	(16000.00)	135.00

DEPTH, m	(ft)	RESIS.	DEPTH, m	(ft)	RESIS.
1.61	(5.30)	378.45	74.95	(245.90)	83.30
2.37	(7.78)	250.87	110.01	(360.93)	89.44
3.48	(11.41)	160.92	161.47	(529.77)	80.68
5.11	(16.75)	121.46	237.01	(777.60)	51.93
7.49	(24.59)	128.73	347.89	(1141.36)	23.90
11.00	(36.09)	158.26	510.63	(1675.29)	17.78
16.15	(52.98)	159.78	749.50	(2458.99)	32.04
23.70	(77.76)	126.09	1100.11	(3609.30)	74.85
34.79	(114.14)	93.27	1614.75	(5297.73)	178.14
51.06	(167.53)	79.69	99999.00	(99999.00)	450.94

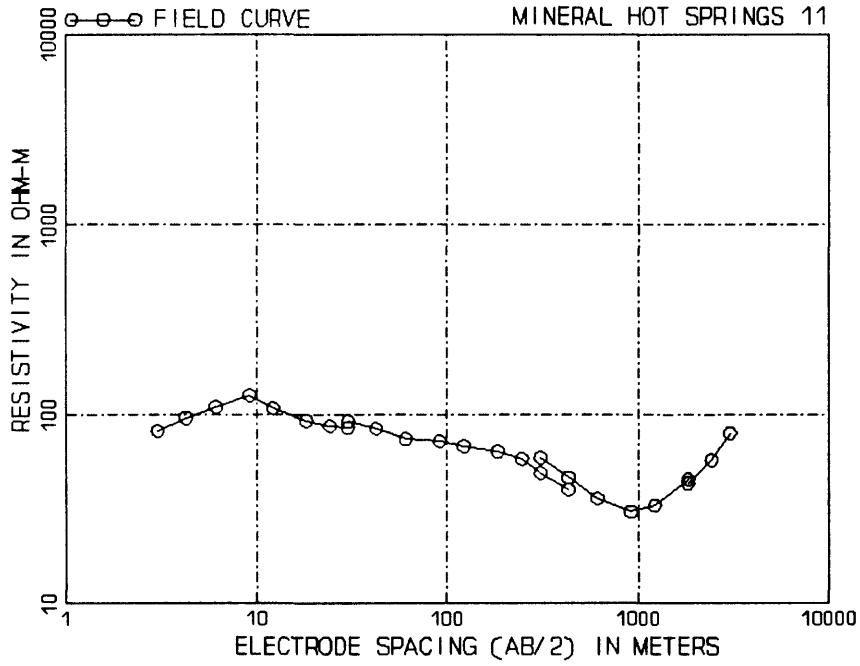

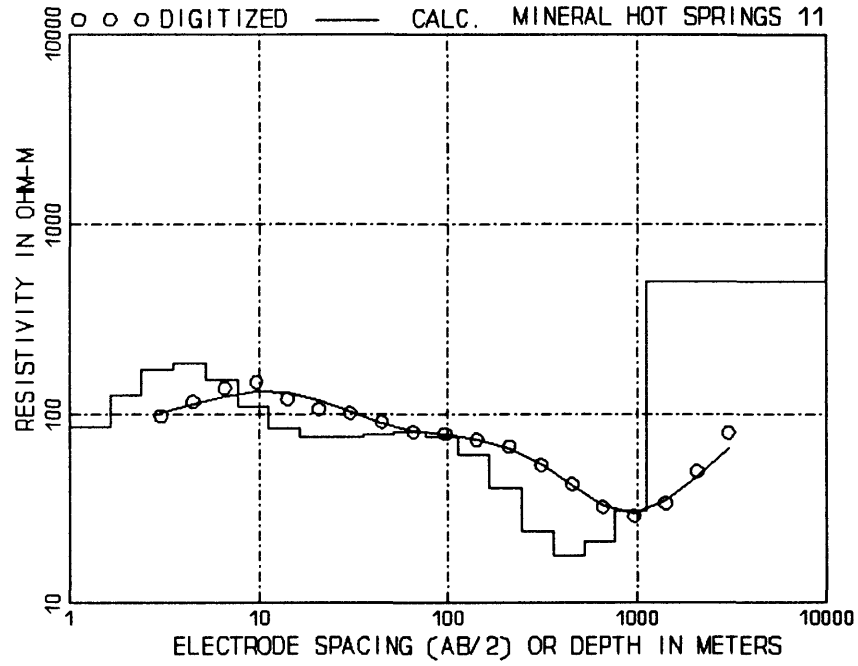

AB/2, m	(ft)	App. Res.	AB/2, m	(ft)	App. Res.
3.05	(10.00)	82.00	182.88	(600.00)	63.50
4.27	(14.00)	96.00	243.84	(800.00)	58.00
6.10	(20.00)	110.00	304.80	(1000.00)	49.00
9.14	(30.00)	126.00	426.72	(1400.00)	40.00
12.19	(40.00)	108.00	304.80	(1000.00)	59.00
18.29	(60.00)	93.00	426.72	(1400.00)	46.50
24.38	(80.00)	87.00	609.60	(2000.00)	36.00
30.48	(100.00)	85.00	914.40	(3000.00)	30.50
30.48	(100.00)	92.00	1219.20	(4000.00)	33.00
42.67	(140.00)	84.00	1828.80	(6000.00)	45.50
60.96	(200.00)	74.00	1828.80	(6000.00)	43.10
91.44	(300.00)	72.00	2438.40	(8000.00)	57.40
121.92	(400.00)	68.00	3048.00	(10000.00)	79.50

DEPTH, m	(ft)	RESIS.	DEPTH, m	(ft)	RESIS.
1.65	(5.40)	86.08	52.05	(170.76)	77.36
2.42	(7.93)	126.44	76.40	(250.65)	79.74
3.55	(11.63)	171.31	112.14	(367.90)	75.61
5.20	(17.08)	184.67	164.59	(540.00)	61.01
7.64	(25.06)	152.30	241.59	(792.61)	40.49
11.21	(36.79)	108.86	354.60	(1163.40)	24.02
16.46	(54.00)	83.82	520.49	(1707.63)	17.97
24.16	(79.26)	75.89	763.97	(2506.46)	21.30
35.46	(116.34)	75.03	1121.35	(3678.98)	30.86
			99999.00	(99999.00)	500.00

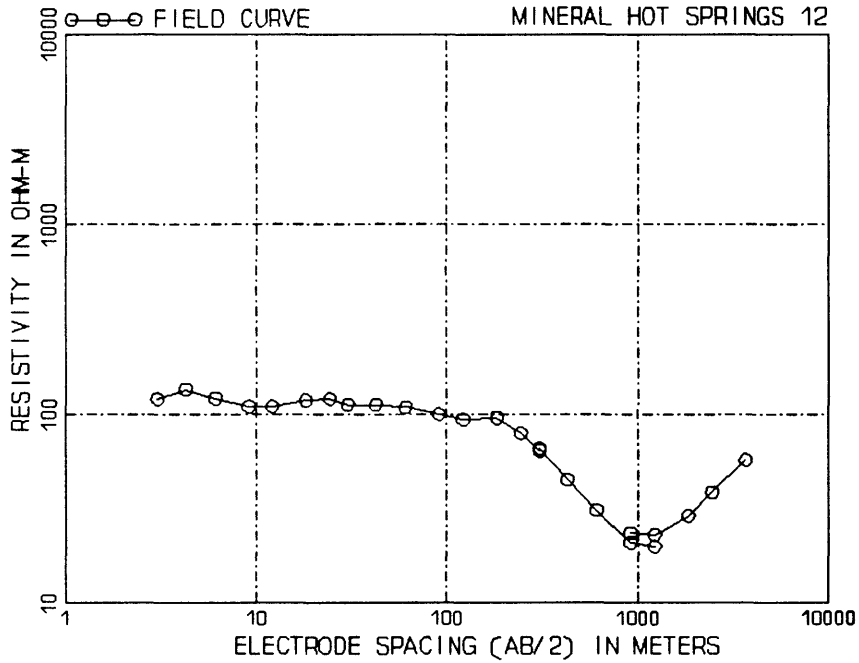

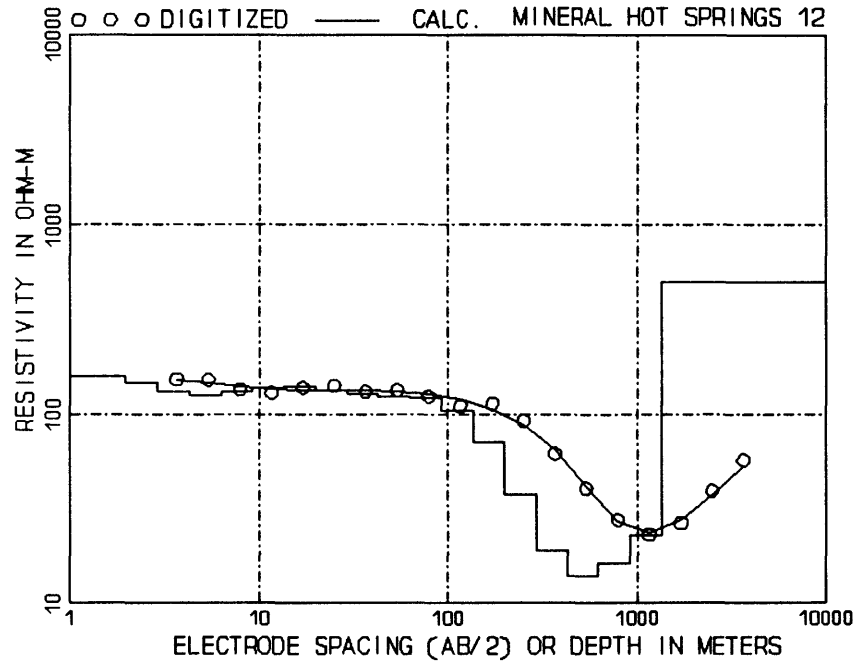

AB/2, m	(ft)	App. Res.	AB/2, m	(ft)	App. Res.
3.05	(10.00)	120.00	182.88	(600.00)	96.00
4.27	(14.00)	135.00	243.84	(800.00)	79.00
6.10	(20.00)	121.00	304.80	(1000.00)	64.00
9.14	(30.00)	110.00	304.80	(1000.00)	66.00
12.19	(40.00)	110.00	426.72	(1400.00)	45.00
18.29	(60.00)	118.00	609.60	(2000.00)	31.00
24.38	(80.00)	120.00	914.40	(3000.00)	21.00
30.48	(100.00)	112.00	1219.20	(4000.00)	20.00
30.48	(100.00)	112.00	914.40	(3000.00)	23.50
42.67	(140.00)	112.00	1219.20	(4000.00)	23.00
60.96	(200.00)	109.00	1828.80	(6000.00)	29.00
91.44	(300.00)	100.00	2438.40	(8000.00)	38.60
121.92	(400.00)	94.00	3657.60	(12000.00)	57.00

DEPTH, m	(ft)	RESIS.	DEPTH, m	(ft)	RESIS.
1.98	(6.48)	159.36	62.46	(204.92)	123.46
2.90	(9.51)	146.82	91.68	(300.77)	121.34
4.26	(13.96)	131.42	134.56	(441.48)	104.91
6.25	(20.49)	125.36	197.51	(648.00)	70.61
9.17	(30.08)	131.44	289.91	(951.13)	37.35
13.46	(44.15)	139.15	425.52	(1396.07)	19.09
19.75	(64.80)	139.87	624.58	(2049.16)	13.93
28.99	(95.11)	134.32	916.76	(3007.75)	16.26
42.55	(139.61)	126.88	1345.62	(4414.77)	23.07
			99999.00	(99999.00)	500.00

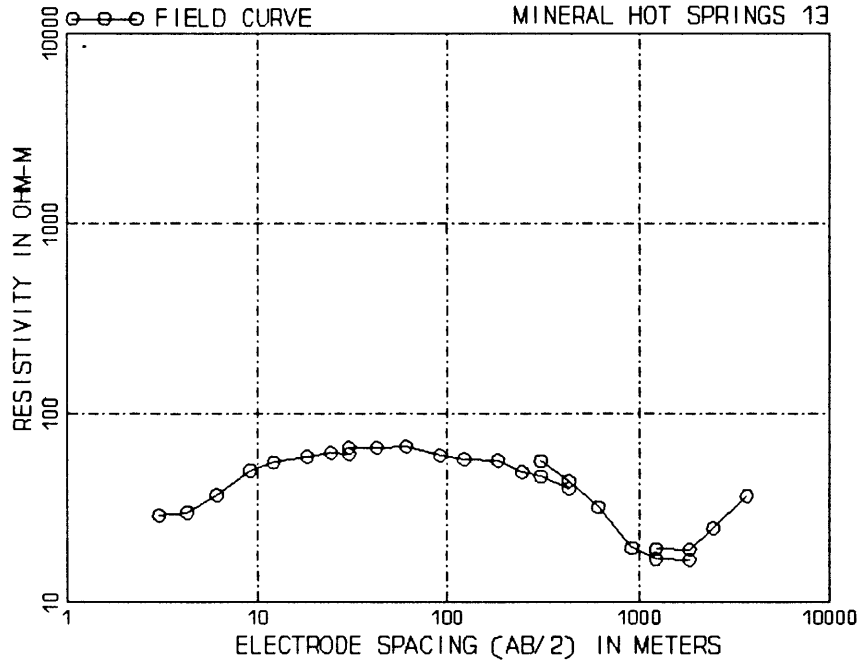

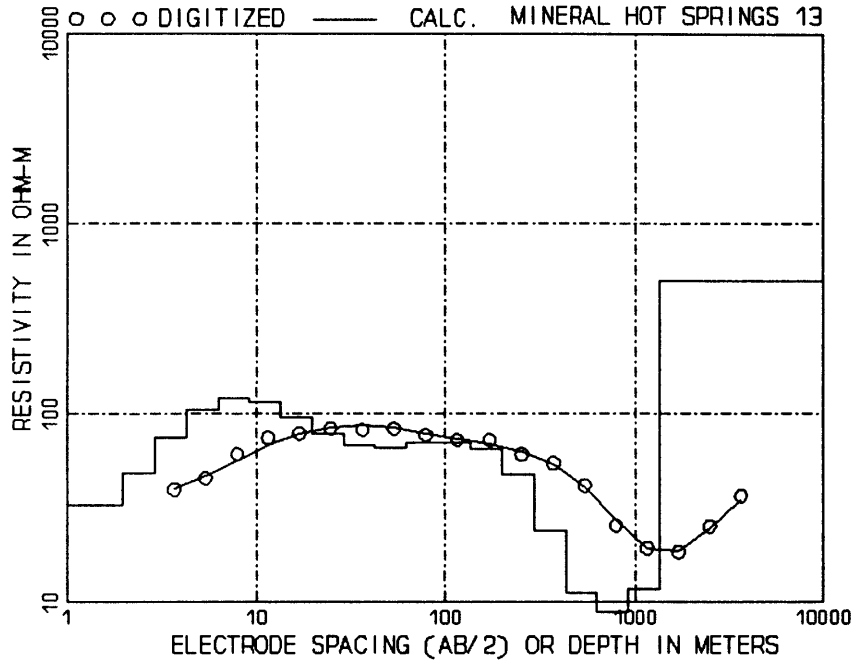

AB/2, m (ft)	App. Res.	AB/2, m (ft)	App. Res.
3.05 (10.00)	29.00	182.88 (600.00)	56.30
4.27 (14.00)	30.00	243.84 (800.00)	49.00
6.10 (20.00)	37.00	304.80 (1000.00)	46.50
9.14 (30.00)	50.00	426.72 (1400.00)	40.00
12.19 (40.00)	55.00	304.80 (1000.00)	56.00
18.29 (60.00)	59.00	426.72 (1400.00)	44.00
24.38 (80.00)	62.00	609.60 (2000.00)	32.00
30.48 (100.00)	61.00	914.40 (3000.00)	19.50
30.48 (100.00)	66.00	1219.20 (4000.00)	17.00
42.67 (140.00)	66.00	1828.80 (6000.00)	16.80
60.96 (200.00)	67.00	1219.20 (4000.00)	19.20
91.44 (300.00)	60.00	1828.80 (6000.00)	19.00
121.92 (400.00)	57.00	2438.40 (8000.00)	24.80
		3657.60 (12000.00)	36.70

DEPTH, m (ft)	RESIS.	DEPTH, m (ft)	RESIS.
1.98 (6.48)	32.64	62.46 (204.92)	66.04
2.90 (9.51)	47.98	91.68 (300.77)	69.42
4.26 (13.96)	74.97	134.56 (441.48)	70.48
6.25 (20.49)	104.56	197.51 (648.00)	64.83
9.17 (30.08)	119.89	289.91 (951.13)	47.24
13.46 (44.15)	114.04	425.52 (1396.07)	24.00
19.75 (64.80)	95.68	624.58 (2049.16)	11.16
28.99 (95.11)	77.85	916.76 (3007.75)	8.93
42.55 (139.61)	67.52	1345.62 (4414.77)	11.68
		99999.00 (99999.00)	500.00

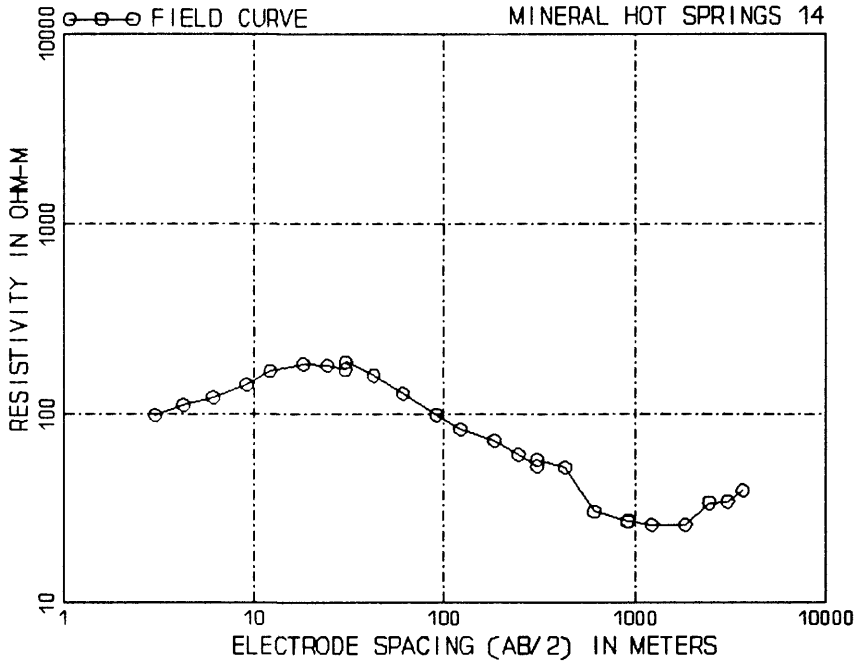

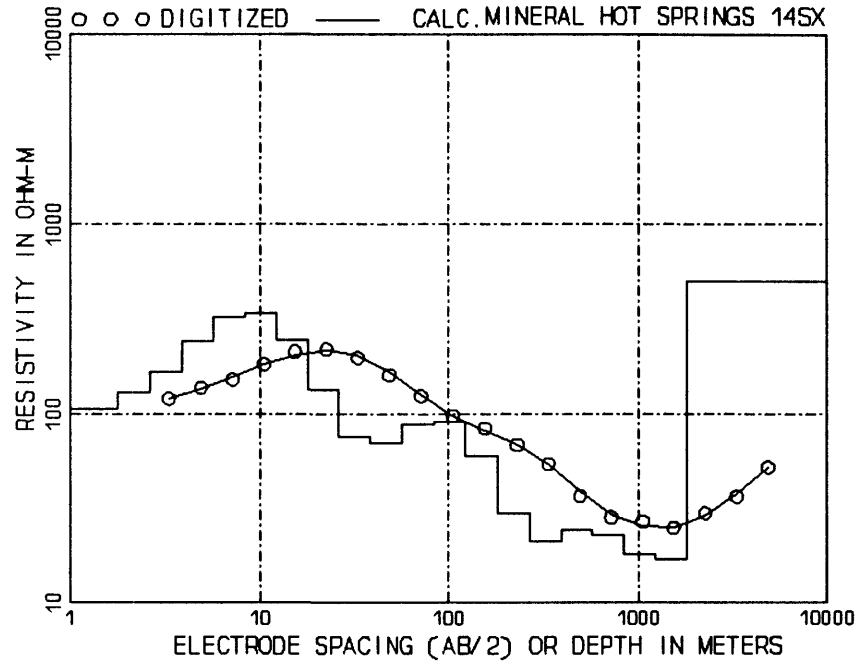

AB/2, m (ft)	App. Res.	AB/2, m (ft)	App. Res.
3.05 (10.00)	98.50	182.88 (600.00)	72.00
4.27 (14.00)	111.00	243.84 (800.00)	61.00
6.10 (20.00)	122.00	304.80 (1000.00)	53.00
9.14 (30.00)	143.00	304.80 (1000.00)	57.00
12.19 (40.00)	168.00	426.72 (1400.00)	52.00
18.29 (60.00)	183.00	609.60 (2000.00)	30.50
24.38 (80.00)	180.00	914.40 (3000.00)	27.00
30.48 (100.00)	171.00	914.40 (3000.00)	27.30
30.48 (100.00)	187.00	1219.20 (4000.00)	26.00
42.67 (140.00)	160.00	1828.80 (6000.00)	26.00
60.96 (200.00)	128.00	2438.40 (8000.00)	34.00
91.44 (300.00)	99.00	3048.00 (10000.00)	34.50
121.92 (400.00)	83.00	3657.60 (12000.00)	39.50

DEPTH, m (ft)	RESIS.	DEPTH, m (ft)	RESIS.
1.79 (5.89)	106.30	83.28 (273.22)	88.94
2.63 (8.64)	128.85	122.23 (401.03)	90.87
3.87 (12.68)	167.81	179.42 (588.64)	60.36
5.67 (18.61)	240.58	263.35 (864.00)	29.75
8.33 (27.32)	324.89	386.54 (1268.18)	21.18
12.22 (40.10)	338.09	567.36 (1861.43)	24.42
17.94 (58.86)	246.09	832.78 (2732.21)	22.98
26.33 (86.40)	133.86	1222.35 (4010.33)	18.03
38.65 (126.82)	76.04	1794.16 (5886.36)	17.20
56.74 (186.14)	70.12	99999.00 (99999.00)	500.00

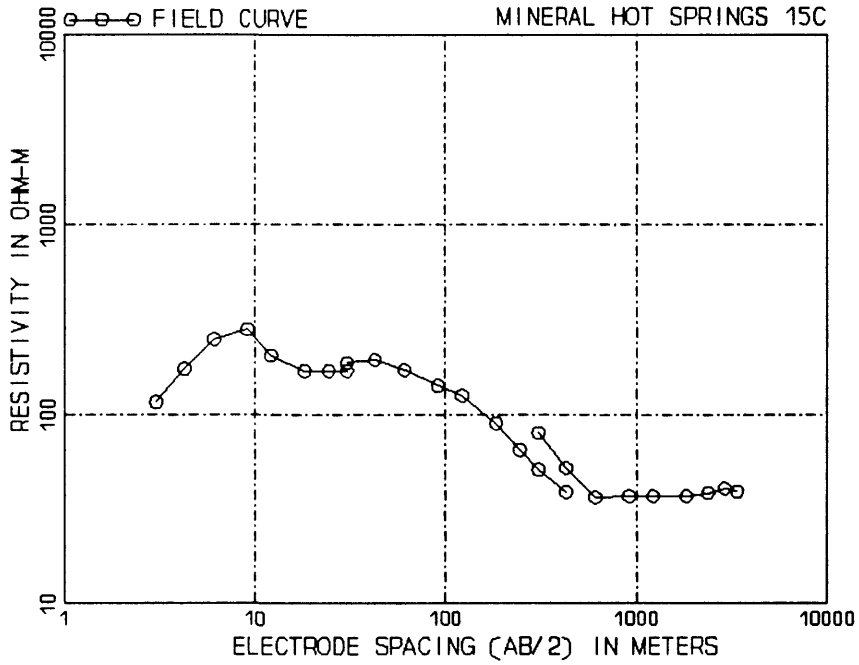

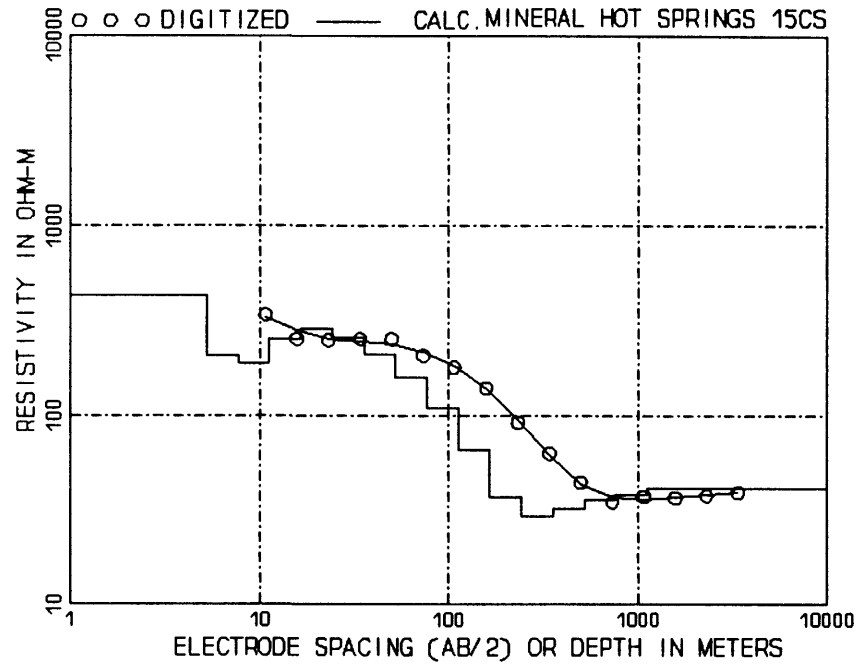

AB/2, m	(ft)	App. Res.	AB/2, m	(ft)	App. Res.
3.05	(10.00)	116.00	182.88	(600.00)	90.00
4.27	(14.00)	174.00	243.84	(800.00)	65.00
6.10	(20.00)	250.00	304.80	(1000.00)	51.00
9.14	(30.00)	280.00	426.72	(1400.00)	39.00
12.19	(40.00)	205.00	304.80	(1000.00)	80.00
18.29	(60.00)	170.00	426.72	(1400.00)	52.00
24.38	(80.00)	170.00	609.60	(2000.00)	36.50
30.48	(100.00)	170.00	914.40	(3000.00)	37.00
30.48	(100.00)	187.00	1219.20	(4000.00)	37.00
42.67	(140.00)	194.00	1219.20	(4000.00)	37.00
60.96	(200.00)	172.00	1828.80	(6000.00)	37.00
91.44	(300.00)	142.00	2374.39	(7790.00)	38.50
121.92	(400.00)	126.00	2903.52	(9526.00)	40.60
			3386.94	(11112.00)	39.20

DEPTH, m	(ft)	RESIS.	DEPTH, m	(ft)	RESIS.
5.21	(17.08)	426.94	112.14	(367.93)	108.86
7.64	(25.07)	206.17	164.61	(540.04)	65.20
11.21	(36.79)	187.16	241.61	(792.68)	36.84
16.46	(54.00)	251.60	354.63	(1163.49)	29.19
24.16	(79.27)	285.75	520.53	(1707.77)	32.38
35.46	(116.35)	256.63	764.03	(2506.66)	35.68
52.05	(170.78)	210.15	1121.44	(3679.27)	38.21
76.40	(250.67)	160.30	99999.00	(99999.00)	41.04

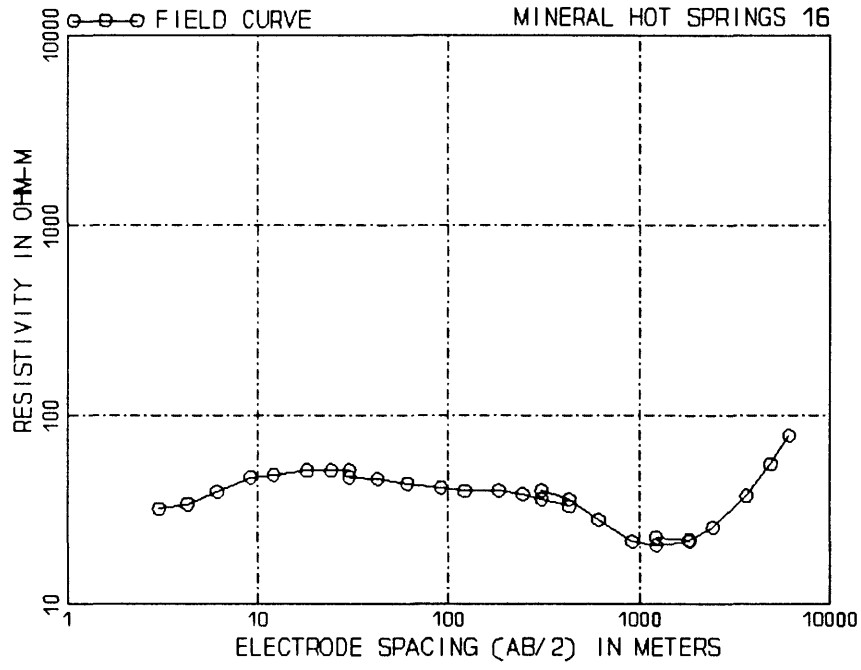

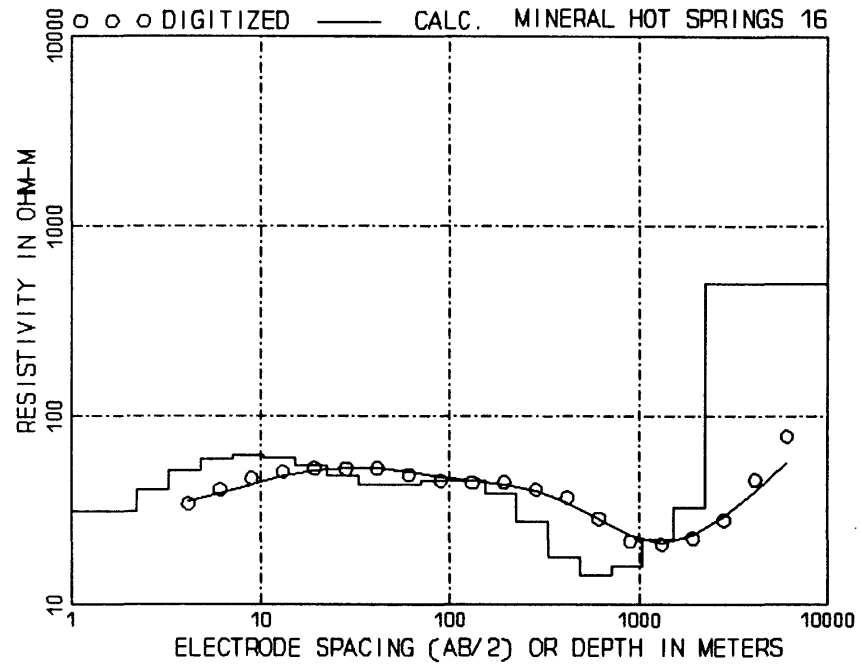

AB/2, m	(ft)	App. Res.	AB/2, m	(ft)	App. Res.
3.05	(10.00)	32.00	243.84	(800.00)	38.20
4.27	(14.00)	34.00	304.80	(1000.00)	36.10
6.10	(20.00)	39.50	426.72	(1400.00)	33.00
9.14	(30.00)	47.00	304.80	(1000.00)	40.00
12.19	(40.00)	48.50	426.72	(1400.00)	36.00
18.29	(60.00)	51.00	609.60	(2000.00)	28.00
24.38	(80.00)	51.00	914.40	(3000.00)	21.50
30.48	(100.00)	51.00	1219.20	(4000.00)	20.50
30.48	(100.00)	47.00	1828.80	(6000.00)	21.50
42.67	(140.00)	46.00	1219.20	(4000.00)	22.70
60.96	(200.00)	43.50	1828.80	(6000.00)	22.00
91.44	(300.00)	41.50	2438.40	(8000.00)	25.50
121.92	(400.00)	39.80	3657.60	(12000.00)	37.50
182.88	(600.00)	40.00	4876.80	(16000.00)	55.00
			6096.00	(20000.00)	77.80

DEPTH, m	(ft)	RESIS.	DEPTH, m	(ft)	RESIS.
2.24	(7.36)	31.35	104.10	(341.53)	45.13
3.29	(10.80)	40.59	152.79	(501.29)	45.21
4.83	(15.85)	50.99	224.27	(735.80)	38.96
7.09	(23.27)	58.87	329.18	(1080.00)	27.52
10.41	(34.15)	61.89	483.18	(1585.22)	18.01
15.28	(50.13)	60.02	709.21	(2326.79)	14.45
22.43	(73.58)	54.58	1040.97	(3415.26)	16.09
32.92	(108.00)	47.90	1527.94	(5012.92)	22.33
48.32	(158.52)	43.34	2242.71	(7357.96)	32.89
70.92	(232.68)	42.96	99999.00	(99999.00)	500.00

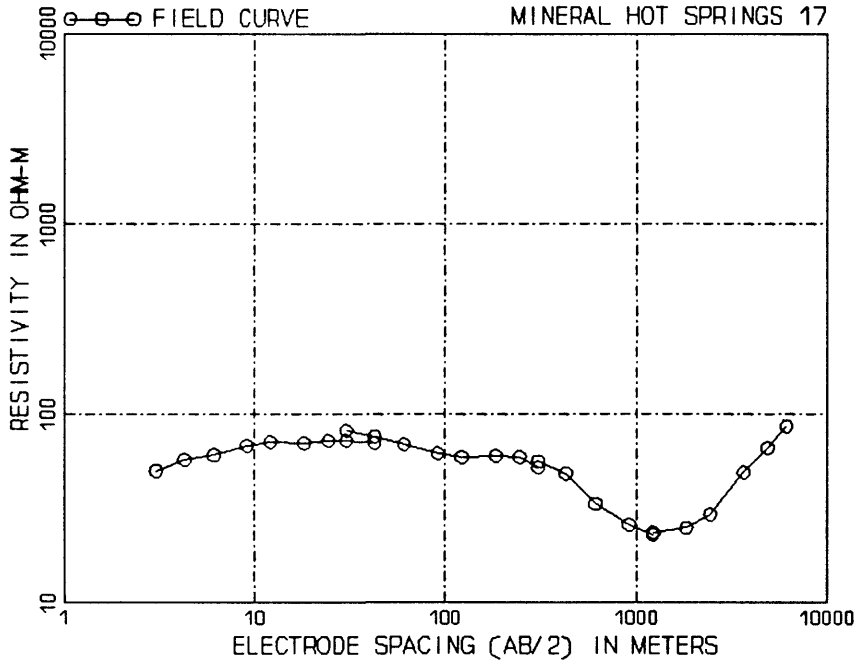

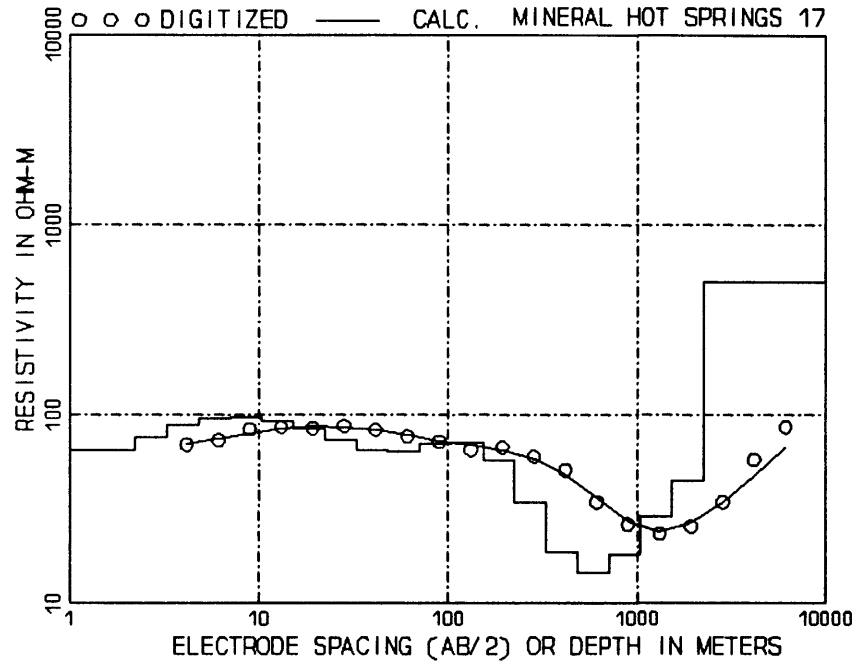

AB/2, m (ft)	App. Res.	AB/2, m (ft)	App. Res.
3.05 (10.00)	50.00	182.88 (600.00)	60.00
4.27 (14.00)	57.00	243.84 (800.00)	59.00
6.10 (20.00)	60.50	304.80 (1000.00)	52.00
9.14 (30.00)	68.00	304.80 (1000.00)	56.00
12.19 (40.00)	71.00	426.72 (1400.00)	48.50
18.29 (60.00)	70.00	609.60 (2000.00)	33.50
24.38 (80.00)	72.00	914.40 (3000.00)	26.00
30.48 (100.00)	72.00	1219.20 (4000.00)	23.00
42.67 (140.00)	70.00	1219.20 (4000.00)	23.70
30.48 (100.00)	81.50	1828.80 (6000.00)	25.00
42.67 (140.00)	76.00	2438.40 (8000.00)	29.50
60.96 (200.00)	69.00	3657.60 (12000.00)	49.00
91.44 (300.00)	62.00	4876.80 (16000.00)	66.00
121.92 (400.00)	59.00	6096.00 (20000.00)	86.00

DEPTH, m (ft)	RESIS.	DEPTH, m (ft)	RESIS.
2.24 (7.36)	64.74	104.10 (341.53)	69.77
3.29 (10.80)	75.27	152.79 (501.29)	71.16
4.83 (15.85)	88.05	224.27 (735.80)	56.98
7.09 (23.27)	95.96	329.18 (1080.00)	34.06
10.41 (34.15)	96.68	483.18 (1585.22)	18.82
15.28 (50.13)	92.64	709.21 (2326.79)	14.59
22.43 (73.58)	84.45	1040.97 (3415.26)	18.22
32.92 (108.00)	73.51	1527.94 (5012.92)	28.69
48.32 (158.52)	64.96	2242.71 (7357.96)	44.37
70.92 (232.68)	64.03	99999.00 (99999.00)	500.00

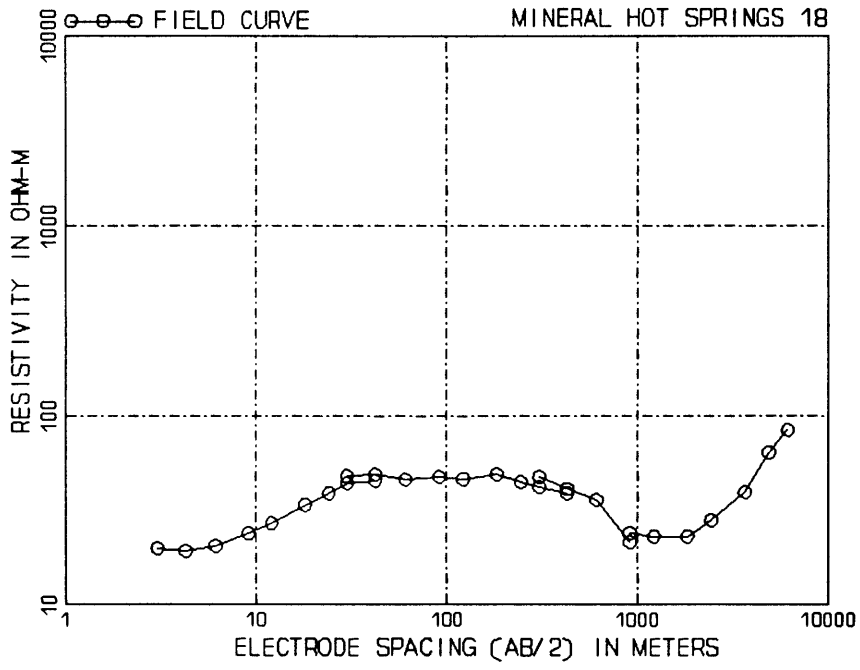

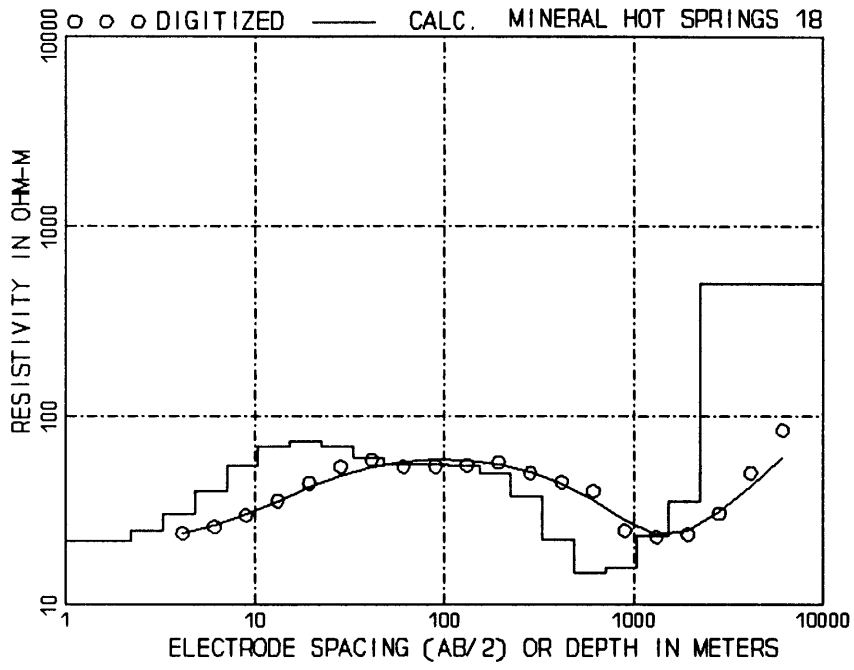

AB/2, m (ft)	App. Res.	AB/2, m (ft)	App. Res.
3.05 (10.00)	20.00	182.88 (600.00)	49.00
4.27 (14.00)	19.40	243.84 (800.00)	44.50
6.10 (20.00)	20.60	304.80 (1000.00)	42.00
9.14 (30.00)	23.90	426.72 (1400.00)	39.00
12.19 (40.00)	27.10	304.80 (1000.00)	47.50
18.29 (60.00)	33.90	426.72 (1400.00)	41.00
24.38 (80.00)	39.00	609.60 (2000.00)	36.00
30.48 (100.00)	44.00	914.40 (3000.00)	21.50
42.67 (140.00)	45.50	914.40 (3000.00)	24.00
30.48 (100.00)	48.00	1219.20 (4000.00)	23.00
42.67 (140.00)	49.00	1828.80 (6000.00)	23.00
60.96 (200.00)	46.00	2438.40 (8000.00)	28.00
91.44 (300.00)	47.50	3657.60 (12000.00)	39.50
121.92 (400.00)	46.30	4876.80 (16000.00)	64.00
		6096.00 (20000.00)	84.00

DEPTH, m (ft)	RESIS.	DEPTH, m (ft)	RESIS.
2.24 (7.36)	22.03	104.10 (341.53)	55.18
3.29 (10.80)	24.62	152.79 (501.29)	54.63
4.83 (15.85)	30.18	224.27 (735.80)	49.69
7.09 (23.27)	40.17	329.18 (1080.00)	37.37
10.41 (34.15)	54.48	483.18 (1585.22)	22.37
15.28 (50.13)	68.43	709.21 (2326.79)	14.85
22.43 (73.58)	73.81	1040.97 (3415.26)	15.89
32.92 (108.00)	68.36	1527.94 (5012.92)	23.25
48.32 (158.52)	59.75	2242.71 (7357.96)	35.15
70.92 (232.68)	55.35	99999.00 (99999.00)	500.00

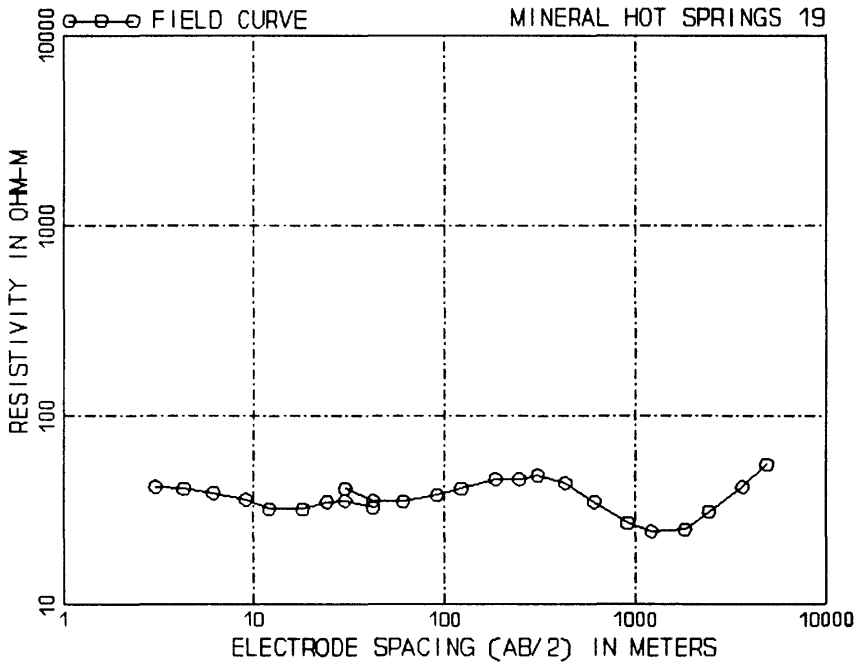

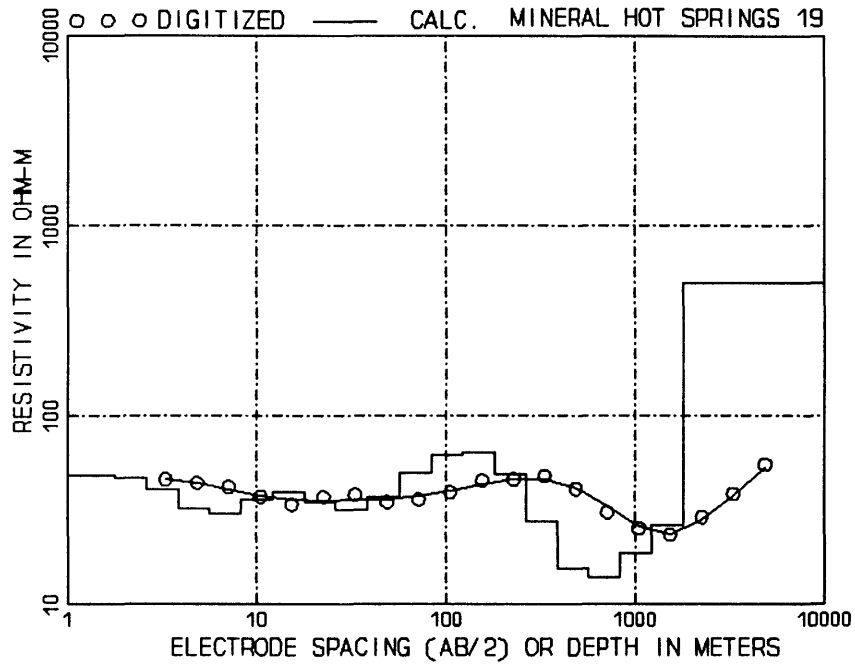

AB/2, m (ft)	App. Res.	AB/2, m (ft)	App. Res.
3.05 (10.00)	42.00	121.92 (400.00)	41.00
4.27 (14.00)	41.00	182.88 (600.00)	46.00
6.10 (20.00)	39.00	243.84 (800.00)	46.00
9.14 (30.00)	36.00	304.80 (1000.00)	48.00
12.19 (40.00)	32.00	426.72 (1400.00)	44.00
18.29 (60.00)	32.00	609.60 (2000.00)	35.00
24.38 (80.00)	35.00	914.40 (3000.00)	27.00
30.48 (100.00)	35.50	914.40 (3000.00)	27.00
42.67 (140.00)	32.50	1219.20 (4000.00)	24.50
30.48 (100.00)	41.00	1828.80 (6000.00)	25.00
42.67 (140.00)	35.50	2438.40 (8000.00)	31.00
60.96 (200.00)	35.20	3657.60 (12000.00)	42.00
91.44 (300.00)	38.00	4876.80 (16000.00)	55.00

DEPTH, m (ft)	RESIS.	DEPTH, m (ft)	RESIS.
1.79 (5.89)	48.01	83.28 (273.22)	49.48
2.63 (8.64)	46.70	122.23 (401.03)	61.71
3.87 (12.68)	40.70	179.42 (588.64)	63.71
5.67 (18.61)	32.45	263.35 (864.00)	48.67
8.33 (27.32)	30.31	386.54 (1268.18)	27.41
12.22 (40.10)	36.01	567.36 (1861.43)	15.50
17.94 (58.86)	39.37	832.78 (2732.21)	14.03
26.33 (86.40)	34.63	1222.35 (4010.33)	18.61
38.65 (126.82)	31.70	1794.16 (5886.36)	26.37
56.74 (186.14)	37.13	99999.00 (99999.00)	500.00

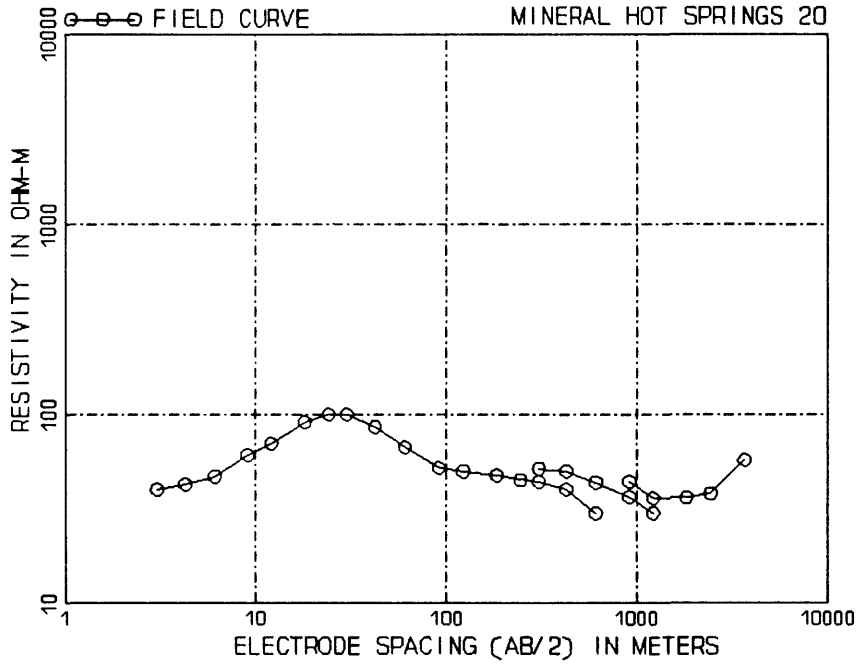

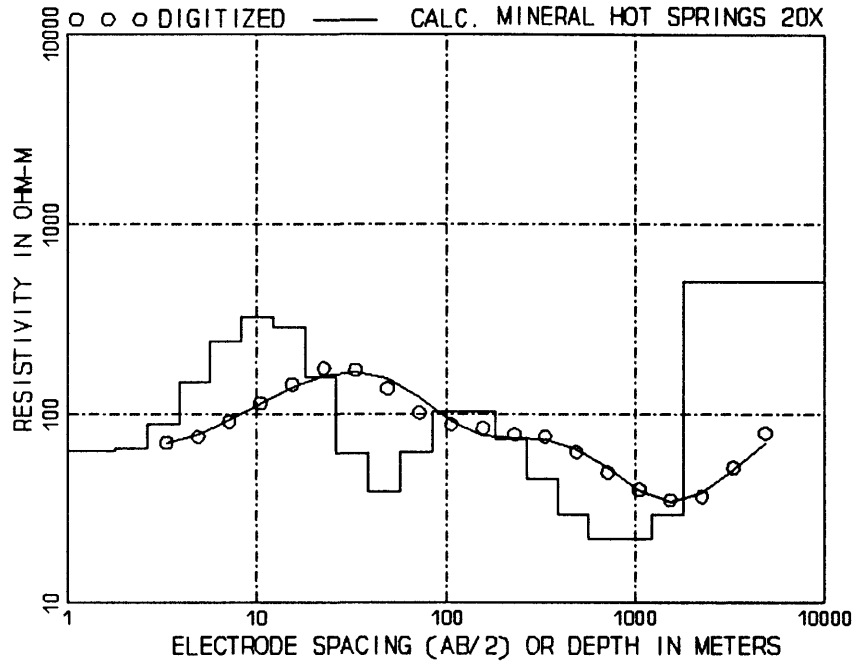

AB/2, m (ft)	App. Res.	AB/2, m (ft)	App. Res.
3.05 (10.00)	40.00	243.84 (800.00)	45.00
4.27 (14.00)	42.50	304.80 (1000.00)	44.00
6.10 (20.00)	47.00	426.72 (1400.00)	40.00
9.14 (30.00)	61.00	609.60 (2000.00)	30.00
12.19 (40.00)	70.00	304.80 (1000.00)	51.50
18.29 (60.00)	91.00	426.72 (1400.00)	50.00
24.38 (80.00)	100.00	609.60 (2000.00)	43.50
30.48 (100.00)	100.00	914.40 (3000.00)	36.50
30.48 (100.00)	100.00	1219.20 (4000.00)	30.00
42.67 (140.00)	86.00	914.40 (3000.00)	44.00
60.96 (200.00)	67.00	1219.20 (4000.00)	36.00
91.44 (300.00)	52.00	1828.80 (6000.00)	36.30
121.92 (400.00)	50.00	2438.40 (8000.00)	38.00
182.88 (600.00)	47.50	3657.60 (12000.00)	57.00

DEPTH, m (ft)	RESIS.	DEPTH, m (ft)	RESIS.
1.79 (5.89)	63.38	83.28 (273.22)	62.94
2.63 (8.64)	65.41	122.23 (401.03)	102.72
3.87 (12.68)	88.87	179.42 (588.64)	102.73
5.67 (18.61)	147.05	263.35 (864.00)	73.36
8.33 (27.32)	243.16	386.54 (1268.18)	45.06
12.22 (40.10)	324.11	567.36 (1861.43)	29.46
17.94 (58.86)	288.40	832.78 (2732.21)	22.02
26.33 (86.40)	156.02	1222.35 (4010.33)	21.73
38.65 (126.82)	62.13	1794.16 (5886.36)	29.52
56.74 (186.14)	38.88	99999.00 (99999.00)	500.00

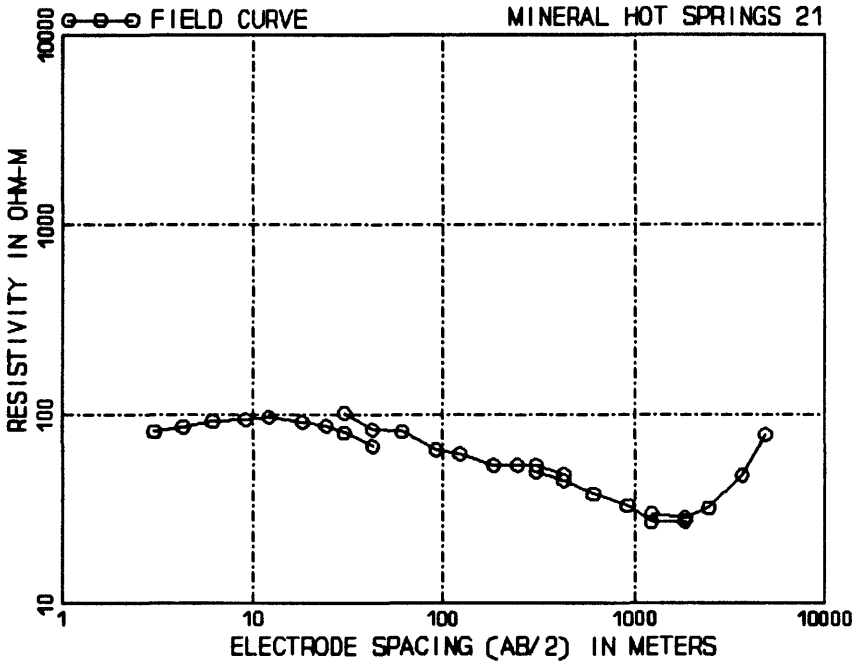

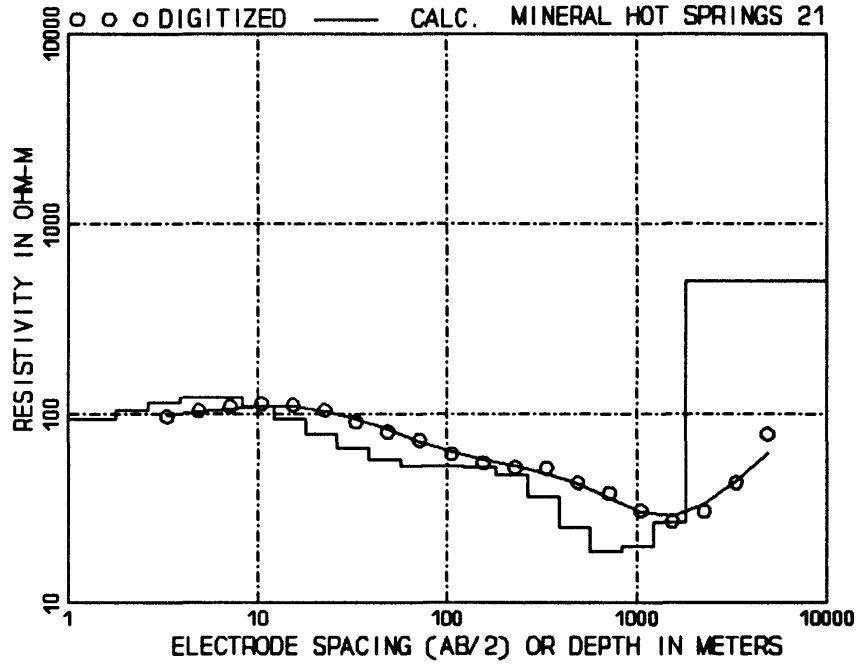

AB/2, m	(ft)	App. Res.	AB/2, m	(ft)	App. Res.
3.05	(10.00)	81.00	182.88	(600.00)	54.00
4.27	(14.00)	86.00	243.84	(800.00)	54.00
6.10	(20.00)	92.00	304.80	(1000.00)	54.00
9.14	(30.00)	94.00	426.72	(1400.00)	48.00
12.19	(40.00)	97.00	304.80	(1000.00)	50.00
18.29	(60.00)	91.00	426.72	(1400.00)	44.50
24.38	(80.00)	87.00	609.60	(2000.00)	38.00
30.48	(100.00)	80.00	914.40	(3000.00)	33.00
42.67	(140.00)	68.00	1219.20	(4000.00)	27.00
30.48	(100.00)	102.00	1828.80	(6000.00)	27.30
42.67	(140.00)	83.00	1219.20	(4000.00)	30.00
60.96	(200.00)	81.00	1828.80	(6000.00)	28.50
91.44	(300.00)	65.00	2438.40	(8000.00)	32.00
121.92	(400.00)	62.00	3657.60	(12000.00)	47.70
			4876.80	(16000.00)	78.00

DEPTH, m	(ft)	RESIS.	DEPTH, m	(ft)	RESIS.
1.79	(5.89)	93.75	83.28	(273.22)	52.63
2.63	(8.64)	104.05	122.23	(401.03)	52.63
3.87	(12.68)	115.06	179.42	(588.64)	52.46
5.67	(18.61)	122.27	263.35	(864.00)	47.20
8.33	(27.32)	121.16	386.54	(1268.18)	36.48
12.22	(40.10)	110.20	567.56	(1861.43)	24.97
17.94	(58.86)	93.50	832.78	(2732.21)	18.76
26.33	(86.40)	77.66	1222.35	(4010.33)	19.77
38.65	(126.82)	65.46	1794.16	(5886.36)	26.75
56.74	(186.14)	56.79	99999.00	(99999.00)	500.00

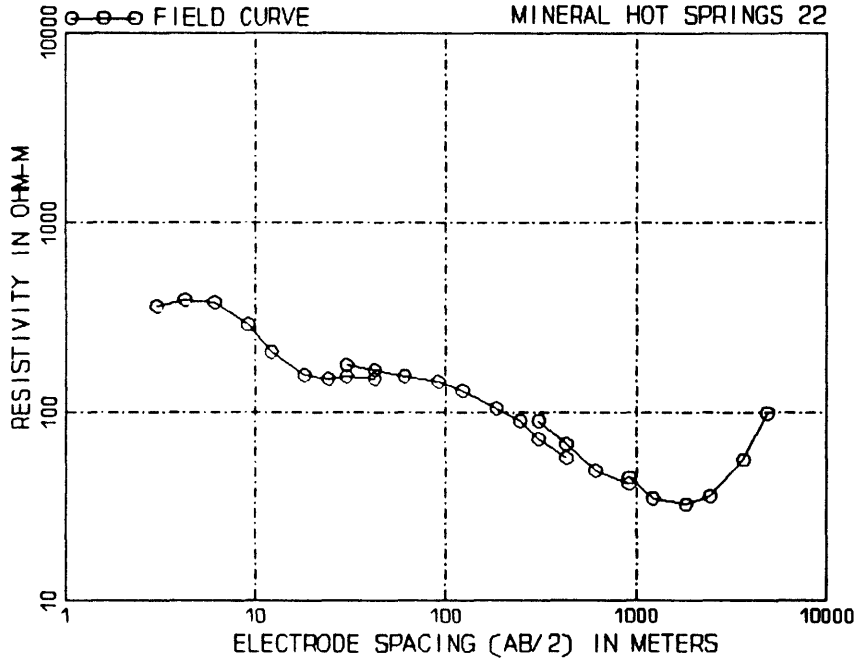

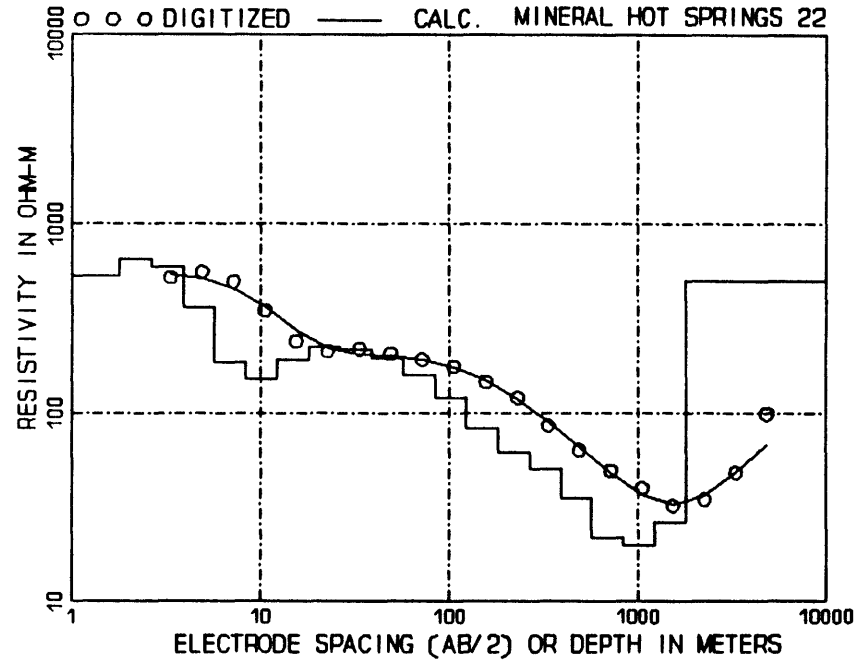

AB/2, m	(ft)	App. Res.	AB/2, m	(ft)	App. Res.
3.05	(10.00)	362.00	182.88	(600.00)	105.00
4.27	(14.00)	390.00	243.84	(800.00)	90.00
6.10	(20.00)	380.00	304.80	(1000.00)	72.00
9.14	(30.00)	290.00	426.72	(1400.00)	57.00
12.19	(40.00)	208.00	304.80	(1000.00)	90.00
18.29	(60.00)	157.00	426.72	(1400.00)	67.50
24.38	(80.00)	150.00	609.60	(2000.00)	49.00
30.48	(100.00)	155.00	914.40	(3000.00)	42.00
42.67	(140.00)	150.00	914.40	(3000.00)	45.00
30.48	(100.00)	177.00	1219.20	(4000.00)	35.00
42.67	(140.00)	166.00	1828.80	(6000.00)	32.50
60.96	(200.00)	155.00	2438.40	(8000.00)	36.00
91.44	(300.00)	145.00	3657.60	(12000.00)	56.00
121.92	(400.00)	130.00	4876.80	(16000.00)	99.00

DEPTH, m	(ft)	RESIS.	DEPTH, m	(ft)	RESIS.
1.79	(5.89)	534.09	83.28	(273.22)	159.32
2.63	(8.64)	650.73	122.23	(401.03)	119.79
3.87	(12.68)	595.00	179.42	(588.64)	83.46
5.67	(18.61)	360.39	263.35	(864.00)	61.82
8.33	(27.32)	186.00	386.54	(1268.18)	50.69
12.22	(40.10)	151.32	567.36	(1861.43)	35.62
17.94	(58.86)	191.09	832.78	(2732.21)	21.93
26.33	(86.40)	222.26	1222.35	(4010.33)	19.77
38.65	(126.82)	217.84	1794.16	(5886.36)	26.21
56.74	(186.14)	193.43	99999.00	(99999.00)	500.00

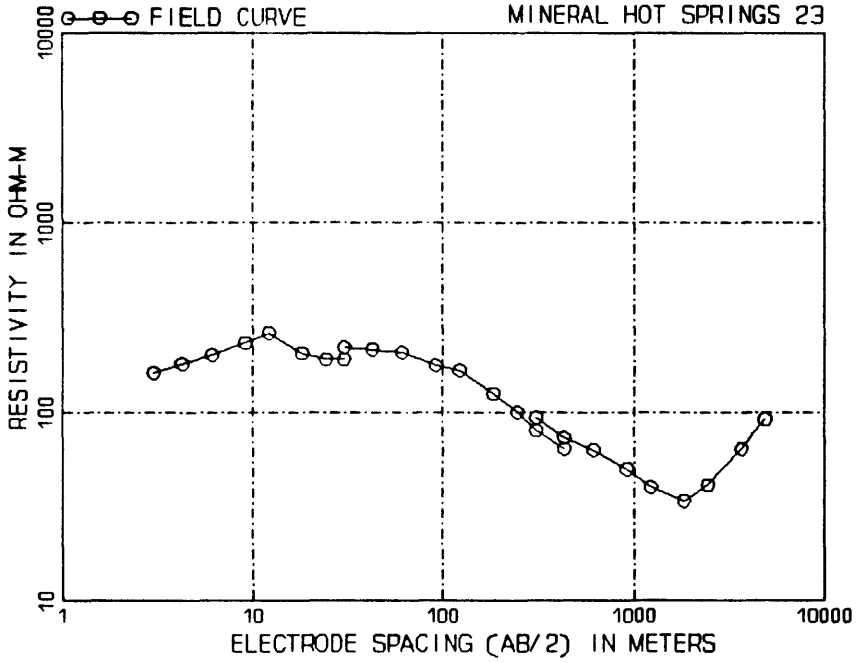

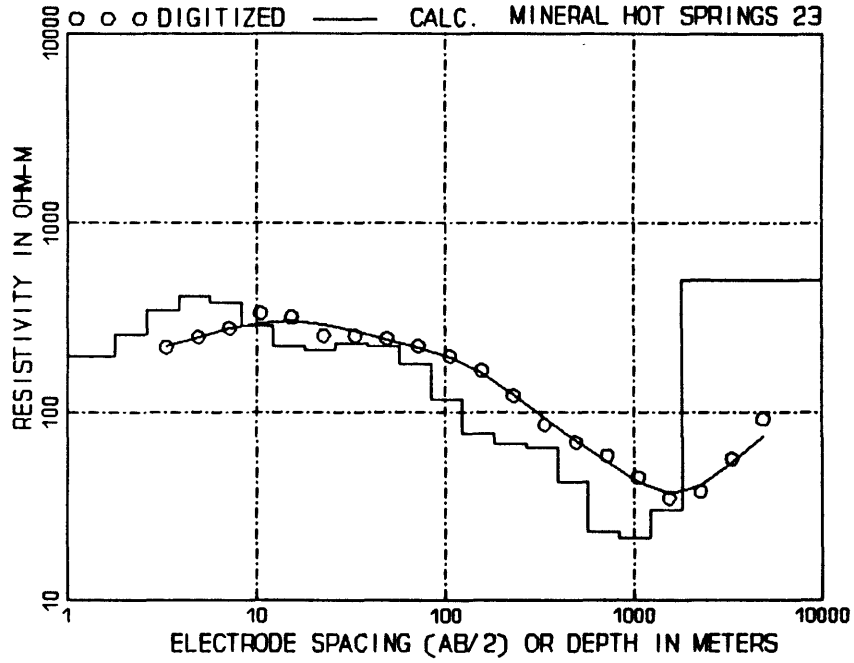

AB/2, m (ft)	App. Res.	AB/2, m (ft)	App. Res.
3.05 (10.00)	162.00	182.88 (600.00)	125.00
4.27 (14.00)	180.00	243.84 (800.00)	100.00
6.10 (20.00)	200.00	304.80 (1000.00)	80.00
9.14 (30.00)	233.00	426.72 (1400.00)	64.00
12.19 (40.00)	263.00	304.80 (1000.00)	94.00
18.29 (60.00)	205.00	426.72 (1400.00)	73.50
24.38 (80.00)	190.00	609.60 (2000.00)	63.00
30.48 (100.00)	190.00	914.40 (3000.00)	50.00
30.48 (100.00)	220.00	1219.20 (4000.00)	40.00
42.67 (140.00)	215.00	1219.20 (4000.00)	40.00
60.96 (200.00)	207.00	1828.80 (6000.00)	34.00
91.44 (300.00)	177.00	2438.40 (8000.00)	41.00
121.92 (400.00)	166.00	3657.60 (12000.00)	64.00
		4876.80 (16000.00)	92.00

DEPTH, m (ft)	RESIS.	DEPTH, m (ft)	RESIS.
1.79 (5.89)	197.04	83.28 (273.22)	178.56
2.63 (8.64)	256.66	122.23 (401.03)	117.17
3.87 (12.68)	344.02	179.42 (588.64)	76.78
5.67 (18.61)	410.18	263.35 (864.00)	67.31
8.33 (27.32)	380.32	386.54 (1268.18)	64.34
12.22 (40.10)	285.76	567.36 (1861.43)	42.51
17.94 (58.86)	222.30	832.78 (2732.21)	23.43
26.33 (86.40)	214.98	1222.35 (4010.33)	21.58
38.65 (126.82)	229.36	1794.16 (5886.36)	30.11
56.74 (186.14)	222.40	99999.00 (99999.00)	500.00

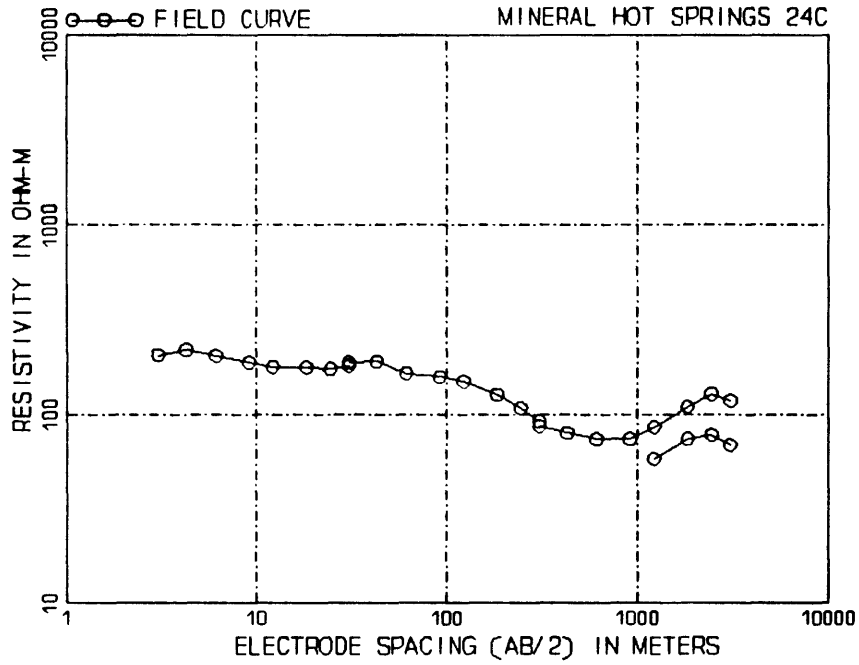

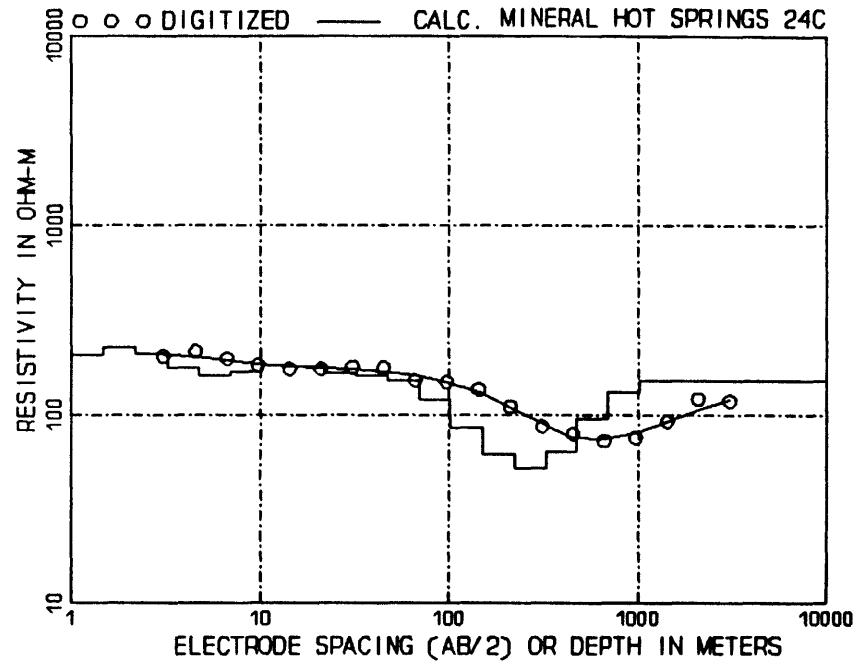

AB/2, m	(ft)	App. Res.	AB/2, m	(ft)	App. Res.
3.05	(10.00)	205.00	243.84	(800.00)	108.00
4.27	(14.00)	219.00	304.80	(1000.00)	92.00
6.10	(20.00)	204.00	304.80	(1000.00)	87.00
9.14	(30.00)	188.00	426.72	(1400.00)	80.00
12.19	(40.00)	178.00	609.60	(2000.00)	74.00
18.29	(60.00)	177.00	914.40	(3000.00)	74.00
24.38	(80.00)	174.00	1222.25	(4010.00)	85.90
30.48	(100.00)	180.00	1825.14	(5988.00)	109.30
30.48	(100.00)	188.00	2433.83	(7985.00)	128.70
42.67	(140.00)	190.00	3064.15	(10053.00)	118.30
60.96	(200.00)	165.00	1219.20	(4000.00)	58.00
91.44	(300.00)	158.00	1828.80	(6000.00)	74.00
121.92	(400.00)	150.00	2438.40	(8000.00)	78.00
182.88	(600.00)	127.00	3048.00	(10000.00)	69.00

DEPTH, m	(ft)	RESIS.	DEPTH, m	(ft)	RESIS.
1.49	(4.89)	205.46	47.09	(154.50)	161.74
2.19	(7.17)	225.69	69.12	(226.78)	151.21
3.21	(10.53)	209.08	101.46	(332.86)	120.66
4.71	(15.45)	176.51	148.92	(488.58)	85.89
6.91	(22.68)	161.07	218.58	(717.13)	61.61
10.15	(33.29)	169.74	320.83	(1052.60)	52.29
14.89	(48.86)	183.12	470.92	(1545.01)	63.54
21.86	(71.71)	178.79	691.22	(2267.77)	95.55
32.08	(105.26)	166.37	1014.57	(3328.63)	131.79
			99999.00	(99999.00)	150.82

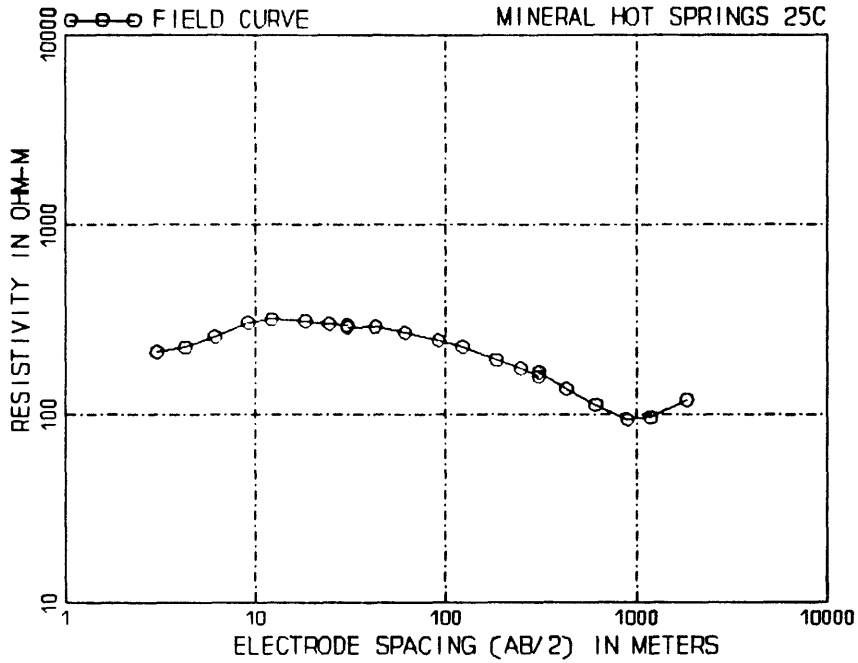

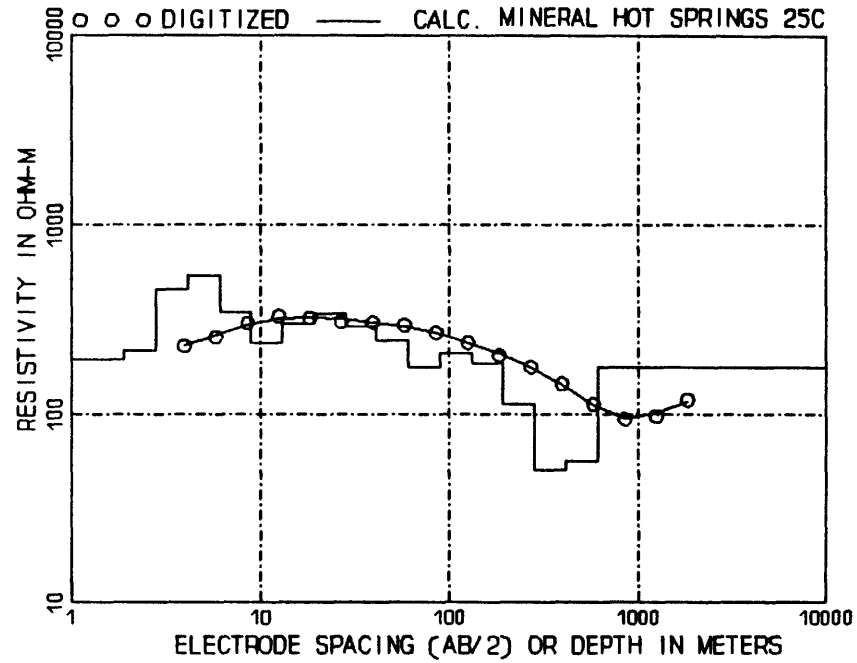

AB/2, m (ft)	App. Res.	AB/2, m (ft)	App. Res.
3.05 (10.00)	214.00	91.44 (300.00)	245.00
4.27 (14.00)	226.00	121.92 (400.00)	228.00
6.10 (20.00)	258.00	182.88 (600.00)	193.00
9.14 (30.00)	305.00	243.84 (800.00)	175.00
12.19 (40.00)	317.00	304.80 (1000.00)	158.00
18.29 (60.00)	311.00	304.80 (1000.00)	167.00
24.38 (80.00)	300.00	426.72 (1400.00)	136.00
30.48 (100.00)	294.00	609.60 (2000.00)	112.00
30.48 (100.00)	288.00	892.76 (2929.00)	93.70
42.67 (140.00)	290.00	1185.98 (3891.00)	96.20
60.96 (200.00)	270.00	1830.93 (6007.00)	119.30

DEPTH, m (ft)	RESIS.	DEPTH, m (ft)	RESIS.
1.92 (6.29)	193.17	41.30 (135.51)	290.62
2.81 (9.23)	215.16	60.62 (198.90)	243.81
4.13 (13.55)	452.84	88.98 (291.94)	176.04
6.06 (19.89)	542.27	130.61 (428.51)	210.89
8.90 (29.19)	346.37	191.71 (628.97)	186.56
13.06 (42.85)	237.96	281.39 (923.20)	113.18
19.17 (62.90)	300.18	413.02 (1355.07)	50.85
28.14 (92.32)	337.59	606.24 (1988.97)	56.25
		99999.00 (99999.00)	176.10

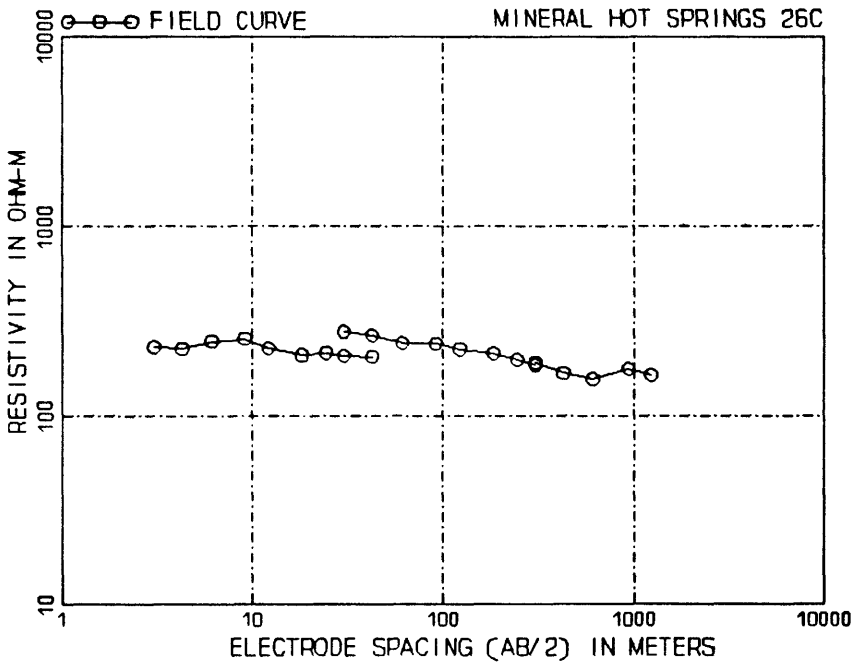

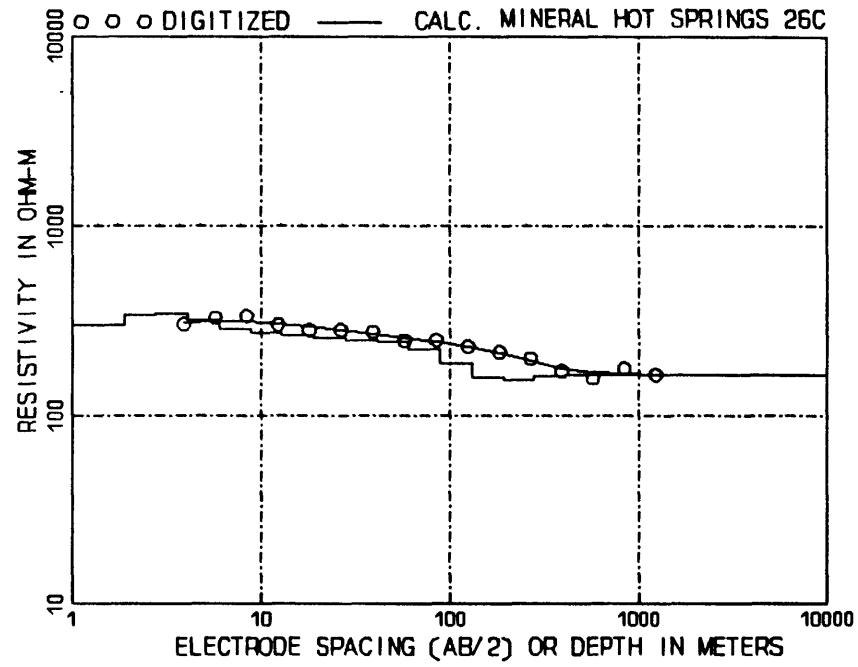

AB/2, m (ft)	App. Res.	AB/2, m (ft)	App. Res.
3.05 (10.00)	230.00	60.96 (200.00)	242.00
4.27 (14.00)	226.00	91.44 (300.00)	240.00
6.10 (20.00)	247.00	121.92 (400.00)	225.00
9.14 (30.00)	255.00	182.88 (600.00)	213.00
12.19 (40.00)	228.00	243.84 (800.00)	198.00
18.29 (60.00)	209.00	304.80 (1000.00)	185.00
24.38 (80.00)	215.00	304.80 (1000.00)	190.00
30.48 (100.00)	207.00	426.72 (1400.00)	168.00
42.67 (140.00)	205.00	609.60 (2000.00)	156.00
30.48 (100.00)	277.00	934.21 (3065.00)	177.60
42.67 (140.00)	265.00	1230.48 (4037.00)	163.90

DEPTH, m (ft)	RESIS.	DEPTH, m (ft)	RESIS.
1.89 (6.20)	298.00	40.74 (133.67)	251.04
2.78 (9.11)	338.62	59.80 (196.20)	243.68
4.07 (13.37)	346.10	87.78 (287.98)	223.60
5.98 (19.62)	317.97	128.84 (422.70)	189.02
8.78 (28.80)	288.02	189.11 (620.43)	159.70
12.88 (42.27)	273.81	277.57 (910.67)	154.38
18.91 (62.04)	264.87	407.42 (1336.68)	162.70
27.76 (91.07)	256.16	99999.00 (99999.00)	164.34

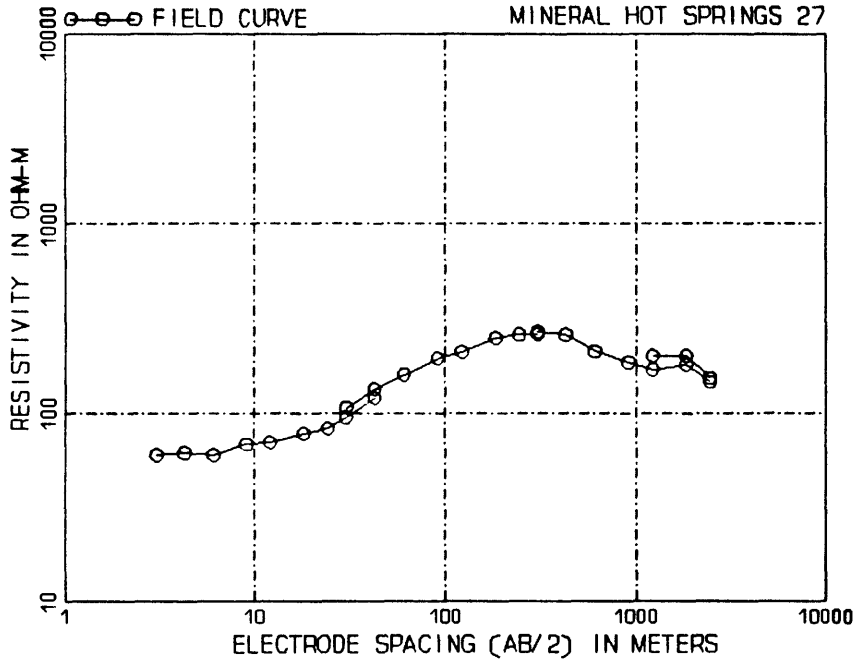

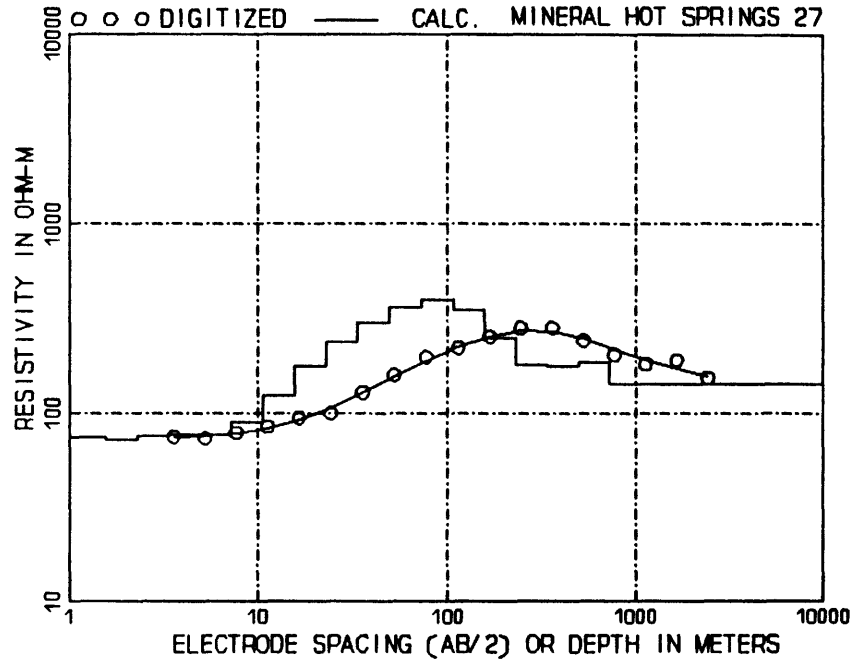

AB/2, m	(ft)	App. Res.	AB/2, m	(ft)	App. Res.
3.05	(10.00)	60.00	121.92	(400.00)	210.00
4.27	(14.00)	61.50	182.88	(600.00)	250.00
6.10	(20.00)	60.00	243.84	(800.00)	260.00
9.14	(30.00)	68.50	304.80	(1000.00)	262.00
12.19	(40.00)	70.00	304.80	(1000.00)	270.00
18.29	(60.00)	78.00	426.72	(1400.00)	260.00
24.38	(80.00)	83.00	609.60	(2000.00)	212.00
30.48	(100.00)	95.00	914.40	(3000.00)	185.00
42.67	(140.00)	120.00	1219.20	(4000.00)	170.00
30.48	(100.00)	107.00	1828.80	(6000.00)	180.00
42.67	(140.00)	134.00	2438.40	(8000.00)	146.00
60.96	(200.00)	160.00	1219.20	(4000.00)	200.00
91.44	(300.00)	195.00	1828.80	(6000.00)	200.00
			2438.40	(8000.00)	153.00

DEPTH, m	(ft)	RESIS.	DEPTH, m	(ft)	RESIS.
1.57	(5.14)	74.01	49.51	(162.42)	298.64
2.30	(7.54)	71.70	72.66	(238.40)	362.44
3.37	(11.07)	75.37	106.66	(349.92)	396.85
4.95	(16.24)	76.80	156.55	(513.61)	352.26
7.27	(23.84)	77.05	229.78	(753.88)	250.44
10.67	(34.99)	89.80	337.27	(1106.54)	181.16
15.65	(51.36)	124.29	495.05	(1624.19)	177.16
22.98	(75.39)	176.77	726.64	(2383.98)	184.45
33.73	(110.65)	236.08	99999.00	(99999.00)	141.94

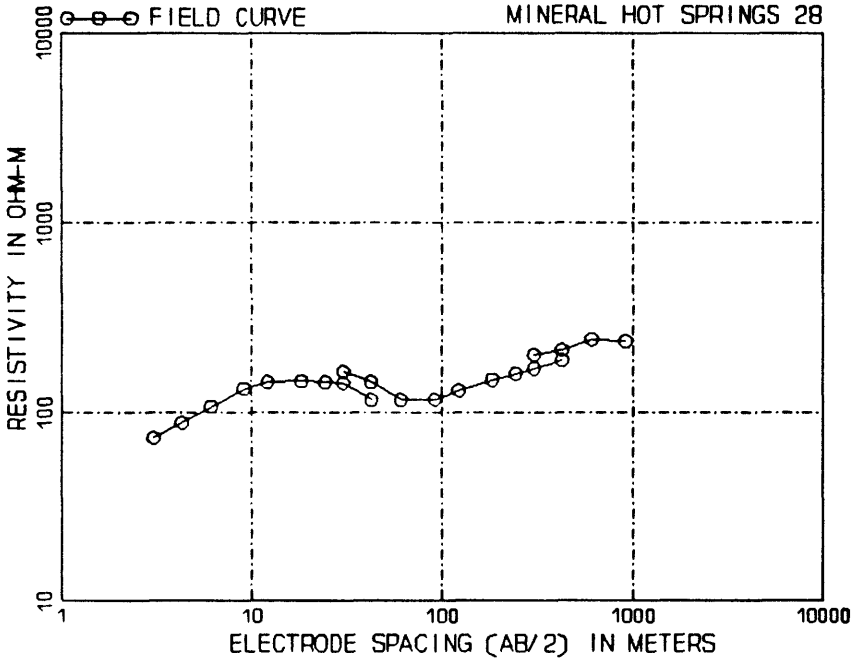

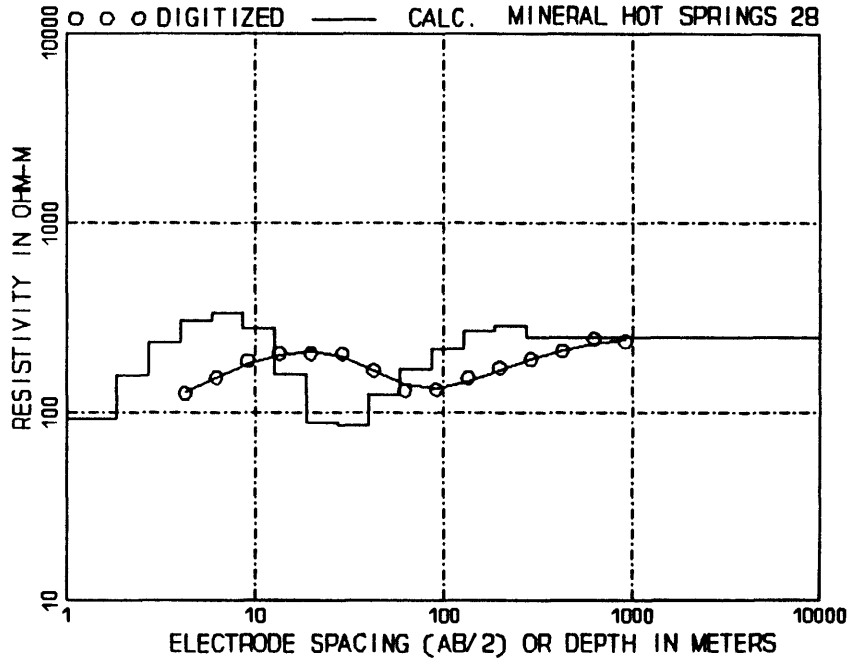

AB/2, m (ft)	App. Res.	AB/2, m (ft)	App. Res.
3.05 (10.00)	73.50	60.96 (200.00)	116.00
4.27 (14.00)	88.00	91.44 (300.00)	117.00
6.10 (20.00)	107.00	121.92 (400.00)	130.00
9.14 (30.00)	133.00	182.88 (600.00)	148.00
12.19 (40.00)	144.00	243.84 (800.00)	160.00
18.29 (60.00)	146.00	304.80 (1000.00)	170.00
24.38 (80.00)	144.00	426.72 (1400.00)	188.00
30.48 (100.00)	143.00	304.80 (1000.00)	200.00
42.67 (140.00)	116.00	426.72 (1400.00)	213.00
30.48 (100.00)	164.00	609.60 (2000.00)	243.00
42.67 (140.00)	144.00	914.40 (3000.00)	237.00

DEPTH, m (ft)	RESIS.	DEPTH, m (ft)	RESIS.
1.86 (6.09)	92.93	27.25 (89.40)	87.69
2.72 (8.94)	156.41	40.00 (131.22)	85.50
4.00 (13.12)	234.78	58.71 (192.60)	123.45
5.87 (19.26)	303.77	86.17 (282.71)	167.99
8.62 (28.27)	333.03	126.48 (414.95)	215.86
12.65 (41.50)	277.13	185.64 (609.07)	268.16
18.56 (60.91)	159.71	272.49 (893.99)	287.99
		99999.00 (99999.00)	250.52

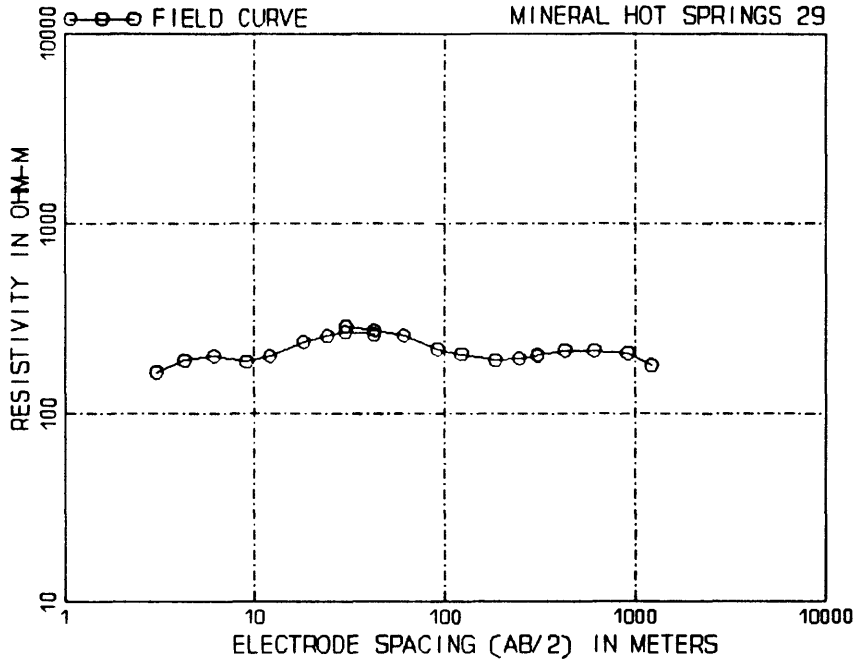

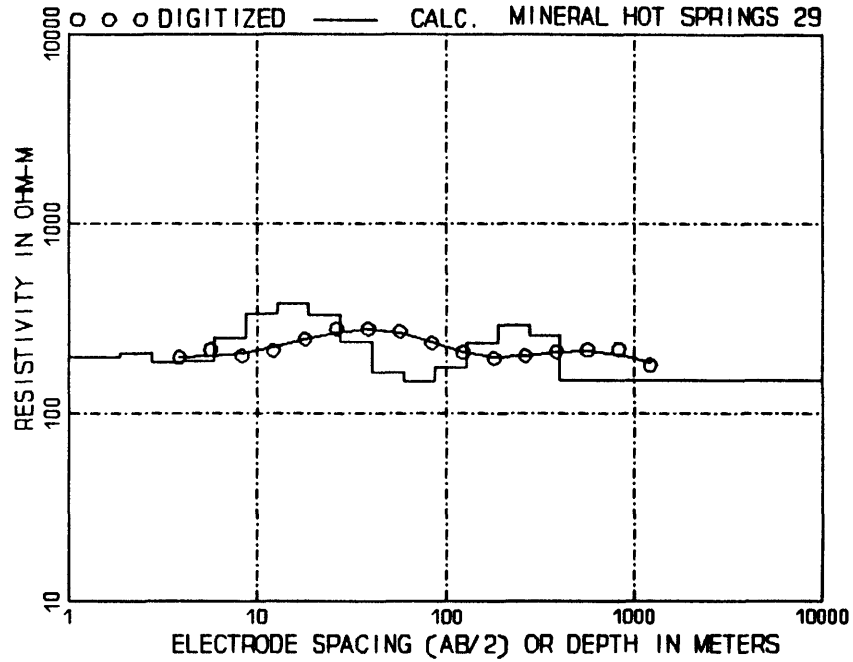

AB/2, m (ft)	App. Res.	AB/2, m (ft)	App. Res.
3.05 (10.00)	165.00	60.96 (200.00)	257.00
4.27 (14.00)	190.00	91.44 (300.00)	218.00
6.10 (20.00)	200.00	121.92 (400.00)	205.00
9.14 (30.00)	187.00	182.88 (600.00)	190.00
12.19 (40.00)	200.00	243.84 (800.00)	195.00
18.29 (60.00)	238.00	304.80 (1000.00)	200.00
24.38 (80.00)	256.00	304.80 (1000.00)	204.00
30.48 (100.00)	268.00	426.72 (1400.00)	215.00
42.67 (140.00)	260.00	609.60 (2000.00)	215.00
30.48 (100.00)	288.00	914.40 (3000.00)	208.00
42.67 (140.00)	273.00	1219.20 (4000.00)	179.00

DEPTH, m (ft)	RESIS.	DEPTH, m (ft)	RESIS.
1.87 (6.15)	196.91	40.37 (132.44)	235.96
2.75 (9.02)	207.86	59.25 (194.40)	164.98
4.04 (13.24)	184.20	86.97 (285.34)	146.71
5.93 (19.44)	188.06	127.66 (418.82)	175.21
8.70 (28.53)	248.83	187.37 (614.75)	235.56
12.77 (41.88)	335.98	275.03 (902.33)	289.36
18.74 (61.47)	376.69	403.69 (1324.43)	258.88
27.50 (90.23)	330.43	99999.00 (99999.00)	149.84

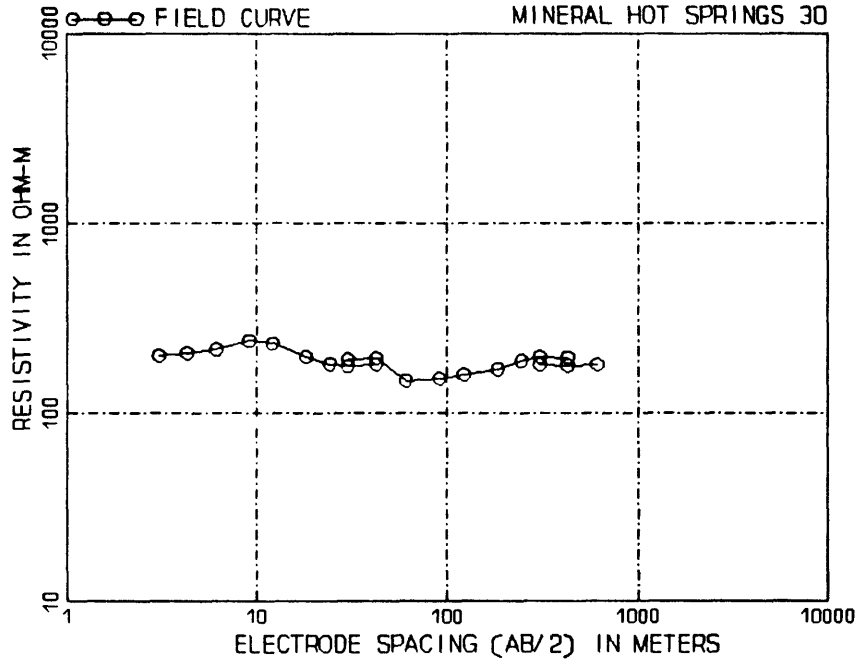

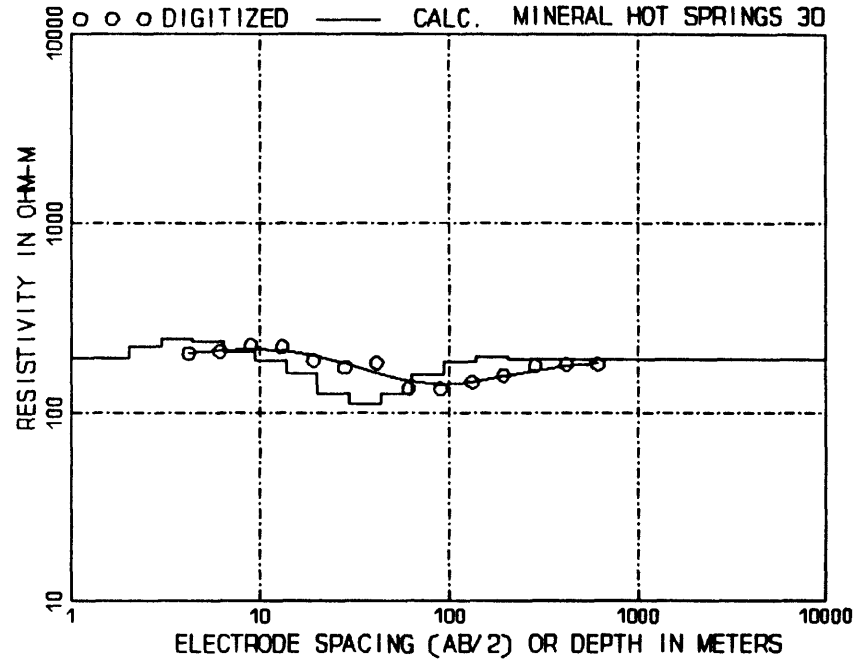

AB/2, m	(ft)	App. Res.	AB/2, m	(ft)	App. Res.
3.05	(10.00)	200.00	42.67	(140.00)	195.00
4.27	(14.00)	207.00	60.96	(200.00)	148.00
6.10	(20.00)	216.00	91.44	(300.00)	152.00
9.14	(30.00)	240.00	121.92	(400.00)	159.00
12.19	(40.00)	233.00	182.88	(600.00)	170.00
18.29	(60.00)	197.00	243.84	(800.00)	188.00
24.38	(80.00)	181.00	304.80	(1000.00)	198.00
30.48	(100.00)	176.00	426.72	(1400.00)	196.00
42.67	(140.00)	181.00	304.80	(1000.00)	180.00
30.48	(100.00)	192.00	426.72	(1400.00)	178.00
			609.60	(2000.00)	180.00

DEPTH, m	(ft)	RESIS.	DEPTH, m	(ft)	RESIS.
2.02	(6.62)	195.37	29.63	(97.20)	126.59
2.96	(9.72)	224.45	43.49	(142.67)	111.50
4.35	(14.27)	246.17	63.83	(209.41)	126.85
6.38	(20.94)	237.45	93.69	(307.37)	158.43
9.37	(30.74)	210.39	137.51	(451.16)	186.28
13.75	(45.12)	189.23	201.84	(662.22)	196.61
20.18	(66.22)	162.70	99999.00	(99999.00)	190.82

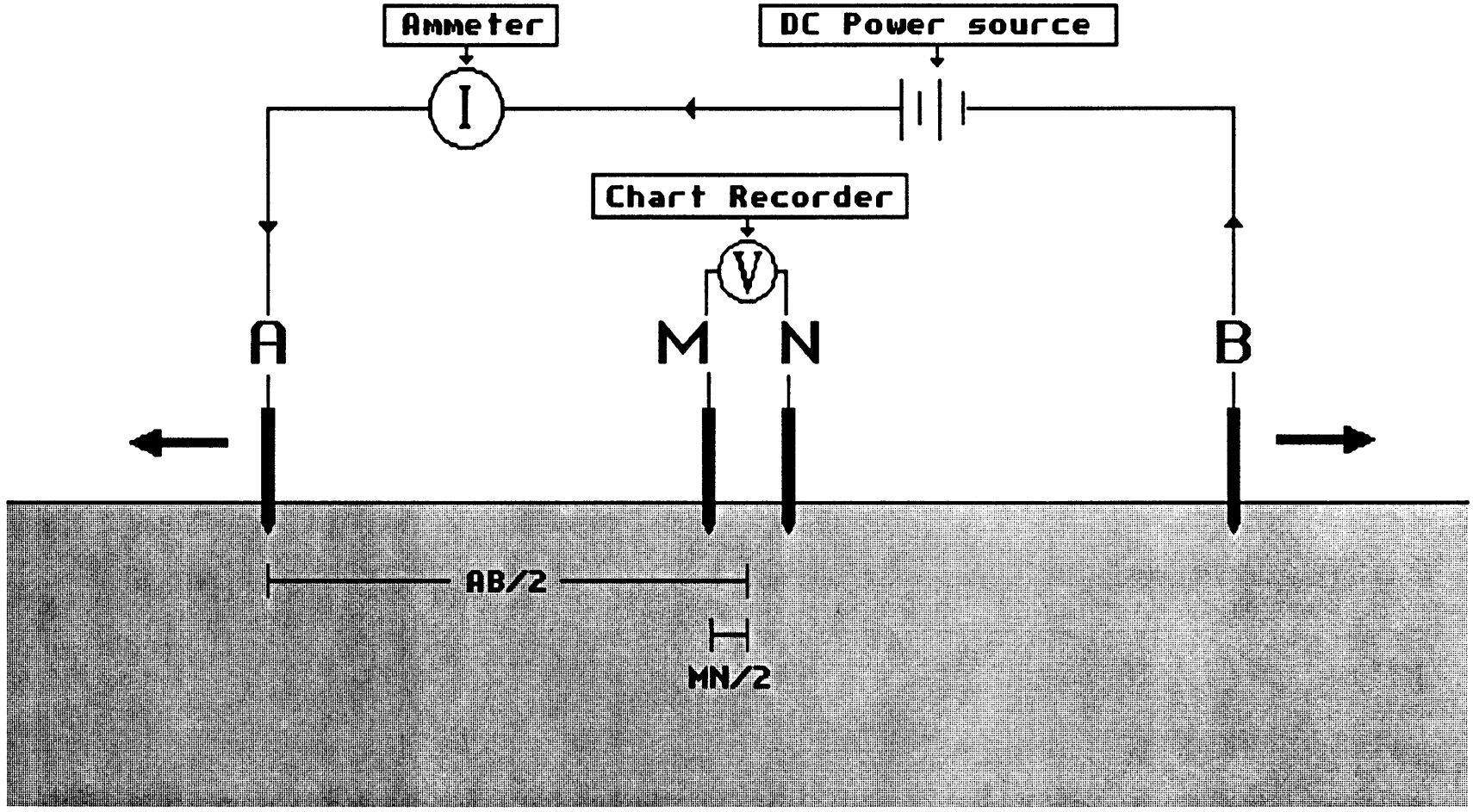

Figure 1. Schlumberger electrode array. A and B, current electrodes; M and N, potential electrodes. Arrows show direction of expansion.

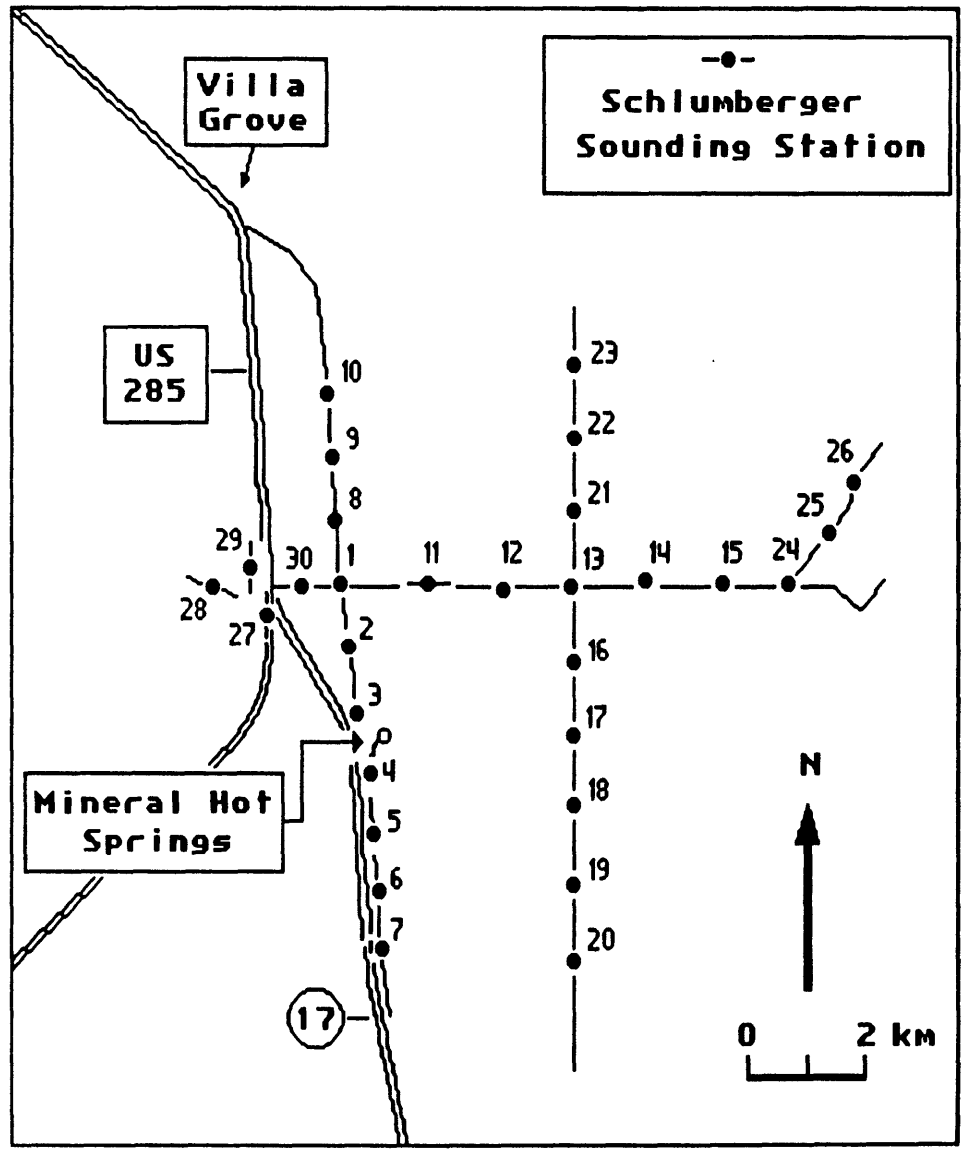

Figure 2. Map showing Schlumberger sounding-station locations and numbers. Soundings expanded parallel to the roads.

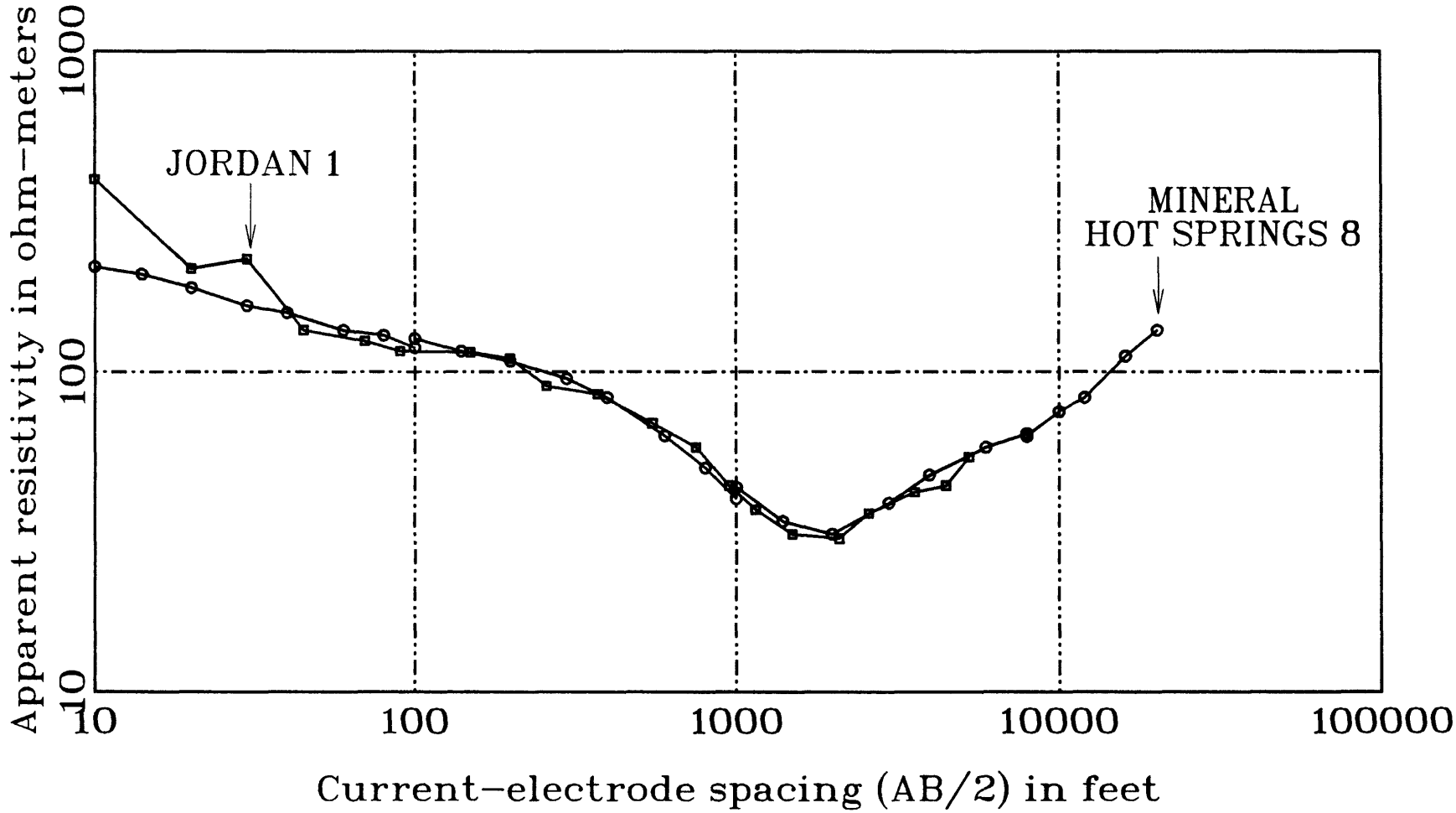

Figure 3. Plot comparing sounding Jordan 1 (Jordan, 1974) and sounding Mineral Hot Springs 8.

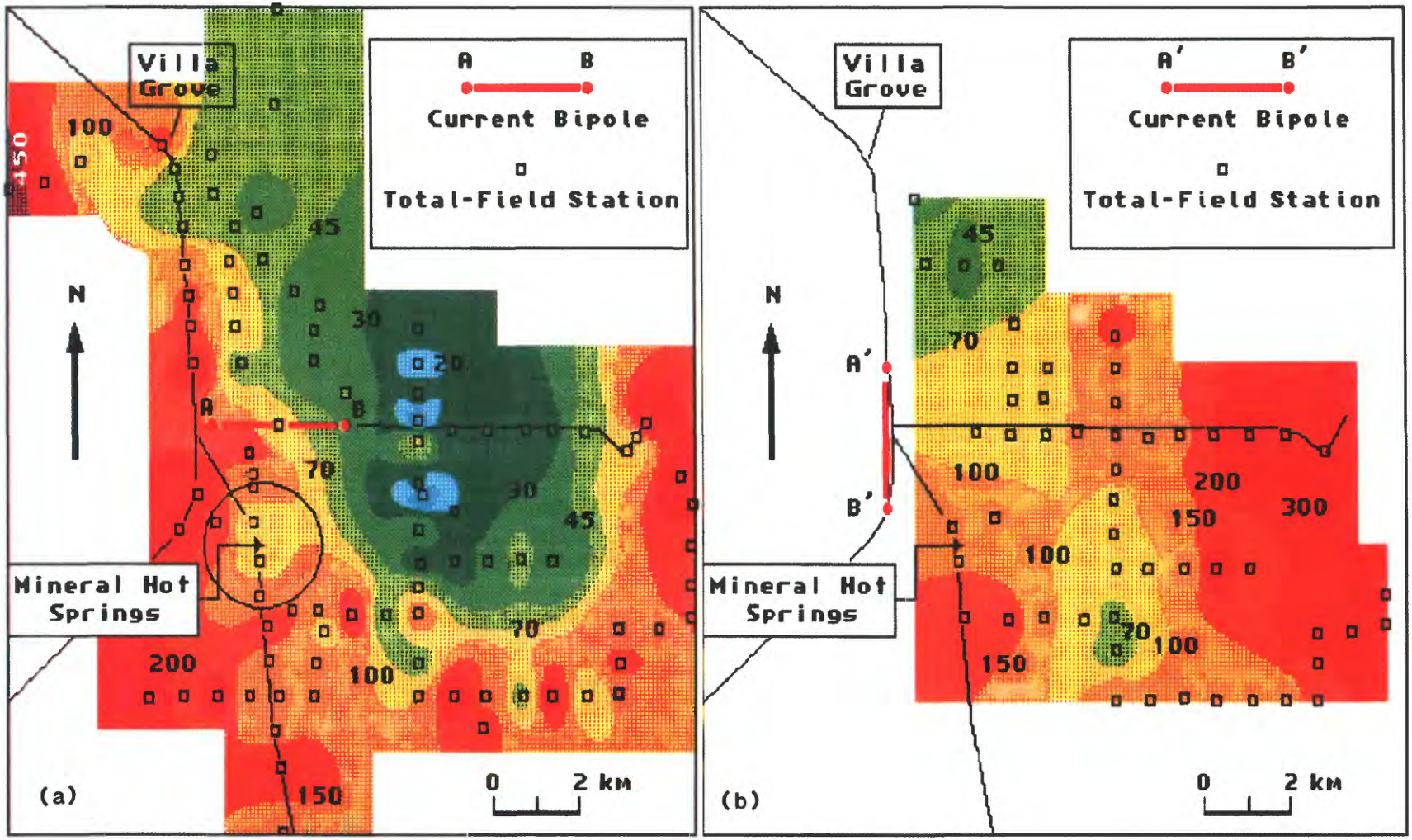

Figure 4 . Recontoured total-field apparent resistivity maps using Jordan (1974) data.

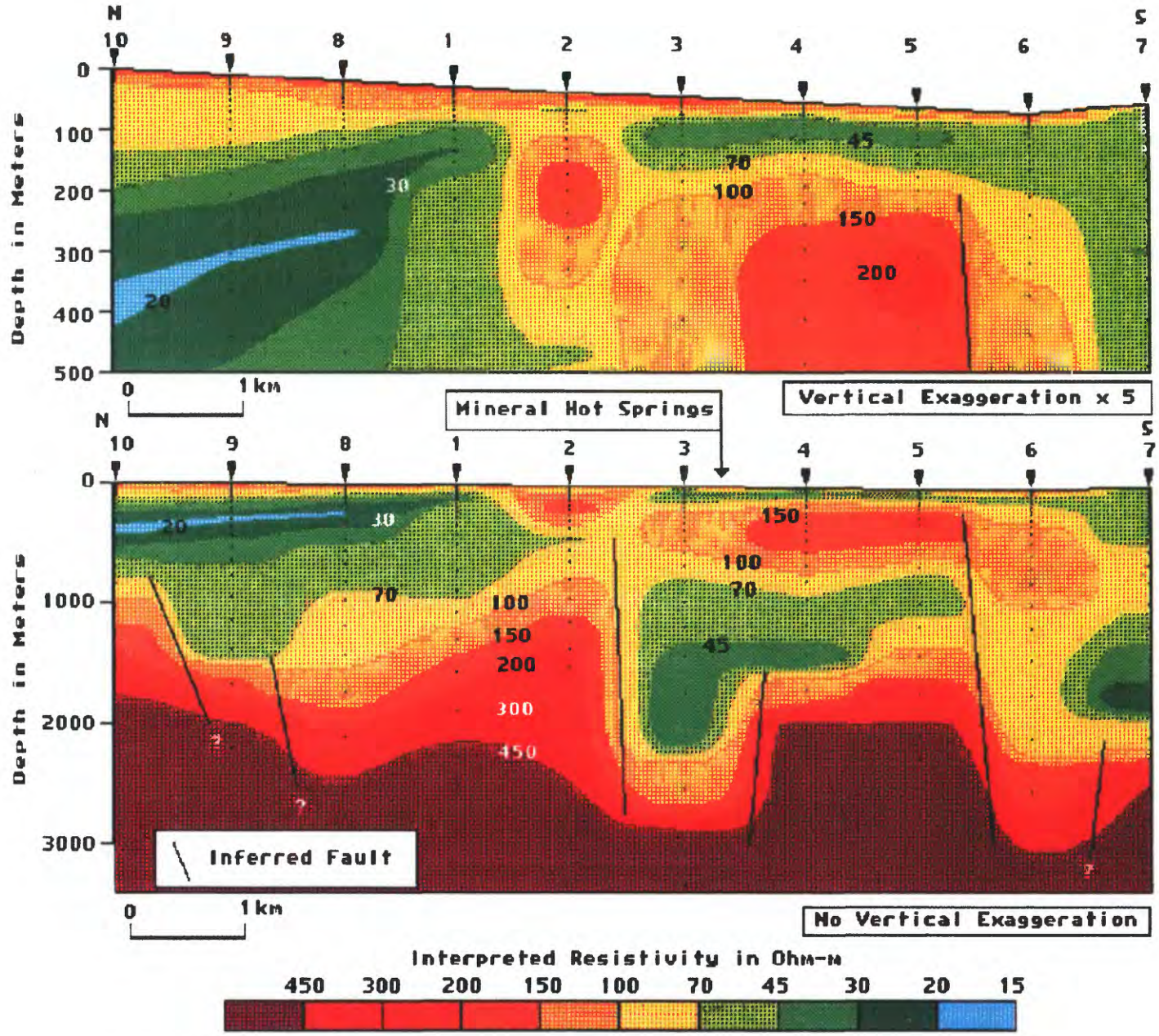

Figure 5. North-south interpreted resistivity cross section.

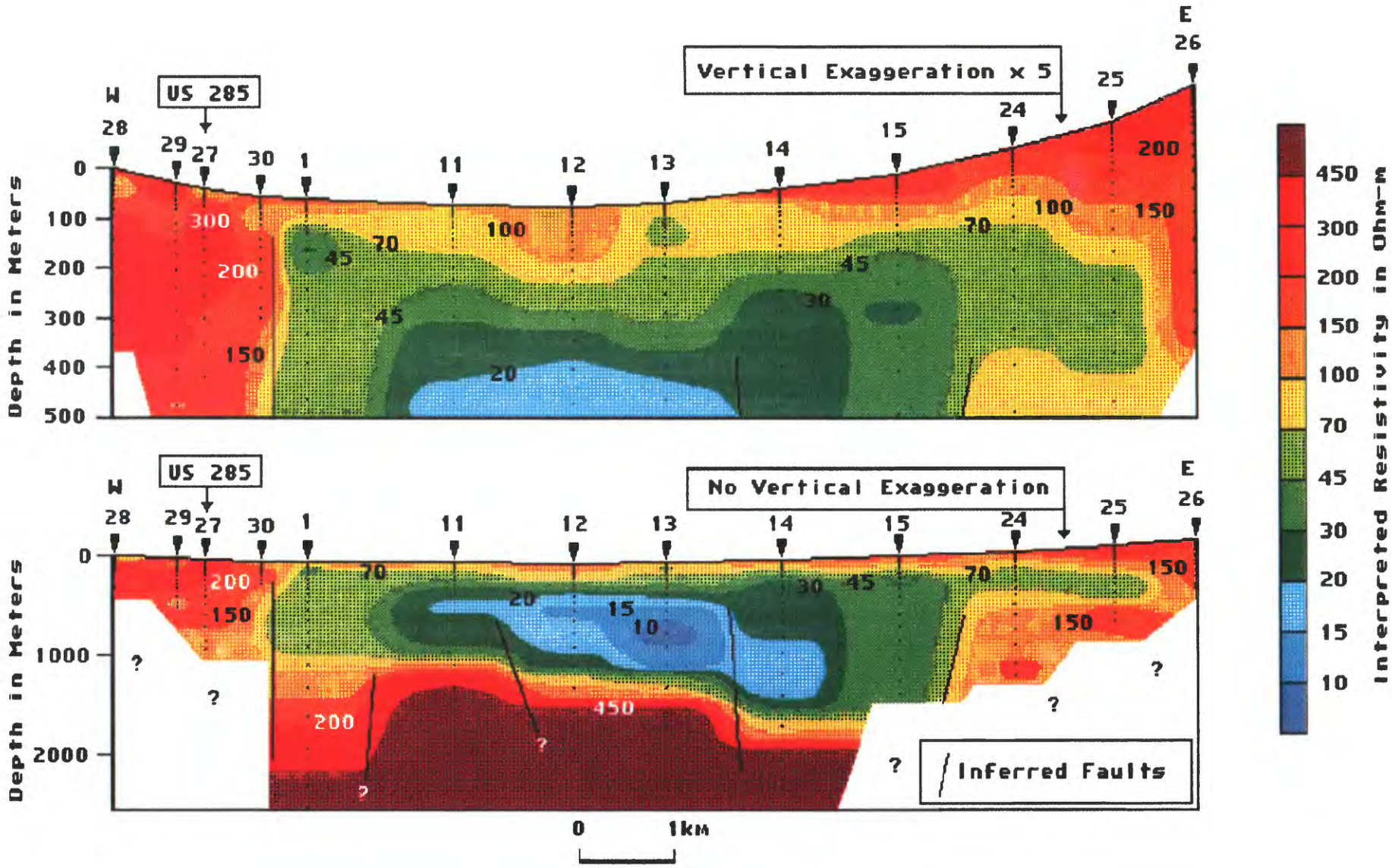

Figure 6 . East-west interpreted resistivity cross section.

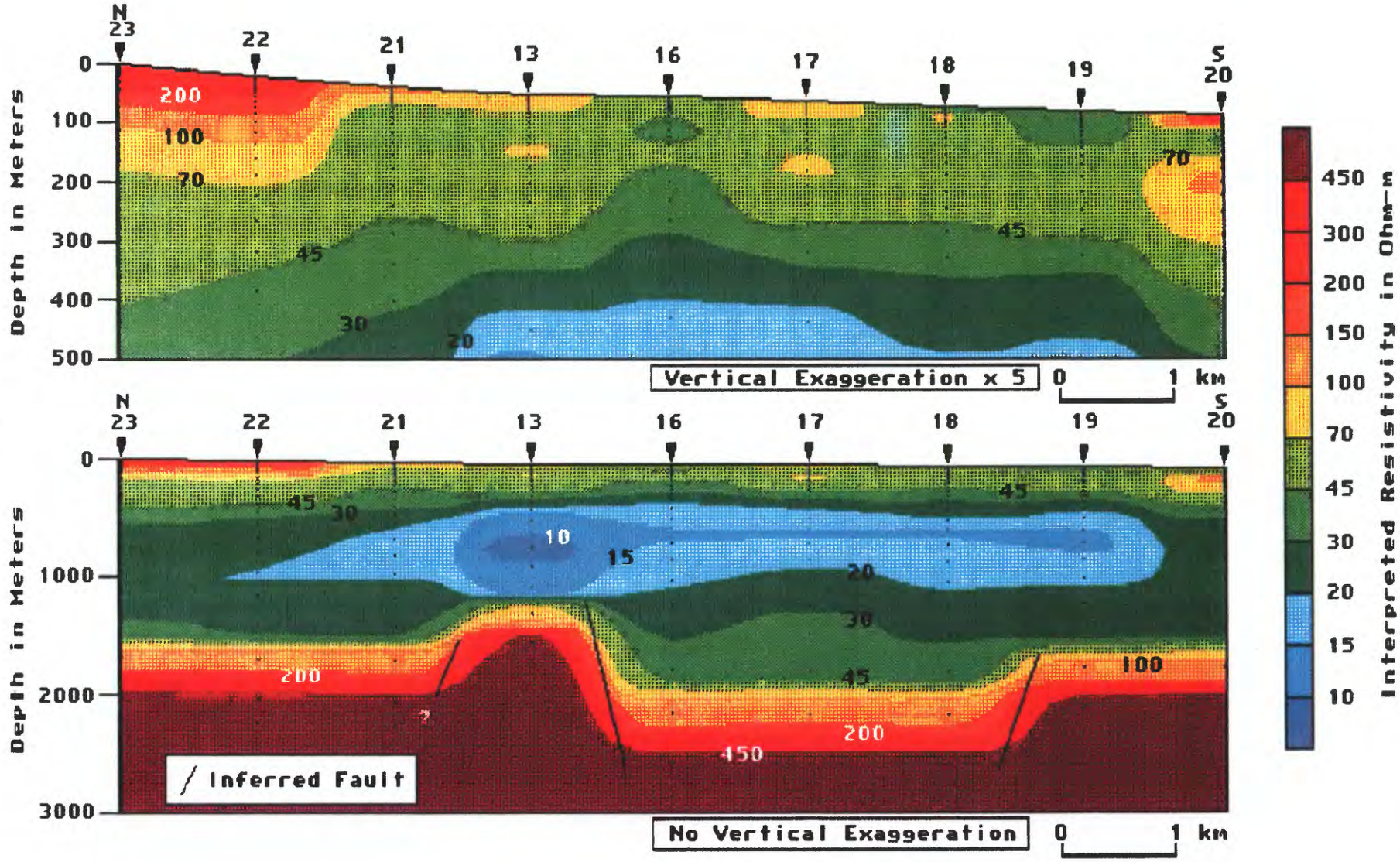

Figure 7 . North-south interpreted resistivity cross section.

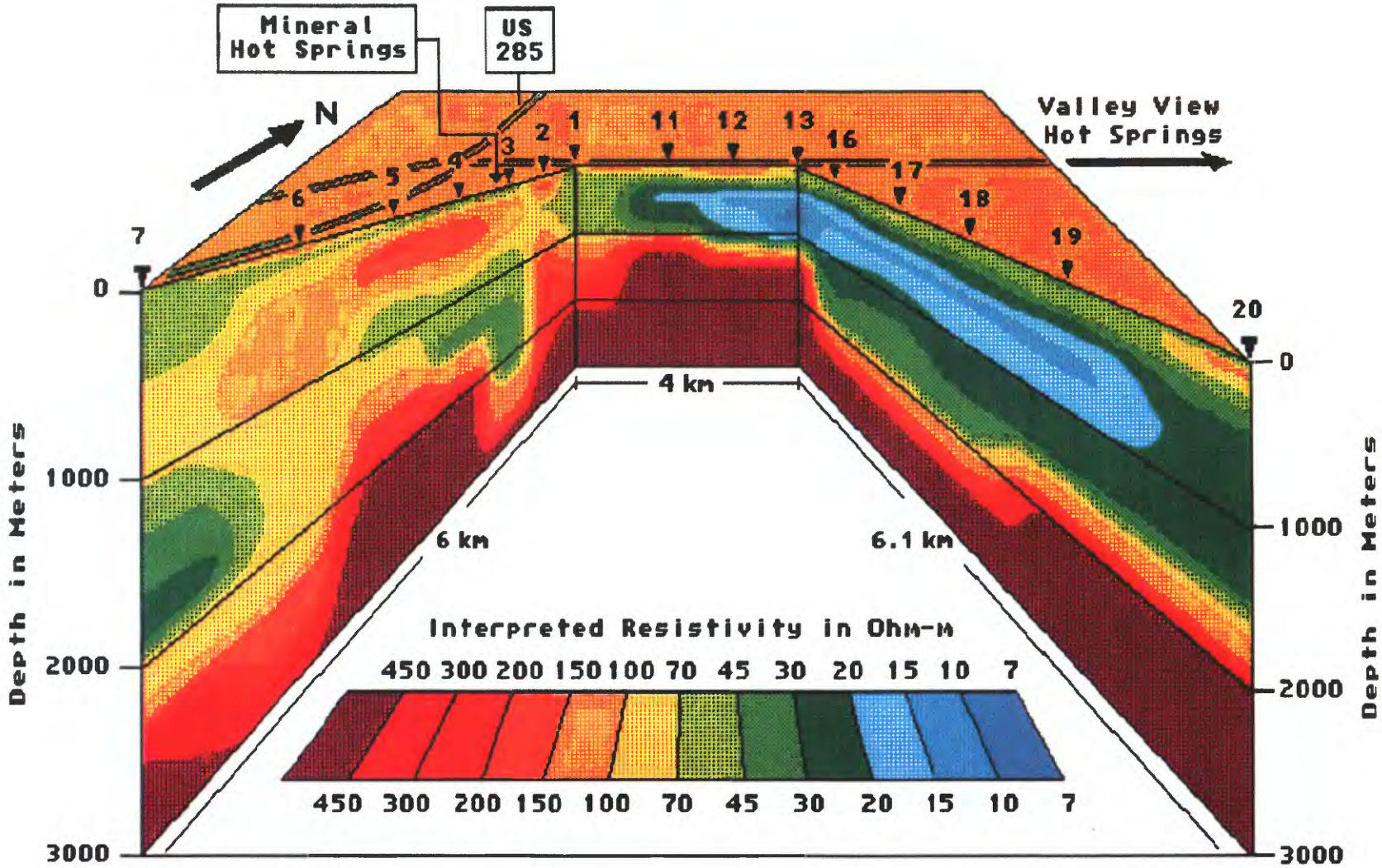

Figure 8. Block diagram showing subsurface geoelectric structures. Looking north.

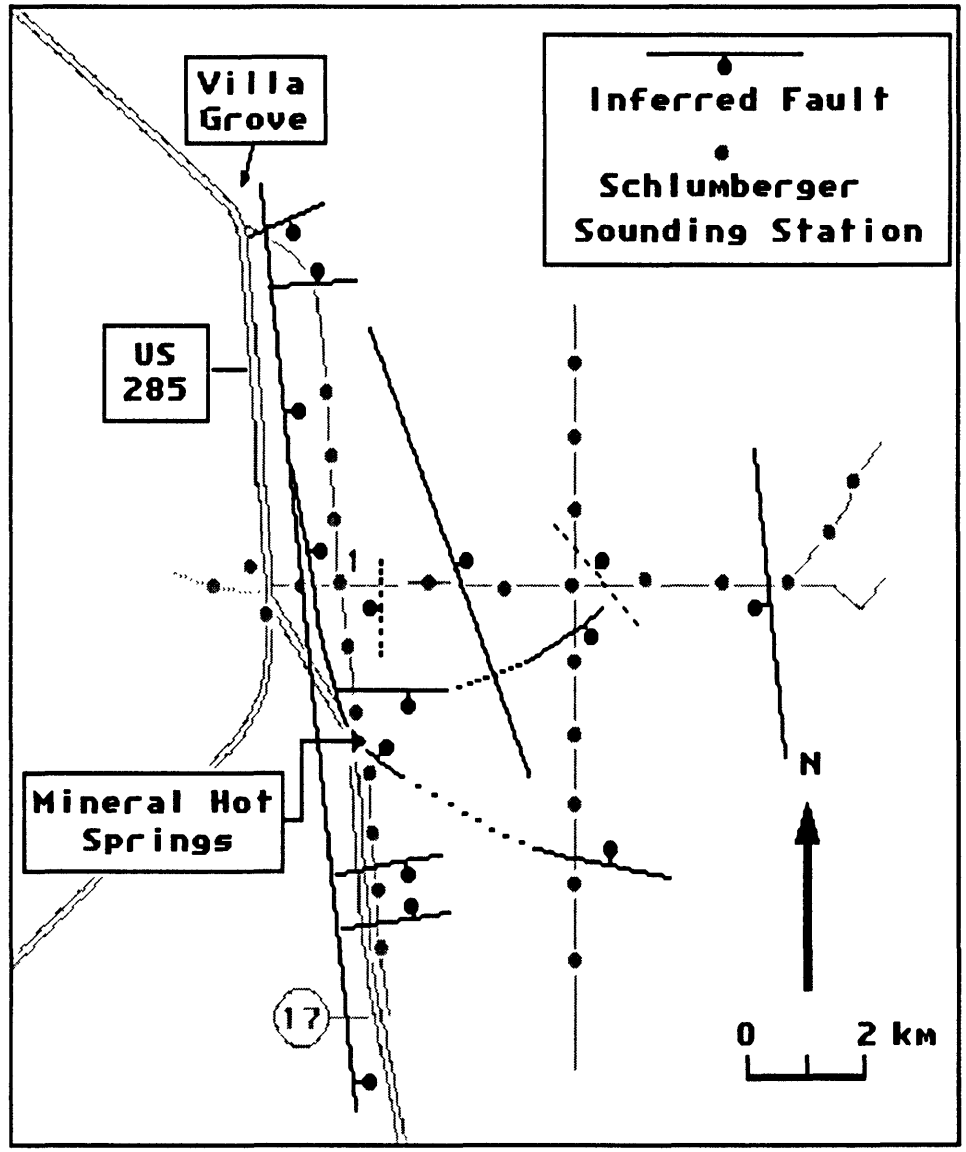

Figure 9. Map showing location of geoelectrically-inferred faults based on both sounding and total-field data.